POLITECNICO DI MILANO

Scuola di Ingegneria Industriale e dell'Informazione

Corso di Laurea Magistrale in Ingegneria Elettrica

POWER SYSTEM STABILIZER OPTIMIZATION ON LARGE ELECTRICAL NETWORKS

Relatore: Prof. Alberto Berizzi

Correlatore: Ing. Vincenzo Asceri

Ing. Davide Stefano Piccagli

Tesi di Laurea Magistrale di:
Ali Rahimzadeh
Matr. 798375

Anno Accademico 2014-2015

Abstract

Electromechanical oscillations were detected in power systems as soon as synchronous generators were interconnected to deliver more power capacity and supply reliability. These oscillations are manifested in the relative motions of generator mechanical axes accompanied by power and voltage oscillations. Some characteristics of modern large-scale electric power systems, such as long transmission distances over weak grids, highly variable generation patterns and heavy loading, tend to increase the probability of appearance of sustained electromechanical oscillations. Both local and inter-area oscillation modes of different frequencies might appear simultaneously in different parts of large-scale systems. Such oscillations threaten the secure operation of power systems and if not controlled efficiently can lead to generator outages, line tripping and even large-scale blackouts.

In general, an insufficient system damping can be the usual reason of electromechanical oscillations. Since the development of current network structures is limited -due to both available resources and environmental considerations- most of the efforts for electromechanical oscillations damping focus on setting different controllers such as Power System Stabilizers (PSSs), Thyristor Controlled Series Compensators (TCSCs) and so on. These damping controllers mostly use local measurements as their inputs. Then, their control rules and parameters are determined in offline studies using time-domain simulations, eigenvalue analysis, and usually remain fixed in practice. Between different controllers available for damping of electromechanical oscillations, PSSs are widely used in power plants. Having the knowledge of limited possible reinforcement in the network together with the fact that PSSs are already accessible in most of the plants, lead us to the idea of maximizing the effect of PSSs by fine-tuning of their parameters.

To this end, this thesis proposes a software development for PSS parameters optimization on large electrical networks with the aim of maximizing the damping of electromechanical oscillations. In particular, this software application is able to import the results of the modal analysis carried out on a large electrical network (e.g. Italian network), and use these outputs as the inputs for the process of optimization of PSSs.

In Italiano:

Nei sistemi di trasmissione di energia elettrica si sono rilevate oscillazioni elettromeccaniche sin da quando, alla ricerca di maggiore capacità produttiva e affidabilità, sono state introdotte le macchine sincrone come sistemi di generazione. Tali oscillazioni si manifestano in moti relativi rispetto all'asse meccanico del generatore, corredati da oscillazioni di tensione e di potenza. Alcune caratteristiche dei moderni sistemi di trasmissione su larga scala, quali ad esempio la trasmissione di energia su lunghe distanze nel caso di reti deboli, la produzione altamente variabile e il forte caricamento delle linee, tendono ad aumentare la probabilità di comparsa di oscillazioni elettromeccaniche. Entrambi i modi di oscillazione locali e inter-area possono apparire contemporaneamente e per varie frequenze in diverse parti del sistema di trasmissione, andando pertanto a influenzarne il funzionamento e la sicurezza. Di fatto, se non controllate in modo efficace, tali oscillazioni possono portare al fuori servizio dei generatori, a scatti intempestivi delle linee e persino blackout su larga scala della rete.

In generale, un insufficiente smorzamento può essere la tipica causa dell'insorgere di oscillazioni elettromeccaniche all'interno della rete di trasmissione. Dal momento che attualmente lo sviluppo delle infrastrutture di rete è limitata, sia dalle risorse disponibili che da considerazioni di carattere ambientale, la maggior parte degli sforzi per poter smorzare le oscillazioni elettromeccaniche è focalizzata sulla taratura dei diversi sistemi di controllo, quali ad esempio i Power System Stabilizer (PSS) o Thyristor Controlled Series Compensator (TCSC). Tali sistemi utilizzano come ingresso per lo più misure locali, avendo inoltre regole di controllo e parametri determinati in studi fuori linea attraverso simulazioni nel dominio del tempo e analisi agli autovalori. Tra i diversi sistemi di controllo disponibili per lo smorzamento delle oscillazioni elettromeccaniche, i PSS sono quelli più ampiamenti utilizzati nel caso di centrali elettriche. Pertanto la limitata possibilità di installazione dei rinforzi nella rete di trasmissione unitamente al fatto che i PSS sono già accessibili nella maggior parte delle centrali, ci portano all'idea di dover massimizzare il loro effetto in modo da ridurre le oscillazioni mediante una corretta configurazione dei parametri.

A tal fine, questa tesi propone lo sviluppo di un tool e di metodologie per l'ottimizzazione dei parametri dei PSS, nel caso di reti elettriche fortemente magliate, con l'obiettivo di massimizzare lo smorzamento delle oscillazioni elettromeccaniche. In particolare, la

soluzione adottata è in grado di importare i risultati dell'analisi modale effettuata su una rete elettrica di grandi dimensioni (quale ad esempio può essere la rete di trasmissione nazionale italiana), e utilizzare tali dati come ingressi per il processo di ottimizzazione dei PSS.

Contents

Figures

Tables

Acknowledgments

The completion of this undertaking could not have been possible without the assistance and guidance of the following:

My supervisor, Prof. Alberto Berizzi, for his excellent advices, caring and helping me prepare my dissertation.

My corporate tutors in CESI, Eng. Davide Piccagli and Eng. Vincenzo Asceri, for the continuous support, guidance, patience and insightful comments during the whole course of the thesis.

Eng. Massimo Pozzi, for offering me the internship opportunity at CESI and allowing me to use all the tools and professional experience of CESI group for my studies.

Last but not the least; I would like to thank my family for supporting me constantly during my studies.

Abbreviations

AC	alternating current
AVR	automatic voltage controller
d	direct axis of a generator
DC	direct current
emf	electro-motive force
HV	high voltage
mmf	magneto-motive force
PSS	power system stabilizer
pu	per unit
q	quadrature axis of a generator
SCR	synchronous generator

1 Introduction

Recently, the number of bulk power exchanges over long distances has increased as a consequence of deregulation of the electrical energy markets worldwide and the extensions of large interconnected power systems. Moreover, the power transfers have also become somewhat unpredictable as dictated by market price fluctuations. The integration of offshore wind generation plants into the existing network is also expected to have a significant impact on the power flow of system as well as the dynamic behavior of the network. The expansion of the transmission grids, on the other hand, is very little due to environmental and cost restrictions. The result is that the available transmission and generation facilities are highly utilized with large amounts of power interchanges taking place through tie-lines and geographical regions. The tie lines operate near their maximum capacity, especially those connected to the heavy load areas. As a result, the system operation can find itself close to or outside the secure operating limits under severe contingencies. Therefore, stressed operating conditions can increase the possibility of electromechanical oscillations between different control areas and even breakup of the whole system [1].

Reliability and good performance are necessary in power system operation to ensure a safe and continuous energy supply. However, weakly damped electromechanical oscillations (both local and inter-area oscillations), inherent to large interconnected power systems during transient conditions, are not only dangerous for the reliability and performance of such systems but also for the quality of the supplied energy. The power flows over certain network branches resulting from generator oscillations can take peak values that are dangerous from the point of view of secure system operation and lead to limitations in network control.

Electromechanical oscillations may cause, in certain cases, operational limitations (due to the restrictions in the power transfers across the transmission lines) and/or

15

interruption in the energy supply (due to loss of synchronism among the system generators). Also, the system operation may become difficult in the presence of these oscillations.

With the heavier power transfers ahead, the damping of electromechanical oscillations will decrease unless new lines are built or other heavy and expensive high-voltage equipment such as series-compensation is added to the grid substations. The construction of new lines, however, is restricted by environmental and cost factors. Therefore, achievement of maximum available transfer capability as well as a high level of power quality and security has become a major concern. This concern requires the need for a better system control, leading to damping improvement.

Simulation studies have shown a high sensitivity of electromechanical oscillations to generator voltage controller and hydro turbine governor settings [6]. Therefore, and because of the relatively low cost, measures to alleviate electromechanical oscillations should be focused on power system controllers. The use of a supplementary control added to the Automatic Voltage Regulator (AVR) is a practical and economic way to supply additional damping to electromechanical oscillations. The first supplementary control for such task was proposed at the end of 1960's [7], and is usually known as Power System Stabilizer (PSS). PSS units have long been regarded as an effective way to enhance the damping of electromechanical oscillations in power system [7]. The PSS provides supplementary control action through the excitation system of generators and thus aids in damping the oscillations of synchronous machine rotors via modulation of the generator excitation. The supplemental damping is provided by an electric torque, applied to the rotor, which is in phase with the speed variation. The action of PSS, in this way, extends the angular stability limits of a power system.

For damping of local generator swings, PSSs have been established in the past [8], [1]. To maximize damping of electromechanical oscillations likewise with PSS, special control structures with additional signal inputs and well adapted parameter tunings are necessary. Since the first proposal of PSS at the end of 1960's, various control methods have been proposed for PSS design to improve overall system performance. Among the classical methods used are the phase-compensation method and the root-locus method. Among these, conventional PSS of the lead-lag compensation type [7], [9], [9] has been adopted

by most utility companies because of its simple structure, flexibility and ease of implementation. Since power systems are highly nonlinear, conventional fixed-parameter PSSs cannot cope with changes in the operating conditions during normal operation and the system sometimes tends to be unstable. Proper design of any control system that takes into account the continual changes in the structure of the network is, therefore, necessary to guarantee robustness over wide operating conditions in the system.

This research mainly focuses on the problem of improving the performance of conventional PSS, for a better damping of electromechanical oscillations, by using instantaneous measurements from synchronous generators of the grid as its supplementary inputs.

The subsequent chapters of this dissertation are organized as follows:

Chapter 2 provides a general description of the power system dynamics and stability phenomena including fundamental concepts, classification, and definitions of associated terms.

Chapter 3 presents the exploited techniques for PSS tuning.

Chapter 4 describes an example of using ALICE as the optimization tool, for the case of a single power plant.

Chapter 5 is the main chapter of this thesis, in which the local optimization of a large network is obtained through using described methods.

In chapter 6, the possible practical modifications on the network will be clarified.

And finally in chapter 7, the results of simulations and their related figures are illustrated.

2   Power System Stability: Electromechanical Oscillation

The purpose of this chapter is to provide a general introduction to the power system stability problem including classification, physical concepts and definition of the related terms. After discussing the general aspects of *power system stability and dynamics*, the focus is on "rotor angle stability", because the electromechanical oscillation problem is a subset of this kind of instability. A good knowledge of the problem and its causes can directly lead us to the solution and a better understanding of different methods to solve it.

The electromechanical stability is related to the dynamic interaction between the turbine-alternators and the network. Regarding this interaction, there are electromechanical oscillations of the rotor of the synchronous generators. The weakly damped oscillations can be pronounced for example during the peak loading periods, but can occur even under light loading conditions. The problems coming from these oscillations are of crucial importance to ensure, mainly within an energy market, a full usability of production plants in their entire design field, as well as to guarantee a behavior consistent with security requirements, in the face of possible network contingencies.

Power System Dynamics and Stability

A power system can be studied, in an intuitive way, as working in two different states, steady-state and dynamic state –considering the variation of generated power and load demands.

One of the characteristic features of power system operation is the continual need to adjust system operating conditions in order to meet the ever-changing load demand. Although the demand from any particular load can vary quite significantly, the total

demand, consisting of a very large number of individual loads changes rather more slowly and in a predictable manner. This characteristic is important as it means that within any small time period the transmission and subtransmission systems can be regarded as being in the steady state and, as time progresses, considered to move slowly from one steady-state condition to another. The steady-state operation is studied to perform the so called "power (or load) flow" calculations of the power system and it is not the case of interest for this thesis, because we want to deal with the stability problem that is discussed when the power system is in a dynamic state.

Separation of stability and dynamics of a power system is difficult, because after a contingency the power system moves to dynamic state, and it is the point where the stability of the system becomes a discussable issue. Thus, stability and dynamics of a power system are two inseparable concepts. However for the sake of simplicity and being clear, first, power system dynamics' concepts and categories are discussed. Then a brief explanation about power system stability is given. In the end, the focus is on a particular case with a specified range of frequency, that is, the electromechanical phenomena.

2.1 Power System Dynamics[1]

An electrical power system consists of many individual elements connected together to form a large, complex and dynamic system capable of generating, transmitting and distributing electrical energy over a large geographical area. Because of this interconnection of elements, a large variety of dynamic interactions are possible, some of which will only affect some of the elements, others are fragments of the system, while others may affect the system as a whole. As each dynamic effect displays certain unique features, power system dynamics can be conveniently divided into groups characterized by their cause, consequence, time frame, physical character or the place in the system where they occur.

---

[1] It is worthy to notice that in North American literature, the term *dynamic stability* has been used mostly to denote small-signal stability in the presence of automatic control devices, but here it is simply denoting the state of the electric power system following any kind of variation in the system, including physical configuration or connection changes, contingencies, load demand increments and etc. In other words, it refers to the dynamic response of power systems to these variations.

Of prime concern is the way the power system will respond to both a changing power demand and to various types of disturbance, that are the two main causes of power system dynamics. A changing power demand introduces a wide spectrum of dynamic changes into the system each of which occurs on a different time scale. In this context the fastest dynamics are due to sudden changes in demand and are associated with the transfer of energy between the rotating masses in the generators and the loads. Slightly slower are the voltage and frequency control actions needed to maintain system operating conditions until finally the very slow dynamics corresponding to the way in which the generation is adjusted to meet the slow daily demand variations take effect. Similarly, the way in which the system responds to disturbances also covers a wide spectrum of dynamics and associated time frames. In this case the fastest dynamics are those associated with the very fast-wave phenomena that occur in high-voltage transmission lines. These are followed by fast electromagnetic changes in the electrical machines themselves before the relatively slow electromechanical rotor oscillations occur. Finally the very slow prime mover and automatic generation control actions take effect.

2.1.1 General Classification of Power System Dynamics – considering the time frame

Based on their physical character, the different power system dynamics may be divided into four groups defined as: wave, electromagnetic, electromechanical and thermodynamic. This classification also corresponds to the time frame involved and is shown in *Figure 2-1*. Although this broad classification is convenient, it is by no means absolute, with some of the dynamics belonging to two or more groups while others lie on the boundary between groups. *Figure 2-1* shows the fastest dynamics to be the wave effects, or surges, in high-voltage transmission lines and correspond to the propagation of electromagnetic waves caused by lightning strikes or switching operations. The time frame of these dynamics is from microseconds to milliseconds. Much slower are the electromagnetic dynamics that take place in the machine windings following a disturbance, operation of the protection system or the interaction between the electrical machines and the network. Their time frame is from milliseconds to a second. Slower still are the electromechanical dynamics due to the oscillation of the rotating masses of the generators

and motors that occur following a disturbance, operation of the protection system and voltage and prime mover control.

The time frame of these dynamics is from seconds to several seconds. The slowest dynamics are the thermodynamic changes which result from boiler control action in steam power plants as the demands of the automatic generation control are implemented. Careful inspection of *Figure 2-1* shows the classification of power system dynamics with respect to time frame to be closely related to where the dynamics occur within the system. For example, moving from the left to right along the time scale in *Figure 2-1* corresponds to moving through the power system from the electrical RLC circuits of the transmission network, through the generator armature windings to the field and damper winding, then along the generator rotor to the turbine until finally the boiler is reached.
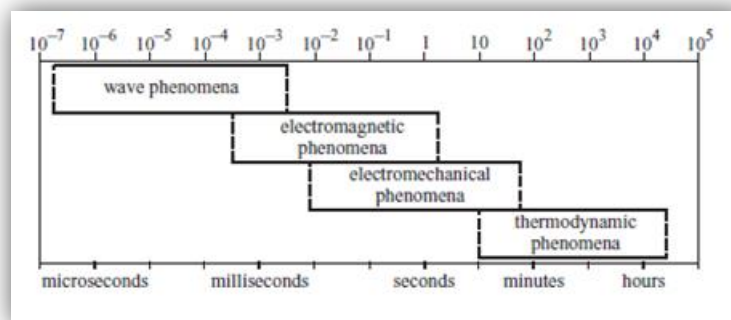
Figure 2-1 Time Frame of the Basic Power Dynamic Phenomena[2]

The fast wave phenomena, due to lightning and switching overvoltages, occur almost exclusively in the network and basically do not propagate beyond the transformer windings. The electromagnetic phenomena mainly involve the generator armature and damper windings and partly the network. These electromechanical phenomena, namely the rotor oscillations and accompanying network power swings, mainly involve the rotor field and damper windings and the rotor inertia. As the power system network connects the generators together, this enables interactions between swinging generator rotors to take place. An important role is played here by the automatic voltage control and the prime mover control. Slightly slower than the electromechanical phenomena are the frequency oscillations, in which the rotor dynamics still play an important part, but are influenced to a

much greater extent by the action of the turbine governing systems and the automatic generation control. Automatic generation control also influences the thermodynamic changes due to boiler control action in steam power plants.

2.2 Power System Stability

As electric power systems have evolved over the last century, different forms of instability have emerged as being important during different periods. The methods of analysis and resolution of stability problems were influenced by the prevailing developments in computational tools, stability theory, and power system control technology. A review of the history of the subject is useful for a better understanding of the electric power industry's practices with regard to system stability.

2.2.1 Historical Review of Power System Stability Problems

As electric power systems have evolved over the last century, different forms of instability have emerged as being important during different periods. The methods of analysis and resolution of stability problems were influenced by the prevailing developments in computational tools, stability theory, and power system control technology. A review of the history of the subject is useful for a better understanding of the electric power industry's practices with regard to system stability.[2]

Power system stability was first recognized as an important problem in the 1920s (Steinmetz, 1920; Evans and Bergvall, 1924; Wilkins, 1926). The early stability problems were associated with remote power plants feeding load centers over long transmission lines.

With slow exciters and non-continuously acting voltage regulators, power transfer capability was often limited by steady-state as well as transient rotor angle instability due to insufficient synchronizing torque.

To analyze system stability, graphical techniques such as the equal area criterion and power circle diagrams were developed. These methods were successfully applied to early systems which could be effectively represented as two machine systems.

As the complexity of power systems increased, and interconnections were found to be economically attractive, the complexity of the stability problems also increased and systems could no longer be treated as two machine systems. This led to the development in the 1930s of the network analyzer, which was capable of power flow analysis of multi-machine systems. System dynamics, however, still had to be analyzed by solving the swing equations by hand using step-by-step numerical integration. Generators were represented by the classical ''fixed voltage behind transient reactance'' model. Loads were represented as constant impedances.

Improvements in system stability came about by way of faster fault clearing and fast acting excitation systems. Steady-state aperiodic instability was virtually eliminated by the implementation of continuously acting voltage regulators. With increased dependence on controls, the emphasis of stability studies moved from transmission network problems to generator problems, and simulations with more detailed representations of synchronous machines and excitation systems were required.

The 1950s saw the development of the analog computer, with which simulations could be carried out to study in detail the dynamic characteristics of a generator and its controls rather than the overall behavior of multi-machine systems.

Later in the 1950s, the digital computer emerged as the ideal means to study the stability problems associated with large interconnected systems. In the 1960s, most of the power systems in the U.S. and Canada were part of one of two large interconnected systems, one in the east and the other in the west. In 1967, low capacity HVDC ties were also established between the east and west systems. At present, the power systems in North America form virtually one large system. There were similar trends in growth of interconnections in other countries.

While interconnections result in operating economy and increased reliability through mutual assistance, they contribute to increased complexity of stability problems and increased consequences of instability. The Northeast Blackout of November 9, 1965,

23

made this abundantly clear; it focused the attention of the public and of regulatory agencies, as well as of engineers, on the problem of stability and importance of power system reliability.

Until recently, most industry effort and interest has been concentrated on transient (rotor angle) stability. Powerful transient stability simulation programs have been developed that are capable of modeling large complex systems using detailed device models. Significant improvements in transient stability performance of power systems have been achieved through use of high-speed fault clearing, high-response exciters, series capacitors, and special stability controls and protection schemes.

The increased use of high response exciters, coupled with decreasing strengths of transmission systems, has led to an increased focus on small signal (rotor angle) stability.

This type of angle instability is often seen as local plant modes of oscillation, or in the case of groups of machines interconnected by weak links, as inter-area modes of oscillation. Small signal stability problems have led to the development of special study techniques, such as modal analysis using eigenvalue techniques (Martins, 1986; Kundur et al., 1990). In addition, supplementary control of generator excitation systems, static Var compensators, and HVDC converters is increasingly being used to solve system oscillation problems.

Present-day power systems are being operated under increasingly stressed conditions due to the prevailing trend to make the most of existing facilities. Increased competition, open transmission access, and construction and environmental constraints are shaping the operation of electric power systems in new ways that present greater challenges for secure system operation. This is abundantly clear from the increasing number of major power-grid blackouts that have been experienced in recent years; for example, Brazil blackout of March 11, 1999; Northeast USA-Canada blackout of August 14, 2003; Southern Sweden and Eastern Denmark blackout of September 23, 2003; and Italian blackout of September 28, 2003. Planning and operation of today's power systems require a careful consideration of all forms of system instability.

2.2.2 **Basic Concepts**

Power system stability is the ability of the system, for a given initial operating condition, to regain a normal state of equilibrium after being subjected to a disturbance.

Stability is a condition of equilibrium between opposing forces; instability results when a disturbance leads to a sustained imbalance between the opposing forces.

The power system is a highly nonlinear system that operates in a constantly changing environment; loads, generator outputs, topology, and key operating parameters change continually.

When subjected to a transient disturbance, the stability of the system depends on the nature of the disturbance as well as the initial operating condition. The disturbance may be small or large. Small disturbances in the form of load changes occur continually, and the system adjusts to the changing conditions. The system must be able to operate satisfactorily under these conditions and successfully meet the load demand. It must also be able to survive numerous disturbances of a severe nature, such as a short-circuit on a transmission line or loss of a large generator.

Following a transient disturbance, if the power system is stable, it will reach a new equilibrium state with practically the entire system intact; the actions of automatic controls and possibly human operators will eventually restore the system to normal state. On the other hand, if the system is unstable, it will result in a run-away or run-down situation; for example, a progressive increase in angular separation of generator rotors, or a progressive decrease in bus voltages. An unstable system condition could lead to cascading outages and a shut-down of a major portion of the power system.

The response of the power system to a disturbance may involve much of the equipment. For instance, a fault on a critical element followed by its isolation by protective relays will cause variations in power flows, network bus voltages, and machine rotor speeds; the voltage variations will actuate both generator and transmission network voltage regulators; the generator speed variations will actuate prime mover governors; and the

voltage and frequency variations will affect the system loads to varying degrees depending on their individual characteristics.

Further, devices used to protect individual equipment may respond to variations in system variables and thereby affect the power system performance. A typical modern power system is thus a very high-order multivariable process whose dynamic performance is influenced by a wide array of devices with different response rates and characteristics. Hence, instability in a power system may occur in many different ways depending on the system topology, operating mode, and the form of the disturbance.

Traditionally, the stability problem has been one of maintaining synchronous operation. Since power systems rely on synchronous machines for generation of electrical power, a necessary condition for satisfactory system operation is that all synchronous machines remain in synchronism or, colloquially, "in step."

This aspect of stability is influenced by the dynamics of generator rotor angles and power-angle relationships. Instability may also be encountered without the loss of synchronism. For example, a system consisting of a generator feeding an induction motor can become unstable due to collapse of load voltage. In this instance, it is the stability and control of voltage that is the issue, rather than the maintenance of synchronism. This type of instability can also occur in the case of loads covering an extensive area in a large system.

In the event of a significant load/generation mismatch, generator and prime mover controls become important, as well as system controls and special protections. If not properly coordinated, it is possible for the system frequency to become unstable, and generating units and/or loads may ultimately be tripped possibly leading to a system blackout. This is another case where units may remain in synchronism (until tripped by such protections as under-frequency), but the system becomes unstable.

Because of the high dimensionality and complexity of stability problems, it is essential to make simplifying assumptions and to analyze specific types of problems using the right degree of detail of system representation.

2.2.3 Different Types of Power System Stability: nature of disturbance

The synchronous stability of a power system can be of several types depending upon the nature of disturbance, and for the purpose of successful analysis it can be classified into the following 3 types as shown below:

1) Steady state stability,

2) Transient stability,

3) Dynamic stability.
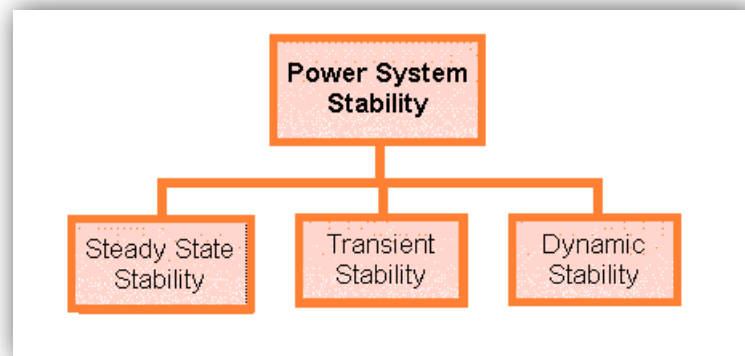
Figure 2-2 Power System Stability Category[1]

Steady-state or Small-signal Stability

The steady state stability of a power system is defined as the ability of the system to bring itself back to its stable configuration following a small disturbance in the network (like normal load fluctuation or action of automatic voltage regulator). It can be considered only during a very gradual and infinitesimally small power change.

In case the power flow through the circuit exceeds the maximum power permissible, then there are chances that a particular machine or a group of machines will cease to operate in synchronism, and result in yet more disturbances. In such a situation,

the steady state limit of the system is said to have reached. Or in other words the steady state stability limit of a system refers to the maximum amount of power that is permissible through the system without loss of its steady state stability.

Transient or Large-Disturbance Stability

Transient stability of a power system refers to the ability of the system to reach a stable condition following a large disturbance in the network condition. In all cases related to large changes in the system like sudden application or removal of load, switching operations, line faults or loss due to excitation the transient stability of the system comes into play. In fact, it deals in the ability of the system to retain synchronism following a disturbance sustaining for a reasonably long period of time.

The maximum power that is allowed to flow through the network without loss of stability following a sustained period of disturbance is referred to as the transient stability of the system. Going beyond that maximum permissible value for power flow, the system would temporarily be unstable.

Dynamic Stability

Dynamic stability of a system denotes the artificial stability given to an inherently unstable system by automatic controlled means. It is generally concerned to small disturbances lasting for about 10 to 30 seconds.

Particularly in the thesis, we want to focus on the steady-state or small signal stability, so we just consider the system conditions following a small disturbance.

2.2.4 Different Types of Power System Stability: quantities of interest

In the previous section we classified power system stability depending on the nature of disturbance. But there is another category for stability of the power system that

can be reached if we consider the parameter of the interest. Three quantities are important for power system operation: (i) angles of nodal voltages δ, also called power or load angles; (ii) frequency f ; and (iii) nodal voltage magnitudes V. These quantities are especially important from the point of view of defining and classifying power system stability. Hence power system stability can be divided into: (i) rotor (or power) angle stability; (ii) frequency stability; and (iii) voltage stability. (*Figure 2-2*)

So if we combine these two categories, we can reach a unique classification of power system stability, shown in *Figure 2-3*, that is useful to lead us to the final point of interest.
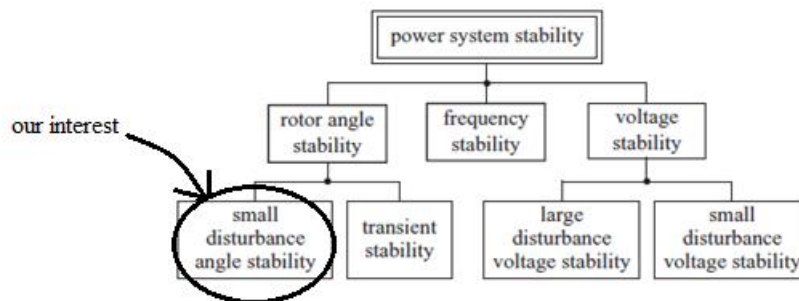
Figure 2-3 Classification of Power System Stability (based on CIGRE No.325)

In the previous section, the dynamics of the power system were discussed and also classified according to the time frame of their occurrence. In the case of electromagnetic phenomenon, as the duration of the disturbance is very short, the generator rotational speed can be considered constant. In this thesis, a longer time scale will be discussed during which the rotor speed will vary and interact with the electromagnetic changes to produce electromechanical dynamic effects. The time scale associated with these dynamics is sufficiently long for them to be influenced by the turbine and the generator control systems. As you can see in *Figure 2-3*, angle stability following small disturbances is our interest.

At this point we know that we need to focus on angle stability, so in the next section a brief description is given and then we will see how the regulation of voltage with AVR can endanger angle stability.

2.2.5 Rotor Angle Stability

Rotor angle stability is the ability of interconnected synchronous machines of a power system to remain in synchronism. The stability problem involves the study of the electromechanical oscillations inherent in power systems. A fundamental factor in this problem is the manner in which the power outputs of synchronous machines vary as their rotors oscillate.

Each synchronous machine has two essential elements: the field and the armature windings. When the rotor is driven by a prime mover (turbine), the rotating magnetic field of the field winding induces alternating voltages in the three-phase armature windings of the stator. The frequency of the induced alternating voltages and of the resulting currents that flow in the stator windings when a load is connected depends on the speed of the rotor. The frequency of the stator electrical quantities is thus synchronized with the rotor mechanical speed: hence the designation "synchronous machine."

When two or more synchronous machines are interconnected, the stator voltages and currents of all the machines must have the same frequency and the rotor mechanical speed of each is synchronized to this frequency. Therefore, the rotor of all interconnected synchronous machines must be in synchronism.

The physical arrangement (spatial distribution) of the stator armature winding is such that the time-varying alternating currents flowing in the three-phase windings produce a rotating magnetic field that, under steady-state operation, rotates at the same speed as the rotor. The stator and rotor fields react with each other and an electromagnetic torque results from the tendency of the two fields to align themselves. In a generator, this electromagnetic torque opposes rotation of the rotor, so that mechanical torque must be applied by the prime mover to sustain rotation. The electrical torque (or power) output of the generator is changed only by changing the mechanical torque input by the prime mover. The effect of increasing the mechanical torque input is to advance the rotor to a new position relative to the revolving magnetic field of the stator. Conversely, a reduction of mechanical torque or power input will retard the rotor position. Under steady-state operating conditions, the rotor field and the revolving field of the stator have the same

30

speed. However, there is an angular separation between them depending on electrical torque (or power) output of the generator.

An important characteristic that has a bearing on power system stability is the relationship between interchange power and angular positions of the rotors of synchronous machines. This relationship is highly nonlinear. Consider *Figure 2-4*. It consists of two synchronous machines connected by a transmission line. Let us assume that machine 1 represents a generator feeding power to asynchronous motor represented by machine 2.
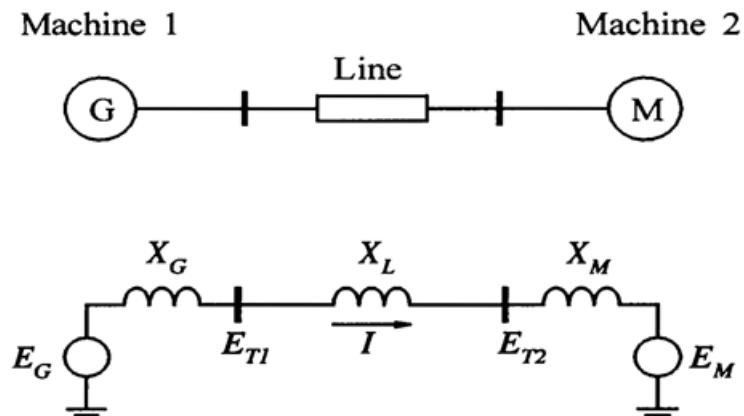
Figure 2-4 Two Machine System

As we already know, the power transferred between these machines has the following relationship:

$$P = \frac{E_G E_M}{X_T} sin\delta \qquad (2\text{-}1)$$

where, δ is the rotor angle difference between two machines and:

$$X_T = X_G + X_L + X_M \qquad (2\text{-}2)$$

The corresponding power versus angle relationship is plotted in *Figure 2-5*.

31
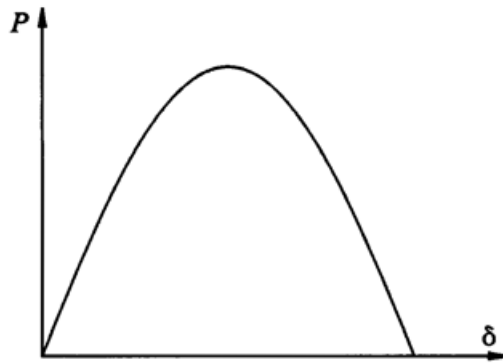
Figure 2-5 Power-angle Characteristic

So we see that the power varies as a sine of the angle: a highly nonlinear relationship. As the angle is increased, the power transfer increases up to a maximum. After a certain angle, nominally 90º, a further increase in angle results in a decrease in power transferred. There is a maximum steady-state power that can be transmitted between the two machines.

2.2.6 Stability Phenomena

Stability is a condition of equilibrium between opposing forces. The mechanism by which interconnected synchronous machines maintain synchronism with one another is through restoring forces, which act whenever there are forces tending to accelerate or decelerate one or more machines with respect to other machines. Under steady-state conditions, there is equilibrium between the input mechanical torque and the output electrical torque of each machine, and the speed remains constant. If the system is perturbed this equilibrium is upset, resulting in acceleration or deceleration of the rotors of the machines according to the laws of motion of a rotating body. If one generator temporarily runs faster than another, the angular position of its rotor relative to that of the slower machine will advance. The resulting angular difference transfers part of the load from the slow machine to the fast machine, depending on the power-angle relationship. This tends to reduce the speed difference and hence the angular separation. The power-angle relationship, as discussed above, is highly nonlinear. Beyond a certain limit, an

32

increase in angular separation is accompanied by a decrease in power transfer; this increases the angular separation further and leads to instability. For any given situation, the stability of the system depends on whether or not the deviations in angular positions of the rotors result in sufficient restoring torques.

When a synchronous machine loses synchronism or "falls out of step" with the rest of the system, its rotor runs at a higher or lower speed than that required to generate voltages at system frequency. The "slip" between rotating stator field (corresponding to system frequency) and the rotor field results in large fluctuations in the machine power output, currents, and voltage; this causes the protection system to isolate the unstable machine from the system.

Loss of synchronism can occur between one machine and the rest of the system or between groups of machines. In the latter case synchronism may be maintained within each group after its separation from the others.

The synchronous operation of interconnected synchronous machines is in some ways analogous to several cars speeding around a circular track while joined to each other by elastic links or rubber bands. The cars represent synchronous machine rotors and the rubber bands are analogous to transmission lines. When all the cars run side by side, the rubber bands remain intact. If force applied to one of the cars causes it to speed up temporarily, the rubber bands connecting it to the other cars will stretch; this tends to slow down the faster car and speed up the other cars. A chain reaction results until all the cars run at the same speed once again. If the pull on one of the rubber bands exceeds its strength, it will break and one or more cars will pull away from the other cars.

With electric power systems, the change in electrical torque of a synchronous machine following a perturbation can be resolved into two components:

$$\Delta T_e = T_s \Delta\delta + T_D \Delta\omega \qquad (2\text{-}3)$$

where

$T_s \Delta \delta$ is the component of torque change in phase with the rotor angle perturbation $\Delta \delta$ and is referred to as the synchronizing torque component; T_s is the synchronizing torque coefficient.

$T_D \Delta \omega$ is the component of torque in phase with the speed deviation $\Delta \omega$ and is referred to as the damping torque component; T_D is the damping torque coefficient.

System stability depends on the existence of both components of torque for each of the synchronous machines. Lack of sufficient synchronizing torque results in instability through an aperiodic drift in the rotor angle. On the other hand, lack of sufficient damping torque results in oscillatory instability. This is our case of interest.

We can characterize the rotor angle stability phenomena in terms of the following two categories:

> *(1)* *Small-signal (or small-disturbance) angle stability* is the ability of the power system to maintain synchronism under small disturbances. Such disturbances occur continually on the system because of small variations in loads and generation. The disturbances are considered sufficiently small for the linearization of the system equations during the analysis. Instability that may result can be of two forms: (i) steady increase in rotor angle due to lack of sufficient synchronizing torque, or (ii) rotor oscillations of increasing amplitude due to lack of sufficient damping torque. The nature of system response to small disturbances depends on a number of factors including the initial operating, the transmission system strength, and the type of generator excitation controls used. For a generator connected radially to a large power system, in the absence of automatic voltage regulators (i.e., with constant field voltage) the instability is due to lack of sufficient synchronizing torque. This results in instability through a non-oscillatory mode. With continuously acting voltage regulators (AVRs), the small-disturbance stability problem is one of ensuring sufficient damping

of system oscillations. Instability is normally through oscillations of increasing amplitude. (*Figure 2-6*)
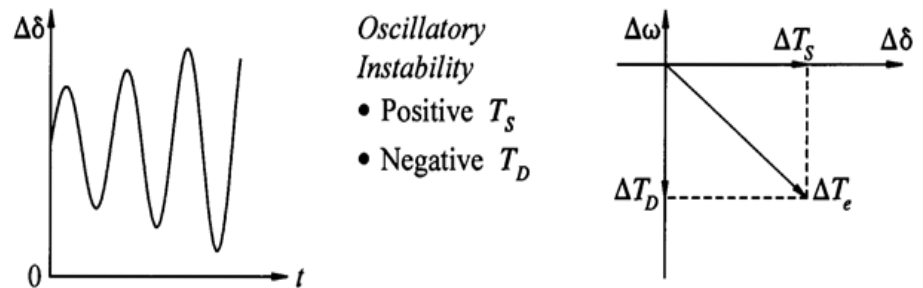
Figure 2-6 Oscillations with Excitation Control

In today's practical power systems, small-signal stability is largely a problem of insufficient damping of oscillations. So in this thesis we are interested in optimization of the mentioned oscillations by using power system stabilizers (PSSs). Later in this chapter we will see how voltage controllers can cause the increasing amplitude of oscillations, and following that we show how the usage of PSS can prevent this increment and even help to damp it sufficiently. But before that, we introduce the following types of oscillations that are of concern:

- Local modes or machine-system modes are associated with the swinging of units at a generating station with respect to the rest of power system. The term local is used because the oscillations are localized at one station or a small part of the power system.
- Inter-area modes are associated with swinging of many machines in one part of the system against machines in other parts. They are caused by two or more groups of closely coupled machines being interconnected by weak ties.

(2)   *Transient stability* is the ability of the power system to maintain synchronism when subjected to a severe transient disturbance. This is not the case for this thesis, so we do not go in details.[1]

2.3 Electromechanical Oscillations Problem in the presence of AVR

It is very important to perfectly understand the process in which we find out the necessity of utilization of *power system stabilizers*. Seeking this goal, it is useful to see some basic concepts of mechanical turbine movements and the related equations, because following that we reach the problem that is caused by the usage of AVRs, and of course the solution to the problem.

When considering free-body rotation the shaft of the synchronous machine can be assumed to be rigid when the total inertia of the rotor J is simply the sum of the individual inertias. According to Newton's second law:

$$J\frac{d_{\omega m}}{dt} + D_d\omega_m = \tau_t - \tau_e \qquad\qquad (2\text{-}4)$$

where J is the total moment of inertia of the turbine and generator rotor ($kg\ m^2$), ω_m is the rotor shaft velocity (mechanical rad/s), τ_t is the torque produced by the turbine (N m), τ_e is the counteracting electromagnetic torque and D_d is the damping-torque coefficient (Nms) that accounts for the mechanical rotational loss due to windage and friction.

Then remembering that the mechanical speed of the rotor is

$$\omega_m = \omega_{sm} + \Delta\omega_m = \omega_{sm} + \frac{d\delta_m}{dt} \qquad\qquad (2\text{-}5)$$

where δ_m is the rotor angle expressed in mechanical radians, $\Delta\omega_m = \frac{d\delta_m}{dt}$ is the speed deviation in mechanical radians per second and ω_{sm} is the synchronous speed of the rotor.

Now we can reach to a fundamental equation governing the rotor dynamics, that is, the *swing equation*

$$M_m \frac{d^2\delta_m}{dt^2} = P_m - P_e - D_m \frac{d\delta_m}{dt} \qquad (2\text{-}6)$$

where $D_m = D_d \omega_{sm}$ is the damping coefficient. Considering δ and ω_s as the electrical angle and electrical synchronous speed, respectively, we can re-write the swing equation as the following equation

$$M \frac{d^2\delta}{dt^2} = P_m - P_e - P_D = P_{acc} \qquad (2\text{-}7)$$

where P_{acc} is the net accelerating power. The time derivative of the rotor angle $\frac{d\delta}{dt} = \Delta\omega = \omega - \omega_s$ is the *rotor speed deviation* in electrical radians per second. Often it is more convenient to replace the second-order differential equation by two first-order equations:

$$M \frac{d\Delta\omega}{dt} = P_m - P_e - P_D = P_{acc}, \qquad \frac{d\delta}{dt} = \Delta\omega \qquad (2\text{-}8)$$

This equation shows that for small deviations in rotor speed the damper windings produce a damping power $P_D = D\Delta\omega$ that is proportional to the rotor speed deviation. To help explain the effect of the damper windings on the system behavior it is convenient to rewrite the swing equation,

$$M \frac{d^2\delta}{dt^2} = P_m - [P_e(\delta) + P_D], \qquad (2\text{-}9)$$

when the damping power is seen either to add to, or to subtract from, the electrical air-gap power $P_e(\delta)$ depending on the sign of the speed deviation. If $\Delta\omega < 0$, then P_D is negative, effectively opposing the air-gap power and shifting the resulting $(P_{E'} + P_D)$ characteristic downwards. If $\Delta\omega > 0$, then P_D is positive, effectively assisting the air-gap power and shifting the resultant characteristic upwards. The rotor will therefore move along a modified power–angle trajectory such as that shown in *Figure 2-7*. To help increase clarity, this diagram shows an enlarged part of the power–angle diagram in the proximity of the equilibrium point.
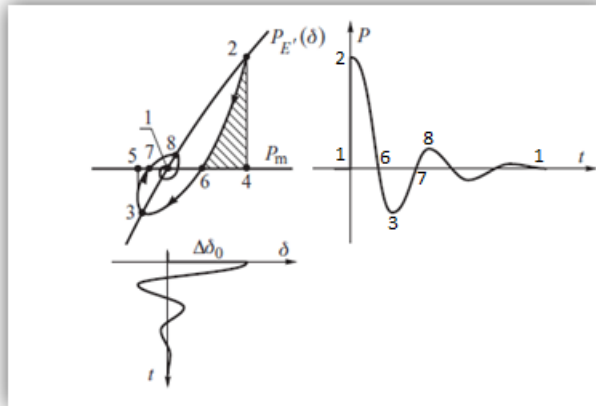
Figure 2-7 Rotor and Power Oscillations with Damping Included[2]

As before, the rotor is initially disturbed, with a stepwise change, from equilibrium point 1 to point 2. At point 2 the driving mechanical power is less than the opposing electrical power and the decelerating torque will force the rotor back towards the equilibrium point. On deceleration the rotor speed drops and P_D becomes negative, decreasing the resulting decelerating torque. The rotor therefore moves along the line 2–6 when the work done by the decelerating torque is equal to the area 2–4–6. This is less than the area 2–4–1 in *Figure 2-7* which represents the work that would have been done if no damping were present. At point 6 the rotor speed reaches a minimum and, as it continues to move along the curve 6–3, the accelerating torque counteracts further movement of the rotor and is assisted by the negative damping term. The rotor again reaches synchronous speed when the area 6–3–5 is equal to the area 2–4–6 which is achieved earlier than in the case without damping. The rotor then starts to swing back, still accelerating, so that the speed increases above synchronous speed. The damping term changes sign, becoming positive, and decreases the resulting accelerating torque. The rotor moves along the curve 3–7 and the work performed during the acceleration is equal to the small area 3–5–7. As a result the rotor reaches synchronous speed at point 8, much earlier than in the case without damping. The rotor oscillations are damped and the system quickly reaches equilibrium point 1.

Steady-state Stability of the Regulated System

This section considers steady-state stability when the action of an AVR is included. It is important for us to see the influence of the voltage regulation on the angular steady-state stability. But before that, it can be useful if we derive the modified steady-state power–angle characteristic.

Type equation here.

2.3.1 Steady-State Power-Angle Characteristic of Regulated Generator

Assuming the unregulated generator, the static power-angle characteristic, $P_{E_q}(\delta)$, can be derived considering the fact that in this condition the excitation e.m.f. is constant, $E_f = E_q = constant$. But, in practice every generator is equipped with an AVR which tries to maintain the voltage at the generator terminals constant (or at some point behind the terminals) by adjusting the value of the excitation voltage and, consequently, E_f. As the resulting formulae for the active and reactive power are more complicated than when $E_f = constant$, the following discussion will be restricted to the case of a round-rotor generator ($x_d{=}x_q$) with resistance neglected (r = 0). For this case the steady-state equivalent circuit and phasor diagram are shown in *Figure 2-8*. The coordinates of $\underline{E_q}$ in the (a, b) reference frame are:

$$E_{qa} = E_q cos\delta, \qquad E_{qb} = E_q sin\delta. \qquad (2\text{-}10)$$
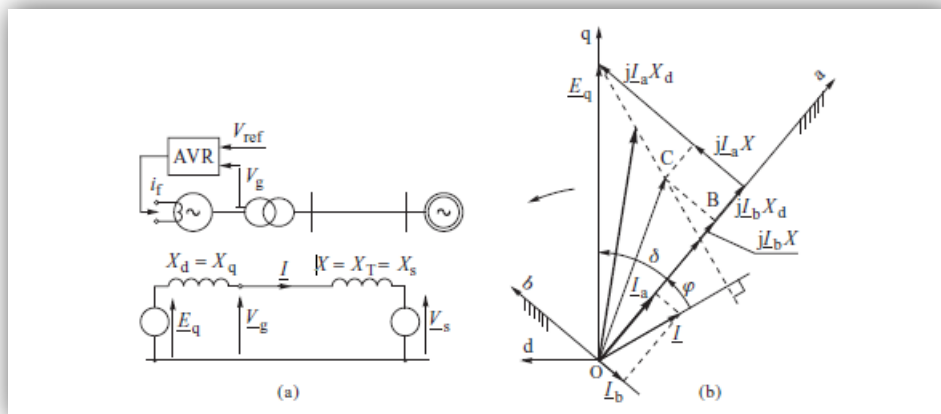
Figure 2-8 Generator Operating on the Infinite Busbars: (a) Schematic and Equivalent Circuit; (b) Phasor Diagram in the (d,q) and (a,b) Reference Frames.[2]

39

Starting from Pythagoras's theorem, we can reach the following equation:

$$(E_{qa} + \frac{X_d}{X}V_s)^2 + E_{qb}^2 = [\frac{X_d+X}{X}V_g]^2 \qquad (2\text{-}11)$$

This equation describes a circle of radius $\rho = (\frac{X_d}{X} + 1)V_g$ with center lying on the a-axis at a distance $A = -X_d V_s/X$ from the origin. This means that with $V_g = constant,$ and $V_s = costant$, the tip of E_q moves on this circle. *Figure 2-9* shows the circular locus centered on the origin made by the phasor $V_g = constant$, and another circular locus (shifted to the left) made by phasor E_q.

The circle defined by the previous equation can be transformed into polar coordinates

$$E^2_q + 2\frac{X_d}{X}E_q V_s cos\delta + (\frac{X_d}{X}V_s)^2 = [\frac{X_d+X}{X}V_g]^2. \qquad (2\text{-}12)$$

One of the roots of this equation is:

$$E_q = \sqrt{(\frac{X_d+X}{X}V_g)^2 - (\frac{X_d}{X}V_s sin\delta)^2} - \frac{X_d}{X}V_s cos\delta, \qquad (2\text{-}13)$$

which corresponds to the $E_f = E_q$ points that lie on the upper part of the circle. Substituting this equation into the round-rotor power-angle equation, gives the generated power as

$$P_{V_g}(\delta) = \frac{V_s}{X_d+X}sin\delta\sqrt{(\frac{X_d+X}{X}V_g)^2 - (\frac{X_d}{X}V_s sin\delta)^2} - \frac{1}{2}\frac{X_d}{X}\frac{V_s^2}{X_d+X}sin2\delta. \quad 2\text{-}14)$$

This equation describes the power-angle characteristic $P_{V_g}(\delta)$ with $V_g = const.$ and is shown, together with P_{E_q}, in *Figure 2-9*. A comparison between them shows that the AVR can significantly increase the amplitude of the steady-state power-angle characteristic.
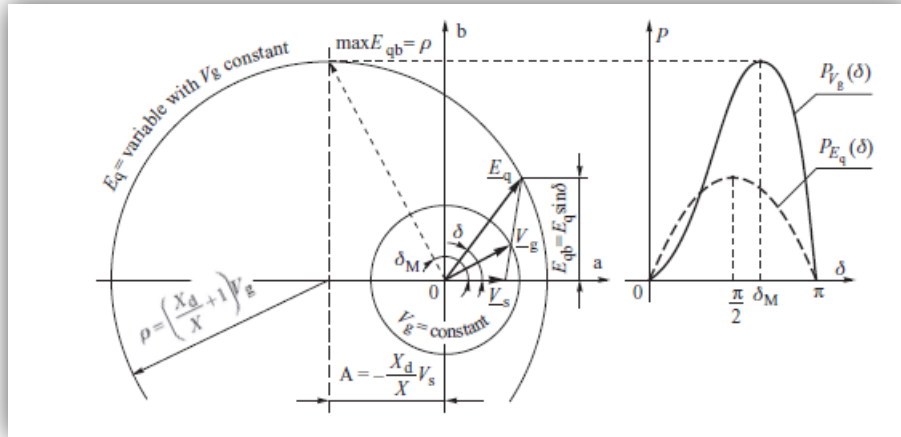
Figure 2-9 The Circle Diagrams and the Power-Angle Characteristic for the Round-Rotor Generator Operating on the Infinite Busbars

On the other hand we know that

$$P_{V_g}(\delta) = \frac{V_s}{X_d + X} E_{qb},$$
(2-15)

indicating that the generated power is proportional to the projection of E_q on the b-axis. This function reaches its maximum value when E_{qb} is a maximum. As it can be seen from the *Figure 2-9*, this occurs at the point on the E_q locus that corresponds to the center of the circle. So the corresponding angle is δ_M.

The angle δ_M at which $P_{V_g}(\delta)$ reaches maximum is always greater than $\frac{\pi}{2}$ irrespective of the voltages V_s and V_g. This is typical of systems with active AVRs.

$$P_{V_gM} = P_{V_g}(\delta) \Big|\delta = \delta_M = \frac{V_g V_s}{X},$$
(2-16)

showing that the amplitude of the power-angle characteristic of the regulated system is independent of the generator reactance. It does, however, depend on the equivalent reactance of the transmission system. The steady-state synchronizing power coefficient of the regulated system is $K_{V_g} = \frac{\partial P_{Vg}(\delta)}{\partial \delta}$ and $K_{V_g} > 0$ when $\delta < \delta_M$.

41

The $sin2\delta$ component in the equation of power-angle characteristic has negative sign, making the maximum of the $P_{V_g}(\delta)$ characteristic shown in *Figure 2-9* occur at $\delta_M > \frac{\pi}{2}$. For small rotor angles $\delta \ll \frac{\pi}{2}$ the characteristic is concave, while for $\delta > \frac{\pi}{2}$ the characteristic is very steep. The $\sin 2\delta$ component has nothing to do with the reluctance power (as the case with $P_{E_q}(\delta)$) because the equation of power-angle characteristic has been derived assuming $x_d = x_q$. The distortion of the characteristic is entirely due to the influence of the AVR.

Physically the shape of the $P_{V_g}(\delta)$ characteristic can be explained using *Figure 2-10*. Assume that initially the generator operates at point 1 corresponding to the characteristic shown by the dashed curve 1. An increase in the generator load causes an increase in the armature current, an increased voltage drop in the equivalent network reactance X, *Figure 2-8*, and therefore a decrease in the generator voltage V_g. The resulting voltage error forces the AVR to increase the excitation voltage so that E_q is increased to a value $E_{q2} > E_{q1}$ and a new operating point is established on a higher characteristic $P_{E_{q2}} = P_{E_q}(\delta)|E_q = E_{q2}$ denoted by 2. Subsequent increases in load will cause the resulting $P_{V_g}(\delta)$ characteristic to cross at the points 2, 3, 4, 5 and 6 lying on consecutive $P_{E_q}(\delta)$ characteristics of increased amplitude. Note that starting from point 5 (for $\delta > \pi/2$) the synchronizing power coefficient $K_{E_q} = \frac{\partial P_{E_q}(\delta)}{\partial \delta}$ is negative while $K_{V_g} = \frac{\partial P_{V_g}(\delta)}{\partial \delta}$ is still positive.
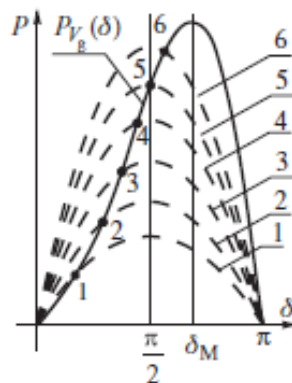
Figure 2-10 Creation of the $P_{V_g}(\delta)$ Characteristic from a Family of $P_{E_q}(\delta)$ Characteristics.

If the AVR is very slow acting (i.e. it has a large time constant) then it may be assumed that following a small disturbance the AVR will not react during the transient state and the regulated and unregulated systems will behave in a similar manner. The stability limit then corresponds to point 5 when $\delta = \pi/2$ (for a round-rotor generator). If the AVR is fast acting so that it is able to react during the transient state, then the stability limit can be moved beyond $\delta = \pi/2$ to a point lying below the top of the $P_{V_g}(\delta)$ curve. In this case stability depends on the parameters of the system and the AVR, and the system stability is referred to as *conditional stability*.

A fast-acting AVR may also reverse the situation when the stability limit is lowered (with respect to the unregulated system) to a point $\delta < \pi/2$, for example to point 4, or even 3, in *Figure 2-10*. In this situation the system may lose stability in an oscillatory manner because of the detrimental effect of the AVR. Such a situation, and the conditional stability condition, will be discussed later in this section. And here is the reason that using the AVR leads us to use PSS to compensate effect of AVR.

Effect of AVR Action on Damper Winding

As shown before in the swing equation one component is $P_D = D\Delta\omega$, that corresponds to the damping power introduced by the damper windings. Remember that a change in the rotor angle δ result in the speed deviation $\Delta\omega$. According to Faraday's law, an emf is induced which is proportional to the speed deviation. The current driven by this emf interacts with the air-gap flux to produce a torque referred to as the *natural damping torque*. To simplify considerations, only the d-axis damper winding will be analyzed.

Figure 2-11a, shows a phasor diagram for the d-axis damper winding, similar to that shown in *Figure 2-10*. The emf induced in the winding $e_{D(\Delta\omega)}$ is shown to be in phase with $\Delta\underline{\omega}$. The damper winding has a large resistance, which means that the current due to speed deviation, $i_{D(\Delta\omega)}$, lags $e_{D(\Delta\omega)}$ by an angle less than $\pi/2$. The component of this current which is in-phase with $\Delta\underline{\omega}$ gives rise to the natural damping torque. The quadrature component, which is in phase with $\Delta\underline{\delta}$, enhances the synchronizing power coefficient.

Now consider the influence of the AVR on the damper windings. The d-axis damper winding lies along the path of the excitation flux produced by the field winding.

43

This means that the two windings are magnetically coupled and may be treated as a transformer *Figure 2-11b*, supplied by $\underline{\Delta E}_f$ and loaded with the resistance R_D of the damper winding. Consequently, the additional current $i_{D(\Delta E_f)}$ induced in the damper winding must lag $\underline{\Delta E}_f$. *Figure 2-11c* shows the position of phasors. The horizontal component of $i_{D(\Delta E_f)}$ directly opposes the horizontal component of $i_{D(\Delta \omega)}$. As the former is due to the AVR while the latter is due to speed deviation and is responsible for the natural damping, it may be concluded that voltage regulation weakens the natural damping. This weakening effect is referred to as *artificial damping*.

Artificial damping is stronger for larger $i_{D(\Delta E_f)}$ currents. This current is, in turn, proportional to the variations in $\underline{\Delta E}_f$ and $\Delta \underline{V}$ caused by $\Delta \underline{\delta}$. Some of the factors influencing this effect were described in the previous subsection and are: generator load, reactance of the transmission network and gain of the voltage controller.
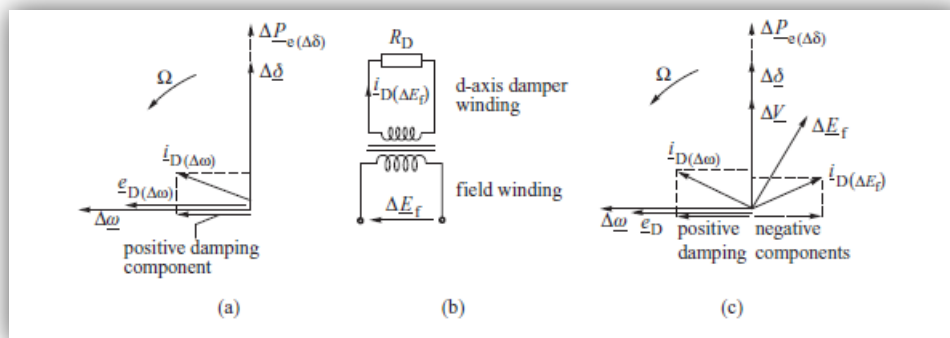
Figure 2-11 Phasor Diagram of Increasing Oscillating with the Swing Frequency Ω (in rad/s) for the Damper Windings: (a) Natural Damping Only; (b) Field and Damper Windings as a Transformer; (c) Natural and Artificial Damping

The main conclusion from the previous sections is that a voltage controller, which reacts only to the voltage error, weakens the damping introduced by the damper and field windings. In the extreme case of a heavily loaded generator operating on a long transmission link, a large gain in the voltage controller gain may result in net negative damping leading to an oscillatory loss of stability. This detrimental effect of the AVR can be compensated using a supplementary control loop referred to as a *power system*

stabilizer (PSS), which is our main field of interest in this thesis, as we will discuss different techniques for PSS tuning in the next chapter.

3 Techniques for PSS Tuning

As it was discussed in the previous chapter, an inadequate excitation control (AVR), as a wrong choice of its parameters setting, can lead to instability conditions that appears as growing oscillations of electrical and mechanical turbine-generator variables. Such oscillations can reach amplitudes so high to prevent the operation of the unit in the working point under consideration. In contrast, a correct excitation control, together with a proper fine-tuning of the regulation parameters, in particular the parameters of the additional power system stabilizer (PSS) for damping the electromechanical oscillations, can ensure a stable operation of the generator and adequate dynamic responses across the full allowable working range and for all the normal network conditions.

In contrast, a correct excitation control, together with a proper fine-tuning of the regulation parameters, in particular the parameters of the additional power system stabilizer for damping the electromechanical oscillations, can ensure a stable operation of the generator and adequate dynamic responses across the full allowable working range and for all the normal network conditions.

It is possible to conduct stability analysis through the calculation of system eigenvalues and the study of the dependence of their location on the complex plan, depending on units operating point and AVR and PSS parameters. A particular and important point of view for stability analysis is the phase evaluation of transfer function between some system variables. The crucial feature is the availability of different optimization procedures capable to determine, in the excitation control of synchronous generators, the most appropriate calibration of the gains of additional stabilizing feedbacks in order to achieve an adequate damping of electromechanical oscillations.

To understand the methods of PSS tuning it is useful to see the model definition of power system elements for different frequencies of oscillations. But before that there is a

short discussion about eigenvalue analysis that is the basic technique, used in this thesis, to observe both the frequency modes which have increasing amplitude of oscillations (oscillatory instability) and the effect of different power plants on those modes. Therefore *eigenvalue analysis* is a kind of tool for our case of study, and it is discussed in this chapter, because well understanding of the concepts behind different PSS tuning techniques is effectively dependent on having enough knowledge about eigenvalue analysis.

It is worth mentioning that the main software -to analyze the electromechanical cycle and then to find the best optimization technique- used in this thesis is ALICE, that is a software package developed by CESI and Terna in MATLAB®, that creates an integrated environment for linearized analysis of the electromechanical cycle. ALICE uses data of synchronous generators AVRs and PSSs to build a model of the power plant-network system.

3.1 Eigenvalue Analysis

As we know the disturbances in a power system can be of two kinds: small or large. After having any kind of disturbances, the system is in its dynamic state, and we are interested to study the stability of the system in this condition. Stability after a large disturbance is called *large perturbation stability* and following a small disturbance is *small perturbation stability*. Since our focus is just on small disturbances, we need to find a method that is optimized for this condition. Eigenvalue and modal analysis describe the small signal behavior of the system – the behavior linearized around one operating point – and do not take into account the non-linear behavior of, for instance, controllers during large perturbations. Therefore, time domain simulation and modal analysis in the frequency domain complete each other in the analysis of power systems.

Table 3-1 Stability Studies

Large perturbation Stability	Small perturbation Stability
dynamic transition	dynamic transition
from one working point to another	around an operating point
non-linear	linear

Eigenvalue analysis investigates the dynamic behavior of a power system under different characteristic frequencies ("modes"). In a power system, it is required that all modes be stable. Moreover, it is desired that all electromechanical oscillations be damped out as quickly as possible. The results of an Eigenvalue analysis are given as frequency and relative damping for each oscillatory mode.

3.1.1 Linear Stability Analysis

Equilibria are not always stable. Since stable and unstable equilibria play quite different roles in the dynamics of a system, it is useful to be able to classify equilibrium points based on their stability.

Suppose that we have a set of autonomous ordinary differential equations, written in vector form:

$$\dot{x} = f(x) \qquad (3\text{-}1)$$

Suppose that x^* is an equilibrium point. By definition, $f(x^*) = 0$. Now suppose that we take a multivariate Taylor expansion of the right-hand side of our differential equation:

$$\dot{x} = f(x^*) + \frac{\partial f}{\partial x}\bigg|x^* (x - x^*) + \cdots$$

$$= \frac{\partial f}{\partial x}\bigg|x^* (x - x^*) + \cdots \qquad (3\text{-}2)$$

The partial derivative in the above equation is to be interpreted as the **Jacobian matrix**. If the components of the state vector **x** are $(x_1, x_2, \ldots, x_n)$ and the components of the rate vector **f** are $(f_1, f_2, \ldots, f_n)$, then the **Jacobian** is:

$$\boldsymbol{J} = \begin{bmatrix} \dfrac{\partial f_1}{\partial x_1} & \dfrac{\partial f_1}{\partial x_2} & \cdots & \dfrac{\partial f_1}{\partial x_n} \\ \dfrac{\partial f_2}{\partial x_1} & \dfrac{\partial f_2}{\partial x_2} & \cdots & \dfrac{\partial f_2}{\partial x_n} \\ \vdots & \vdots & \cdots & \vdots \\ \dfrac{\partial f_n}{\partial x_1} & \dfrac{\partial f_n}{\partial x_2} & \cdots & \dfrac{\partial f_n}{\partial x_n} \end{bmatrix} \qquad (3\text{-}3)$$

Now defining $\Delta x = x - x^*$ and taking a derivative of this definition, we get $\Delta \dot{x} = \dot{x}$. If Δx is small, then only the first term in the above equation is significant since the higher terms involve powers of our small displacement from equilibrium. If we want to know how trajectories behave *near* the equilibrium point, e.g. whether they move toward or away from the equilibrium point, it should therefore be good enough to keep just this term. Then we have

$$\Delta \dot{x} = \boldsymbol{J}^* \Delta x \qquad (3\text{-}4)$$

where $\boldsymbol{J}^*$ is the Jacobian evaluated at the equilibrium point. The matrix $\boldsymbol{J}^*$ is a constant, so this is just a linear differential equation. According to the theory of linear differential equations, the solution can be written as a superposition of terms of the form $e^{\lambda_j t}$ where $\{\lambda_j\}$ is the set of eigenvalues of the Jacobian.

The eigenvalues of the Jacobian are, in general, complex numbers. Let $\mu_j + i v_j$, where μ_j and v_j are, respectively, the real and imaginary parts of the eigenvalue. Each of the exponential terms in the expansion can therefore be written as

$$e^{\lambda_j t} = e^{\mu_j t} e^{i v_j t} \qquad (3\text{-}5)$$

The complex part of the eigenvalue therefore only contributes an oscillatory component to the solution. It's the real part that matters: If $\mu_j > 0$ for any j, $e^{\mu_j t}$ grows with time, which means that trajectories will tend to move away from the equilibrium point. This leads us to a very important theorem:

Theorem 1 *An equilibrium point x^* of the differential equation 1 is stable if all the eigenvalues of J^*, the Jacobian evaluated at x^*, have negative real parts. The equilibrium point is unstable if at least one of the eigenvalues has a positive real part.*

Because we are only keeping a locally linear approximation to the vector field, an analysis based on this theorem is called a linear stability analysis.

Note that the theorem is silent on the issue of what happens if some of the eigenvalues have zero real parts while the others are all negative. This case can't be decided based on linear stability analysis. The nonlinear terms we left out of equation 2 in fact determine the stability in this case. Dealing with this case requires a nonlinear theory which we do not discuss here.

In the following there is a *Figure 3-1* summarizing the visual representations of stability that the eigenvalues represent:
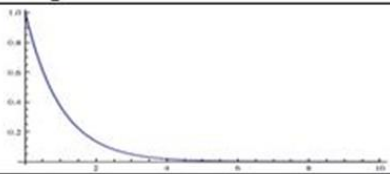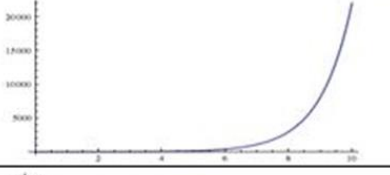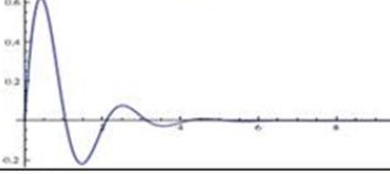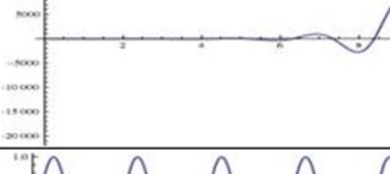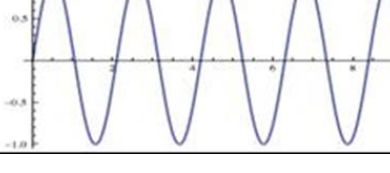
Eigenvalues	Graph
All real and negative	
All real and one or more are positive	
All real eigenvalues are negative and there are imaginary parts	
One or more eigenvlaues have a positive real part and there are imaginary parts	
Real parts of the eigenvlaues are zero and there are imaginary parts	

Figure 3-1 Stability Representation with Eigenvalues

3.2 Model Definition

3.2.1 Type of Electromechanical Oscillation Modes

Electromechanical oscillations affecting power systems are reported in range 0.1-2 Hz and divided in two types:
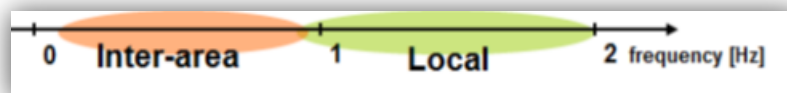
Figure 3-2 Types of electromechanical oscillation modes.

- **Local Oscillations:** they concern single (or coherent group of) machines against the rest of the system (usually 1-2 Hz).
- **Inter-area Oscillations:** they are dynamic modes typically between coherent groups of generators (usually 0.1-1 Hz).

For both the types of oscillations, damping depends on the operating point of the units (i.e. actual power flows, reactive point on the capability plan), as well as on the external lines conditions (i.e. network meshing, lack of interconnections).

We want to analyze stability of the power plant-network system both in local and in inter-area frequency interval, evaluating damping of oscillation modes and tuning of PSS according to the typical damping objectives.
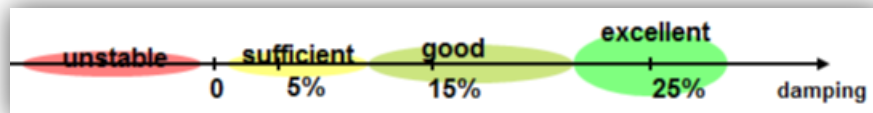
Figure 3-3 Oscillations damping evaluation scale

3.2.2 Local Oscillation Modes Modelling

To analyze the interaction between the turbine-alternator and the network it is possible to build a model where a synchronous generator is connected with an infinite power network through an equivalent reactance.
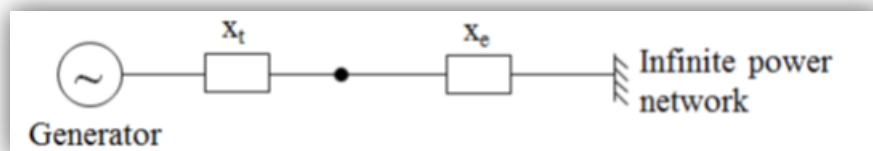
Figure 3-4 Model representation of a synchronous generator connected with an infinite power network.

It is how ALICE models the network for analyzing the local oscillation modes. Because PSS works based on a feedback control loop, it is useful to model the whole

power plant, including synchronous generator, AVR and PSS, with equivalent block diagrams.

The system modelling is organized into different modules, so it's quite easy to change the models of AVR and PSS or to create a custom model as close as possible to the real one. Into this linearized environment the user can analyze the electromechanical cycle and verify the behavior of the generator towards the local oscillation modes.
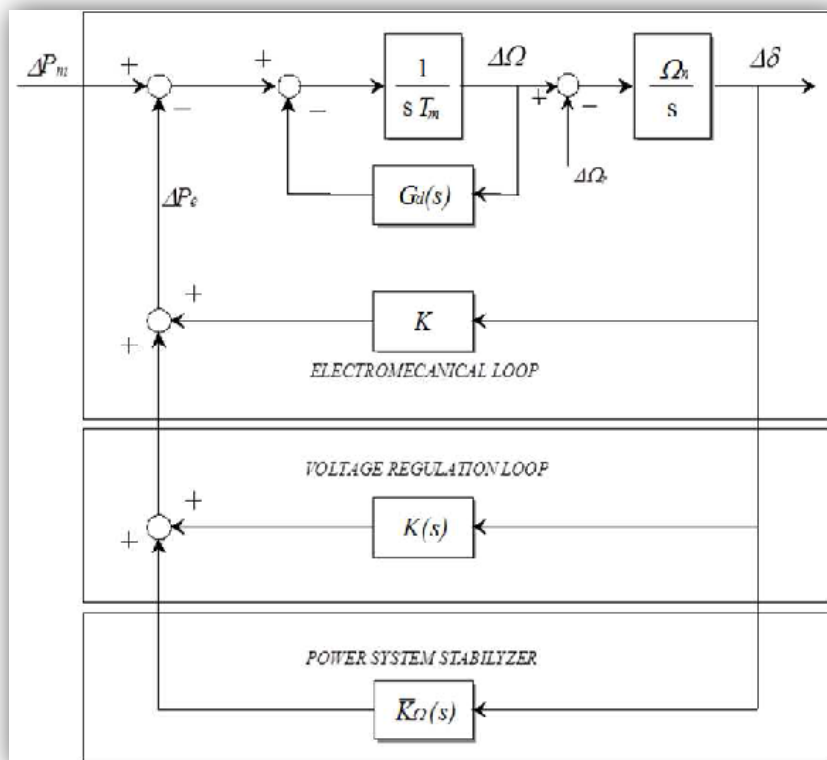
Figure 3-5 Block diagram of the control model of a synchronous generator with AVR and additional PSS

Using the same model of the generators, it's also possible to simulate a small network where the different machines are connected by equivalent reactances and loads.
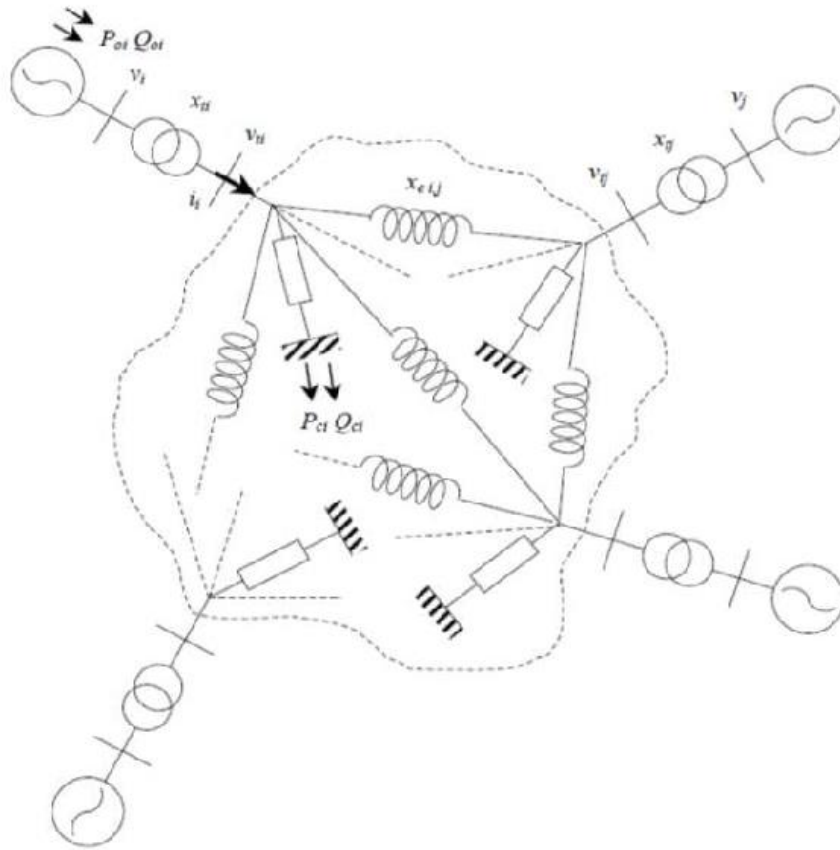
Figure 3-6 Representation of the multi-machine model

Furthermore in a multi-machine environment there are not only local oscillation modes, but also inter-area oscillations ones, determined by the units parameters and by the connection lines between different generators.

3.2.3 Inter-area Oscillation Modes Modelling

The generic multi-machine model available in ALICE can be specifically tailored to simulate a particular inter-area mode that affects a generator. The objective is reached calculating the parameters of the loads and the values of the reactance necessary to obtain the desired frequency and damping.
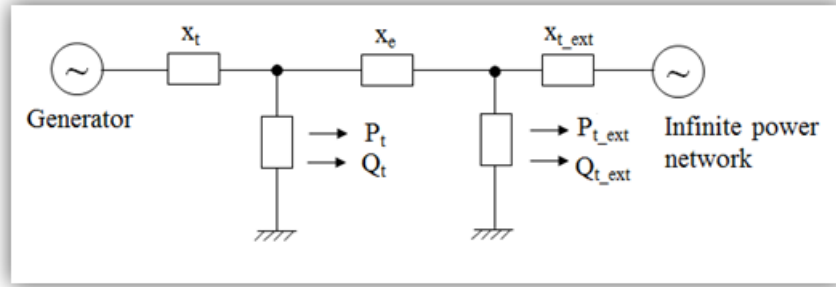
Figure 3-7 Model representation capable to simulate a particular inter-area mode that affects a generator

In the configuration shown in *Figure 3-7*, all the parameters of the plant remain unchanged and the variables to be calibrated are:

- *Xe*: the external reactance determines the length of the "rope" that connects the power plant and the dominant network, its value decreases with the increase of the system oscillation frequency.
- *Pto*: (the initial value of P_t) the active power absorbed by the load in the operating point (the reactive powers are determined by the load flow solution), its value increases with the increase of the system oscillation damping.

This model changes only the connection parameters (*Xe, Pto*) with the external network, so it could be very useful to evaluate the behavior of the generator towards inter-area modes.

3.3 Stability Analysis Criteria

To evaluate the stability of the linearized system, ALICE allows two possible approaches; a) the analysis of the system eigenvalues position in the complex plan; b) the analysis of the transfer function phase between some system variables.

3.3.1 **Precise Criterion: Analysis of Eigenvalues Position in the Complex Plan**

The simplest technique to evaluate the stability of a system is to observe the position of its eigenvalues in the complex plan, ensuring that all of them are located in the left part and, in particular, on the left of the two half-lines which represent the minimum acceptable damping (i.e. 20%). This criterion gives an overview of the stability of the system in the operating point under consideration, for example:
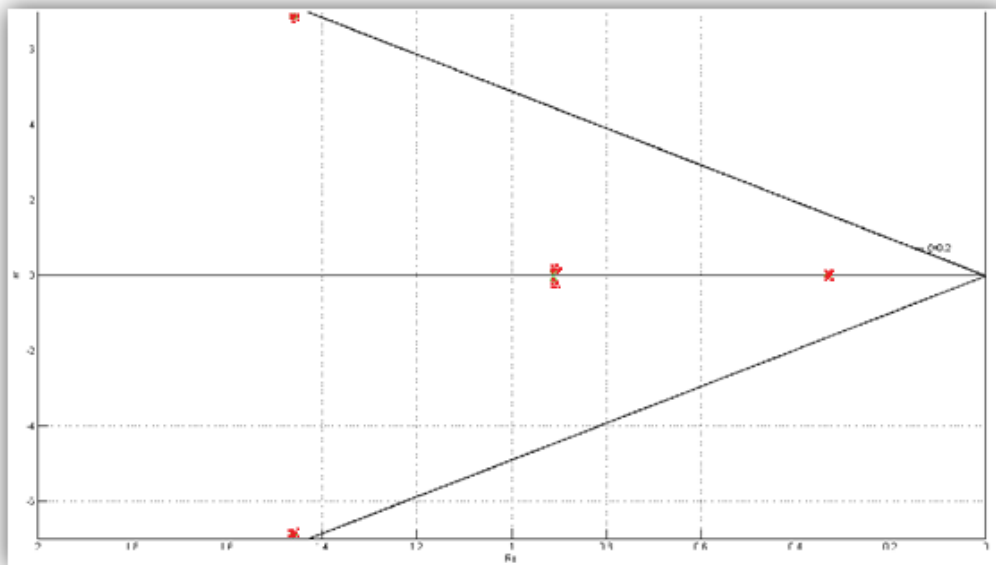
Figure 3-8 Representation of system eigenvalues and minimum acceptable damping in the complex plan.

3.3.2 **Simplified Criterion: Analysis of Transfer Function Phase Between Some System Variables**

This criterion analyses the phase of a certain number of open-loop transfer functions among some system variables; the most significant of them is the one between unit speed and electrical active power. This method is not as precise as the previous one, but reveals to be very useful for evaluating the effectiveness of PSS parameterization. The objective of the optimization of the PSS, in fact, can also be expressed by saying that this must be calibrated so that its phase contribution is sufficient to compensate, totally or at least in part, the phase difference between speed and electric active power. In particular, this compensation should be effective in the electromechanical oscillations frequency

range (0.1-2 Hz) to smooth them. As shown in *Figure 3-9* the compensation can be considered satisfying when the phase of the transfer function is between +/-30° around 0° in the band of interest.
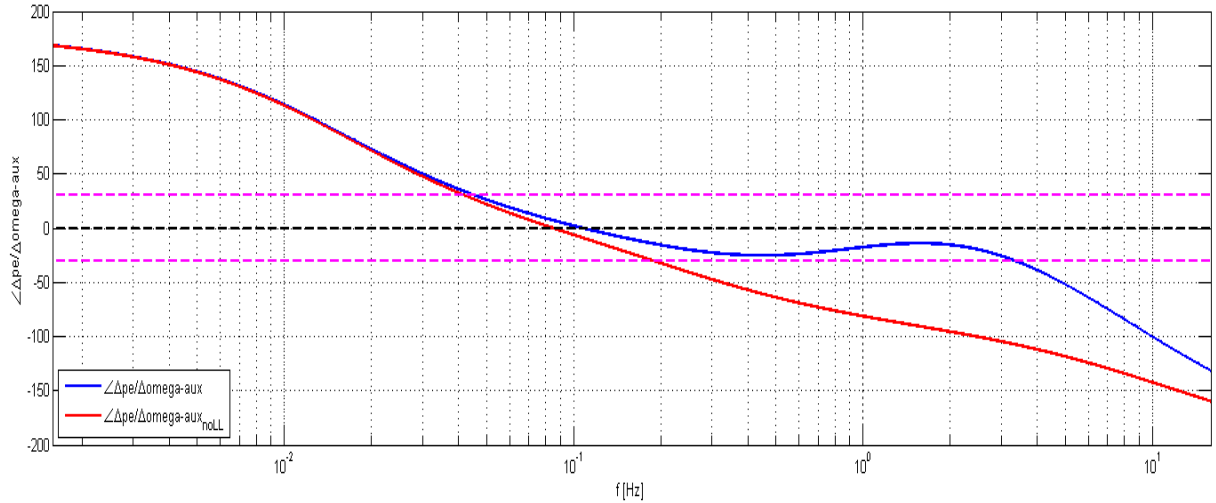
*Figure 3-9 Phase of the open-loop transfer function phase
between speed and electrical active power (in this example
the compensation can be considered satisfying).*

3.4 PSS Optimization Methods

For stabilizers calibration, different methods are available in ALICE, so it is possible to have different options to improve system stability. Depending on the situation (i.e. position of the power plant in the network, measurements accuracy, typical points of operation, etc.) and, in particular, on AVR and PSS models, one of them can be better than the others. For a more detailed explanation and formulas, about the following methods, the reader can refer to [11].

3.4.1 Residuals Method on Double Feedback PSS

This technique aims to optimize stabilizers gains searching a compromise between the requirements of stability and energy containment associated with the control stabilizing

signal called $v_{feedback}$ or v_{ret} in Italian.[1] This setting guideline is influenced also by the need to limit the measurement noises introduced through the additional feedbacks in the voltage loop. There is the need to identify the criteria for the analytical determination of the "optimal" gains and it is possible to use only one feedback channel or a couple of them (K_p for electrical power channel with K_f for frequency channel or K_w for speed channel) for the optimization. A cost function can be defined as follows:

$$J(K_p, K_f) = K_p^2 + \alpha^2 * K_f^2 \qquad (3\text{-}6)$$

The function J in (3-6) represents the weight of each feedback channel according to value α which is defined later. This function can be minimized leading to a choice of "optimal" gains in compliance with a constraint that imposes a satisfying value of the electromechanical damping. In other words, it moves the eigenvalues of the electromechanical system from the original position (λ, λ^*) - without stabilizing feedbacks - to the new location $(\lambda_{ott}, \lambda_{ott}^*)$ - characterized by the desired damping value (ξ_{ott}). The determination of the optimal gains can be entrusted to an iterative procedure that aims to place the electromechanical eigenvalues associated in the left-half plan defined by the half-lines representing the minimum acceptable damping. Firstly it is needed to identify residues which are associated with complex eigenvalues:

$$G_P^i(s) = \frac{\Delta P_e}{\Delta v_{ret}} = \cdots + \frac{C_P^i}{s - \lambda^i} + \frac{C_P^{i^*}}{s - \lambda^{i^*}} + \cdots \qquad (3\text{-}7)$$

$$G_f^i(s) = \frac{\Delta f}{\Delta v_{ret}} = \cdots + \frac{C_f^i}{s - \lambda^i} + \frac{C_f^{i^*}}{s - \lambda^{i^*}} + \cdots \qquad (3\text{-}8)$$

where the superscript i indicates the initial values of variables' gains of stabilizing feedback and transfer function, P_e is the electrical power, v_{ret} is the feedback voltage, s is the Laplace variable, λ is the eigenvalue or poles of $G(s)$ and C is the corresponding residue. The displacement of the pair of electromechanical eigenvalues (λ_i, λ_i^*) from the original position to the optimal one:

$$\lambda_{ott} = \rho_{ott} * (-\xi_{ott} + j\sqrt{1 - \xi_{ott}^2}), \quad \lambda_{ott}^* = \rho_{ott} * (-\xi_{ott} - j\sqrt{1 - \xi_{ott}^2}) \qquad (3\text{-}9)$$

---

[1] due to using ALICE in this thesis, the Italian symbols and abbreviations are used

is obtained by applying an appropriate change to the gains. The deviation of K_p and K_f can be determined by evaluating the sensitivity of the eigenvalues of the dynamic system using the following approximate expression:

$$\Delta\lambda = \lambda_{ott} - \lambda^i = -\left(\rho_{ott}\xi_{ott} + \sigma^i\right) + j\left(\rho_{ott}\sqrt{1 - \xi_{ott}^2} - w^i\right)$$

$$\cong -C_P^i \Delta K_p + C_f^i \Delta K_f \qquad\qquad (3\text{-}10)$$

and separating the equalities written in real and imaginary components, a linear expression of ΔK_p and ΔK_f is obtained depending on the parameter ρ_{ott}. These expressions are substituted in the function (3-6) of which the minimum is sought by requiring the cancellation of the derivative part with respect to ρ_{ott}, then the value of ρ_{ott} allows to identify the optimal gains of the stabilizing feedback. Due to the simplifications introduced in equation (3-9), it is necessary to iterate the procedure, because its validity is limited to small deviations of K_p and K_f, defining an appropriate test to evaluate the optimal convergence of the solution obtained in every iteration. If the coefficient α is set equal to the modules of the residues associated with eigenvalues of the electromechanical transfer function $G_P(s)$ and $G_f(s)$ defined in absence of feedback stabilizers, the function in (3-6) is directly proportional to the energy associated with stabilizing signal v_{ret}.

In the multi-machine case, the stabilizing signal v_{ret}, acting on a machine has also effect on other generators: thus, the system is characterized by complex residues matrices. So a new quadratic cost function can be defined:

$$\min(0.5x'\mathbf{H}x + f'x) \quad \text{with} \quad \mathbf{A}x \leq \mathbf{B} \qquad\qquad (3\text{-}11)$$

where H is an identity matrix of size NxN (where N is the generators number), if it is used only one feedback channel for stabilization, vice-versa is a $2Nx2N$ diagonal matrix whose generic element $H(i,i)$ is defined by:

$$H(i,i) = \begin{cases} \dfrac{1}{\sum_{j=1}^{N} C_P^2(i,j)} & if \quad 1 \leq i \leq N \\[4mm] \dfrac{1}{\sum_{j=1}^{N} C_f^2(1,j)} & if \quad N+1 \leq i \leq 2N \end{cases} \qquad (3\text{-}12)$$

$C_P(i,j)$ is the residue associated with $i'th$ electromechanical eigenvalue and the $j'th$ stabilizing signal. The vector f is unitary if it's used only one feedback channel for stabilization; vice-versa introduces a normalization of optimized gains. Finally the vector x contains the gains and the terms A and B, which define the constraints of the problem, given by the equation:

$$\left| \sqrt{1 - \xi_{ott}^2} \cdot Re(C_P') - \xi_{ott} \cdot Im(C_P') \right| \cdot \Delta K_P \leq \left| \sqrt{1 - \xi_{ott}^2} \cdot Re(\lambda) - \xi_{ott} \cdot Im(\lambda) \right|$$

(3-13)

3.4.2 Lead-lags Method on Single Feedback PSS

This method optimizes the gain and lead-lags time constants for one feedback channel; it is very useful when only one input of PSS is available or one of the input measurement is not enough accurate. For simplicity here the speed channel is considered and the lead-lags time constants T_1 (the zero) and T_2 (the pole); the procedure is the same for the other two channels (electric power and frequency). This methods is iterative like the previous, even if, in this case, it's necessary to optimize not a gain, but the transfer function that is:

$$K_w \cdot \frac{(1 + jwT_1)}{(1 + jwT_2)} \qquad (3\text{-}14)$$

So (3-10) becomes:

$$\Delta\lambda = \lambda_{ott} - \lambda^i = -\left(\rho_{ott}\xi_{ott} + \sigma^i\right) + j\left(\rho_{ott}\sqrt{1 - \xi_{ott}^2} - w^i\right)$$

$$\cong C_w^i \cdot \Delta\left(K_w^i \cdot \frac{\left(1 + jwT_1^i\right)}{\left(1 + jwT_2^i\right)}\right)$$

$$= C_{wK}^i \Delta K_w + C_{wT1}^i \Delta T_1 + V_{wT2}^i \Delta T_2 \qquad (3\text{-}15)$$

Having to calculate the three contributions due to the gain and time constants by calculating:

$$\Delta\left(K_w^i \frac{\left(1+jwT_1^i\right)}{\left(1+jwT_2^i\right)}\right) = \Delta K_w \cdot \left[\frac{(1+jwT_1)}{(1+jwT_2)}\right] + K_w \cdot \Delta \left[\frac{(1+jwT_1)}{(1+jwT_2)}\right]$$

$$= \Delta K_w \cdot \left[\frac{(1+jwT_1)}{(1+jwT_2)}\right] + \Delta T_1 \cdot \left[\frac{jwK_w}{(1+jwT_2)}\right] + \Delta T_2 \cdot \left[\frac{j.w.(1+jwT_1)K_w}{(1+jwT_2)^2}\right] \qquad (3\text{-}16)$$

Equating real and imaginary parts separately we obtain two equations, but another one is necessary, because there are three unknown variables. So, in order to maximize the contribution of lead-lags filters at the electromechanical oscillation pulse ($w_\circ$), while leaving as much as possible PSS transfer function phase the same in the rest of the spectrum, we chose to center the pole-zero pair precisely around $w_\circ$.

This constraint is expressed by:

$$\sqrt{(T_1 + \Delta T_1)(T_2 + \Delta T_2)} = \frac{1}{w_\circ} \qquad (3\text{-}17)$$

There are cases where the contribution of a single lead-lag filter could not be sufficient; it is therefore possible to optimize a transfer function which includes two lead-lags in cascade. Following the same principle used to write equation (3-17), the chain of two filters is constructed as a double multiplicity filter centered around $w_\circ$, namely:

$$K_w \frac{(1+jwT_1)}{(1+jwT_2)} \cdot \frac{(1+jwT_3)}{(1+jwT_4)} = K_w \frac{(1+jwT_1)^2}{(1+jwT_2)^2} \qquad (3\text{-}18)$$

where T_3 and T_4 are respectively the time constants for the zero and the pole of the second lead-lags filter. Using two lead-lags the equations for residues calculation are modified, but the optimization procedure remains unchanged.

This optimization technique is very useful also when the residual method using a couple of channel for stabilization is not able to reach the desired damping value. In this case, in fact, it's possible to fix the value of one of the gains calculated by the residual method and to apply lead-lags calibration on the other channel.

3.4.3 Lead-lags Method for Inter-area Mode Damping

In real cases could happen that the measurement of frequency and/or speed is not accurate or that the gain necessary to damp oscillation is too high. In this situation ALICE can optimize electric power channel gain and lead-lags to replace the contribution of frequency or speed channel and to aid inter-area mode damping. Assuming the use of one lead-lag filter, the stabilizing signal can be expressed as:

$$v_{ret} = -K_p K_s \frac{1+sT_1}{1+sT_2} P_e = K_P K_s \left(\frac{T_1}{T_2} + \frac{1-\frac{T_1}{T_2}}{1+sT_2} \right) P_e \qquad (3\text{-}19)$$

where K_s is the global gain of the PSS, after the algebraic sum of all inputs. Considering that:

$$P_e = -2Hsw \qquad (3\text{-}20)$$

where H is the inertia constant of the unit under consideration, s is showing the Laplacian domain, thus, the second term of the third member of equation (3-19) becomes:

$$K_{weq}w = 2K_P K_s Hs(\frac{1-\frac{T_1}{T_2}}{1+sT_2})w \qquad (3\text{-}21)$$

showing the equivalent gain K_{weq} on speed channel. Then, by choosing:

$$sT_2 \gg 1 \qquad (3\text{-}22)$$

that is:

$$T_2 \gg \frac{1}{w_\circ} \qquad (3\text{-}23)$$

where $w_\circ$ is the electromechanical oscillation pulse to damp. Therefore we can assert that the overall gain on electric power channel (that remains unchanged) and the equivalent gain on speed channel are:

$$\begin{cases} K_{peq} = K_P K_S \dfrac{T_1}{T_2} = K_P \\ K_{weq} = \dfrac{K_P K_S 2H\left(1-\frac{T_1}{T_2}\right)}{T_2} \end{cases} \qquad (3\text{-}24)$$

So we have:

$$\begin{cases} K_S \dfrac{T_1}{T_2} = 1 \\ K_S = 1 + \dfrac{T_2}{2.H} \dfrac{K_{weq}}{K_P} \end{cases} \qquad 3\text{-}25)$$

and the equations necessary to design the lead-lag filter are:

$$\begin{cases} T_2 \gg \dfrac{1}{w_\circ} \\ K_S = 1 + \dfrac{T_2}{2H} \dfrac{K_{weq}}{K_P} > 1 \\ T_1 = \dfrac{T_2}{K_S} < T_2 \end{cases} \qquad 3\text{-}26)$$

It is possible to implement the dual method where the use of lead-lags of frequency or speed channel replaces the contribution of the electric power channel, which is the same objective of the technique described in 4.2.

3.4.4 Quadratic Programming Method

Finally, to develop another technique for gain and lead-lag time constants optimization, we can exploit the quadratic programming used for the residual method in the multi-machine situation. Differing from the technique described in 3.4.2, in this case it is not either required that pole and zero lags of leads are centered on the electromechanical oscillation pulse or that in the case of two lead-lags ($T_1 = T_3$ and $T_2 = T_4$). In addition, this method, in the case of optimization with two feedback channel, does not force the gain of one channel to be constant. So, no external constrains are necessary and it is sufficient to write the generic problem (3-12), where the inequality system, in case of speed channel with one lead-lag, becomes:

$$\sqrt{1-\xi_{ott}^2}\, Re\big(C_{wK}^i\big)\Delta K_w + \xi_{ott}\, Im\big(C_{wK}^i\big)\Delta K_w + \sqrt{1-\xi_{ott}^2}\, Re\big(C_{wT1}^i\big)\Delta T_1 +$$

$$\xi_{ott}\, Im\big(C_{wT1}^i\big)\Delta T_1 + \sqrt{1-\xi_{ott}^2}\, Re\big(C_{wT2}^i\big)\Delta T_2 + \xi_{ott}\, Im\big(C_{wT2}^i\big)\Delta T_2 \le \sqrt{1-\xi_{ott}^2}\, Re(\lambda) +$$

$$\xi_{ott}\, Im(\lambda) \qquad (3\text{-}27)$$

While to write the matrix H and the vector f is necessary to express a quadratic cost function:

$$J^i = \left[K_w^i \frac{(1+jwT_1^i)}{(1+jwT_2^i)} + \Delta\left(K_w^i \frac{(1+jwT_1^i)}{(1+jwT_2^i)}\right)\right]' \left[K_w^i \frac{(1+jwT_1^i)}{(1+jwT_2^i)} + \Delta\left(K_w^i \frac{(1+jwT_1^i)}{(1+jwT_2^i)}\right)\right]'$$

$$(3\text{-}28)$$

where the quadratic terms make up the diagonal of the matrix H, whereas the first order ones the vector f.

4 Applications and Examples on Real Power Plants

The final objective of this chapter is to show how the PSS parameters tuning is achieved for a single power plant by using ALICE. The result is an optimized[1] damping ratio of local electromechanical oscillations for the mentioned power plant, and following that a better *rotor angle stability* regarding to it. So our general approach is to reach the maximum damping of electromechanical oscillations, first for an individual power plant, that is *the local optimization* of a single power plant, and then in the next chapter we will try to develop it to a large network with different kinds of AVRs and PSSs, that is the local optimization of the whole network –that will be a large network- and as a result, to prepare the network for the global optimization discussed in chapter six.

Starting from a single power plant, it is useful to divide it into three different parts including, *synchronous generator (SCR), automatic voltage regulator (AVR)* and *power system stabilizer (PSS).* In this way, it is easier to see the effect of each section separately.

4.1 Dynamic model of a mono-machine system, alternator-network

For the purpose of local optimization that is our goal in this chapter, the synchronous generator is assumed to be connected to an infinite busbar with a simple transmission line. Except for the considered generator, the rest of the network is assumed to have a prevailing voltage that is independent from this generator and always with a constant voltage value. Therefor we have a nonlinear dynamic system, whose equilibrium condition is defined as the operation of the generator in synchronism with the frequency and voltage of the infinite network.

---

[1] In the whole thesis, by optimization we mean 'tuning the parameters of the PSS in such way that the damping of electromechanical oscillations is maximized'.

As discussed in the previous chapter, the analysis of the stability of a nonlinear dynamic system can be done by linearization of the system itself around a certain equilibrium point, and using the instruments provided by the theory of linear dynamic systems (e.g. superposition principle…). So the electrical model used for this discussion is as shown in *Figure 4-1*.
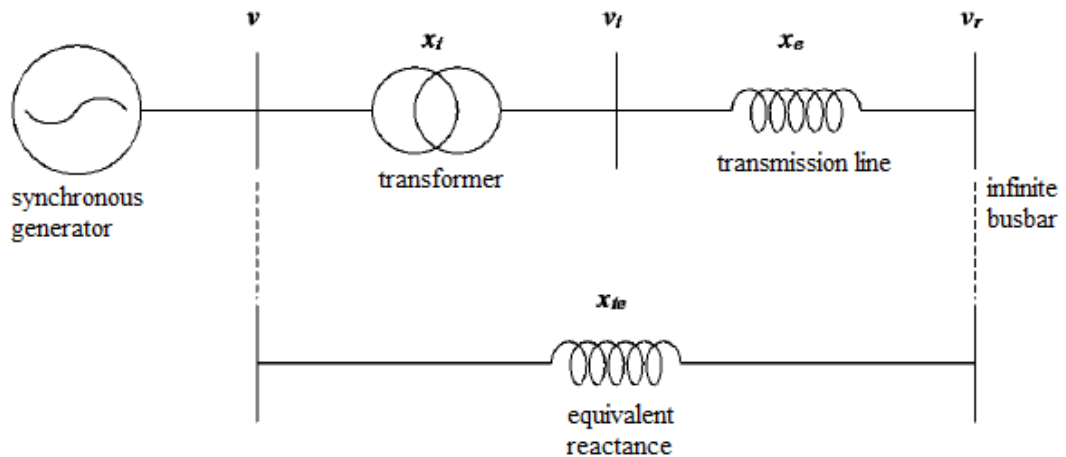
Figure 4-1 mono-machine system, alternator-infinite busbar

4.1.1 Mathematic Model of the Synchronous Machine

For the purpose of stability and control, it is not enough to model a synchronous machine with a simple first or second order model. The most useful models used in this topic are fifth or sixth order model.

As established by the Unified Theory of Electrical Machines, a synchronous machine can be represented in a reference system with two axes dq, rotating at the synchronous speed and having the q axis perpendicular to the vector of the excitation voltage - or defining an equivalent machine obtained by a transformation operation of the electrical quantities (Park's transformation) originating from the three-phase system to that of two orthogonal axes. The transform operation is conservative from the point of view of energy balances, and the synchronous machine in the dq axis system is described by the following set of equations of state:

66

$$
\begin{cases}
\dfrac{de'_q}{dt} &= \dfrac{1}{T'_{do}}\left(-e'_q - x'_{dq}i_d + \left(1 - \dfrac{T_{AA}}{T'_{do}}\right)v_f\right) \\[4mm]
\dfrac{de''_q}{dt} &= \dfrac{1}{T''_{do}}\left(e'_q - e''_q - x''_{dq}i_d + \dfrac{T_{AA}}{T'_{do}}v_f\right) \\[4mm]
\dfrac{de'_d}{dt} &= \dfrac{1}{T'_{qo}}\left(-e'_d + x'_{qd}i_q\right) \\[4mm]
\dfrac{de''_d}{dt} &= \dfrac{1}{T''_{qo}}\left(e'_d - e''_d + x''_{qd}i_q\right) \\[4mm]
\dfrac{d}{dt}\cdot\dfrac{\Omega}{\Omega_n} &= \dfrac{1}{T_m}\left(P_m - P_e - D_\Omega\dfrac{\Omega}{\Omega_n}\right) \\[4mm]
\dfrac{d\delta}{dt} &= \Omega_n\left(\dfrac{\Omega}{\Omega_n} - \dfrac{\Omega_r}{\Omega_n}\right) \tag{4-1}
\end{cases}
$$

Where

$$
x'_{dq} = x_d - x'_d - \dfrac{T''_d}{T''_{do}}(x_d - x'_d) \qquad x''_{dq} = x'_d - x''_d + \dfrac{T''_d}{T''_{do}}(x_d - x'_d) \quad \text{4-2)}
$$

$$
x'_{qd} = x_q - x'_q - \dfrac{T''_q}{T''_{qo}}(x_q - x'_q) \qquad x''_{qd} = x'_q - x''_q + \dfrac{T''_q}{T''_{qo}}(x_q - x'_q) \quad \text{4-3)}
$$

With

$$
x'_d = x_d\ \dfrac{T'_d}{T'_{do}} \qquad x''_d = x'_d\ \dfrac{T''_d}{T''_{do}} \qquad \text{4-4)}
$$

$$
x'_q = x_q\ \dfrac{T'_q}{T'_{qo}} \qquad x''_q = x'_q\ \dfrac{T''_q}{T''_{qo}} \qquad \text{4-5)}
$$

d and q components of the armature voltage, v_d, v_q are:

$$
v_d = e''_d + x''_q i_q \qquad v_q = e''_q - x''_d i_d \qquad \text{(4-6)}
$$

while the active and reactive electrical power, $P_e\ and\ Q_e$, are calculated as follow:

$$
P_e = v_d\cdot i_d + v_q i_q \qquad Q_e = v_q\cdot i_d - v_d i_q \qquad \text{(4-7)}
$$

Finally, the absolute value of the voltage and armature current is:

$$v = \sqrt{v_d^2 + v_q^2} \qquad\qquad i = \sqrt{i_d^2 + i_q^2} \qquad\qquad (4\text{-}8)$$

In the case of the mono-machine system, as shown in *Figure 4-1*, where the equivalent reactance $x_{te} = x_t + x_e$, represents the transformer-line system, the components of the armature current i_d *and* i_q are given by the following equations:

$$i_d = \frac{e_q'' - v_r.\cos\delta}{x_{te} + x_d''} \qquad\qquad i_q = \frac{v_r.\sin\delta - e_d''}{x_{te} + x_q''} \qquad\qquad 4\text{-}9)$$

where v_r is the (ideal) voltage of the infinite busbar, where the generator is connected to. So the dynamic model of the system, described with the above equations, is illustrated as in *Figure 4-2*.
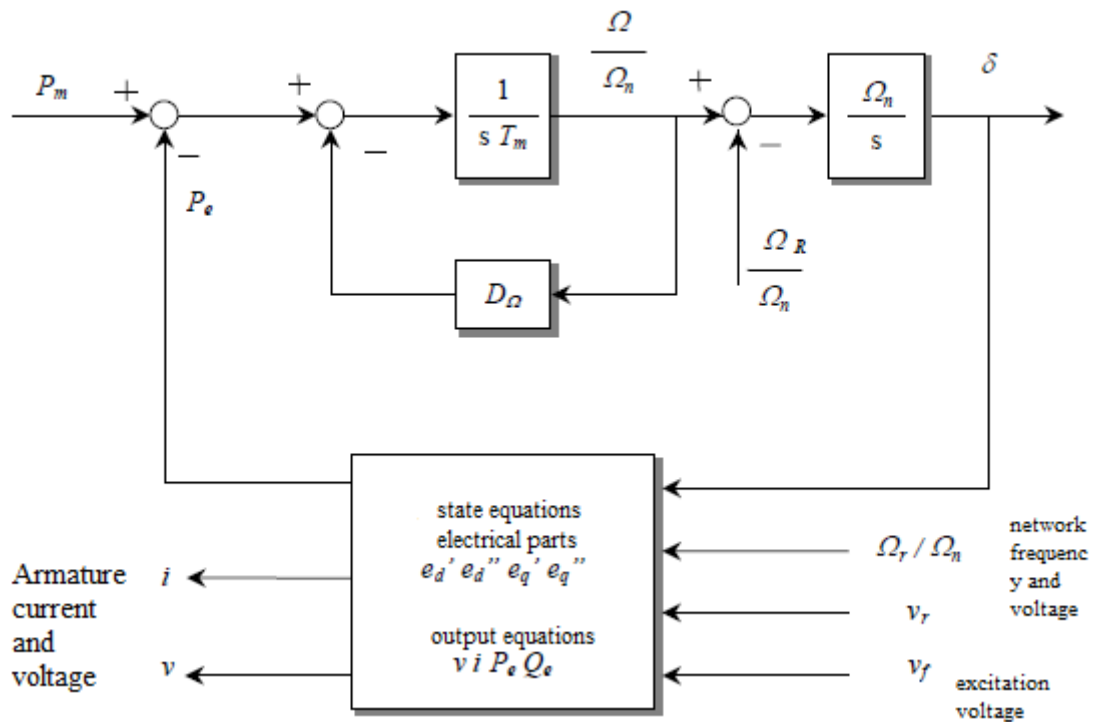
Figure 4-2 block diagram of the mono-machine alternator-network system

The meaning of the quantities that appear in previous equations is given in *Table 4-1*.

Table 4-1 characteristic quantities of a synchronous machine

symbol	Description	unit
e_q'	quadrature axis component of transient emf	p.u.
e_q''	quadrature axis component of subtransient emf	p.u.
e_d'	direct axis component of transient emf	p.u.
e_d''	direct axis component of subtransient emf	p.u.
v_f	field voltage supplied by the excitation system	p.u.
T_{AA}	leakage time constant of the additional damper along direct axis	s
x_d	operational reactance along direct axis	p.u.
x_q	operational reactance along quadrature axis	p.u.
T_d'	transient time constant along direct axis	s
T_d''	subtransient time constant along direct axis	s
T_{do}'	open-circuit transient time constant along direct axis	s
T_{do}''	open-circuit subtransient time constant along direct axis	s
T_q'	transient time constant along quadrature axis	s
T_q''	subtransient time constant along quadrature axis	s
T_{qo}'	open-circuit transient time constant along quadrature axis	s
T_{qo}''	open-circuit subtransient time constant along quadrature axis	s
i_d	armature current along direct axis	p.u.
i_q	armature current along quadrature axis	p.u.
i	absolute value of the armature current	p.u.
v_d	armature voltage along direct axis	p.u.
v_q	armature voltage along quadrature axis	p.u.
v	absolute value of the armature voltage	p.u.
P_m	mechanical power of the rotor	p.u.
P_e	active power generated by the alternator	p.u.
Q_e	reactive power generated by the alternator	p.u.

4.1.2 Voltage Regulator

The above mentioned dynamic system will be completed by adding a voltage regulator that can be modeled with the following second order transfer function:

$$G_v(s) = \mu_\circ . \frac{1 + sT_c}{(1 + sT_b)(1 + sT_a)} \qquad (4\text{-}10)$$

It is taking into account, the gain of the voltage transducer and the effects of filtering (pole in $\left(-\frac{1}{T_a}\right)$) in high frequency, in the control loop; the selected transfer function allows to correctly present the intervention of the regulator in the frequency range of interest for the study of electromechanical phenomena (1: 10 rad/s).

4.1.3 Dynamic Friction

In the *Figure 4-2*, the feedback element D_Ω represents the mechanical friction phenomena: it can suitably be replaced by an element of dynamic friction described by a transfer function $G_d(s)$:

$$G_d(s) = D_\Omega \frac{sT_d}{1 + sT_d} \qquad (4\text{-}11)$$

In *Figure 4-3*, the effect of voltage regulator and dynamic friction is also added:
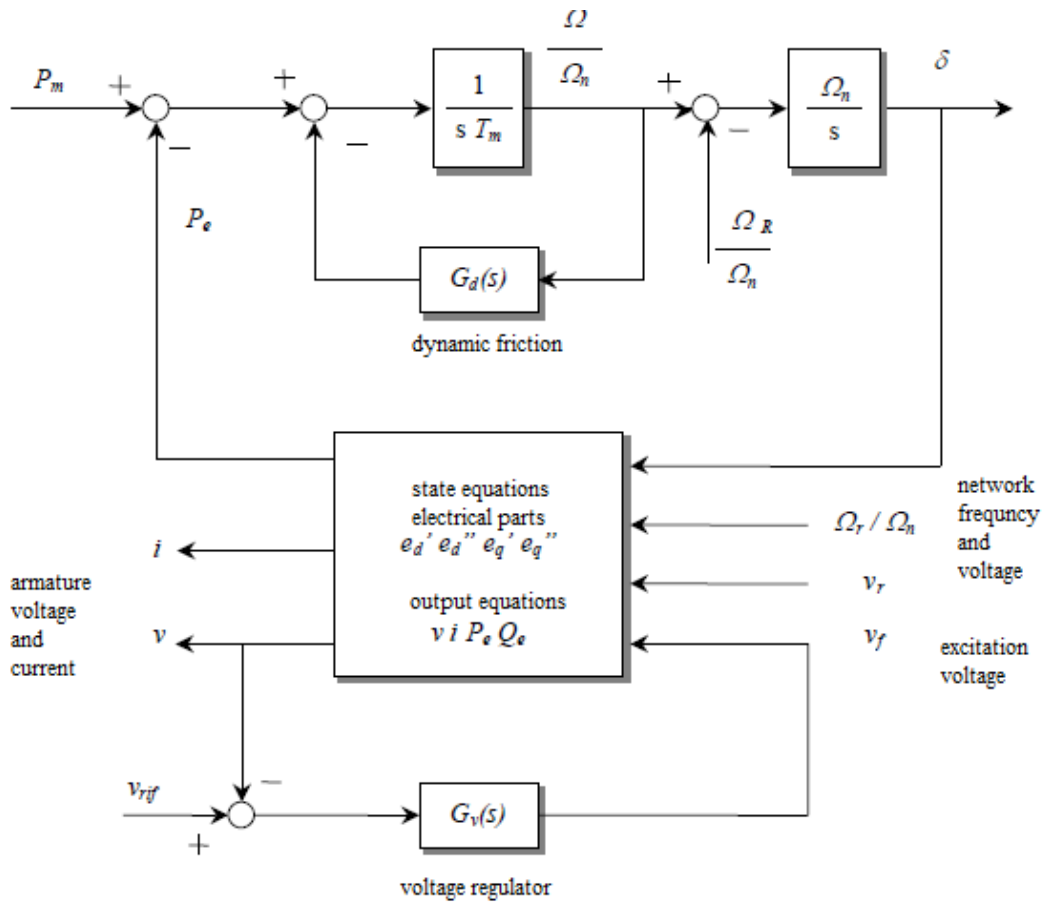
Figure 4-3 block diagram of a mono-machine alternator-network system with dynamic friction element $G_d(s)$ and voltage regulator $G_v(s)$

4.1.4 Linearization: electromechanical and voltage cycle

Proceeding to the linearization of non-linear mathematical model of the system described (mono-machine), around an appropriate point of equilibrium, leads us to a formulation of the same which allows a block representation presented in *Figure 4-4*.
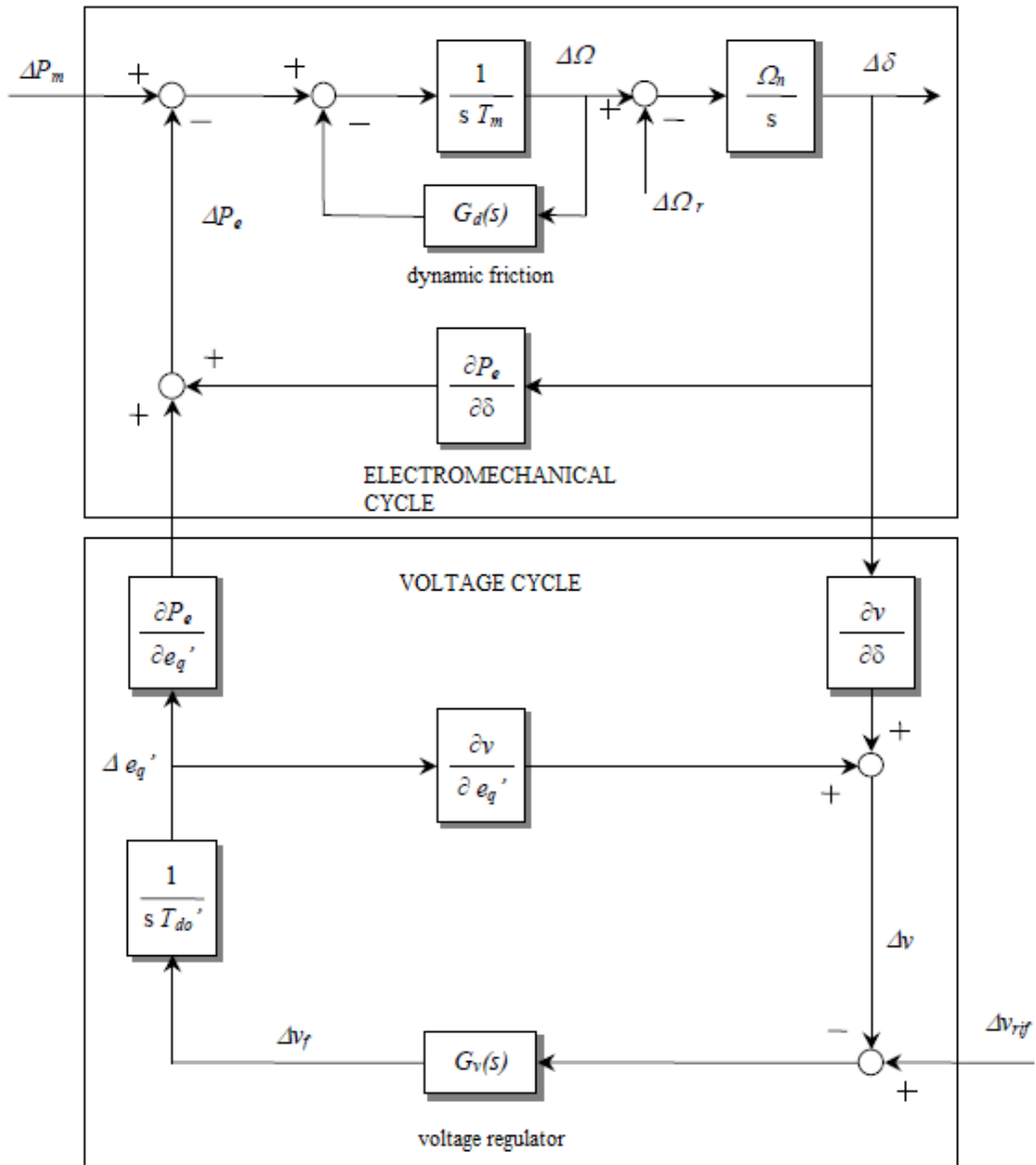
Figure 4-4 linearized block diagram of the mono-machine alternator-network system: with presence of the electromechanical and voltage cycles

It can be seen, in particular, an electromechanical cycle and a voltage cycle. As it is shown in *Figure 4-4*, it is possible to simplify the block diagram, by combining the effects of the cycle of voltage on the variation of active electric power P_e in a single term as *K(s),* which makes it easier to evaluate the stabilizing and destabilizing effects as a whole.
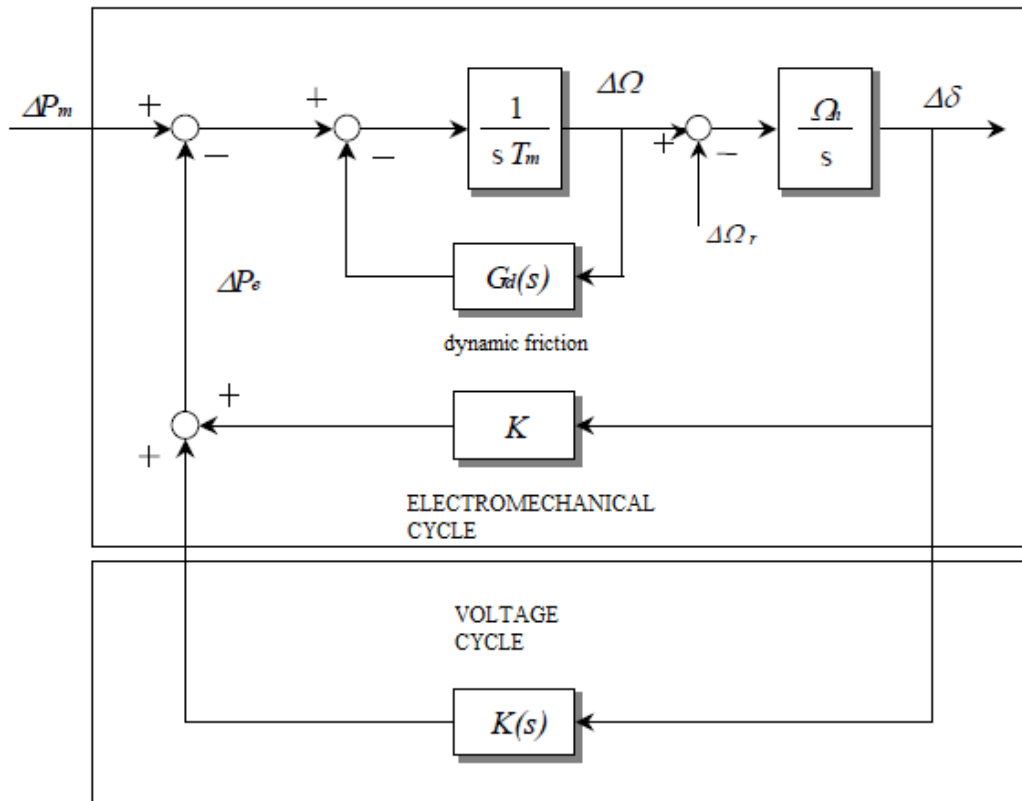
Figure 4-5 linearized block diagram of the mono-machine alternator-network system

The linearized model of *Figure 4-5*, is therefore a mono-machine alternator-network system without additional feedback stabilizers. In the absence of the term of dynamic friction, the electromechanical cycle is characterized by two poles in the origin, the first associated with the rotational dynamics (with time constant T_m), the second one is the load angle δ, the sign of which determines the direction of the active power injected or absorbed by the network.

First, one can observe that, with open loop voltage, or with manual adjustment of the excitation voltage (assumed constant $\Delta v_f = 0$), the linearized system has two complex poles purely imaginary

$$\lambda, \lambda^* = \pm j \sqrt{\frac{\Omega_n}{T_m} \left(\frac{\Delta P_e}{\Delta \delta}\right)_\circ} \qquad (4\text{-}12)$$

which corresponds, as it is known, an oscillatory behavior without damping. However, it is necessary to emphasize that the real part of the poles is zero because of the

adopted simplification: in fact they have negative real parts, although they are still positioned very close to the imaginary axis.

The algebraic block *K*, in *Figure 4-5*, represents the partial derivative of the electrical power with respect to the load angle δ and is referred to as synchronizing power coefficient. The electromechanical cycle therefore, consists of two integrators in series and by the gain in the negative feedback *K*, it has zero phase margins.

The corresponding transfer function of the block *K* is the following:

$$K(s) = -\frac{\left(\frac{\Delta v}{\Delta \delta}\right)\cdot\left(\frac{\Delta P_e}{\Delta e_q'}\right)}{\left(\frac{\Delta v}{\Delta e_q'}\right)} \frac{1}{1+\frac{sT_{do}'}{G_v(s)}\left(\frac{\Delta v}{\Delta e_q'}\right)} \qquad (4\text{-}13)$$

It represents the characteristics of a low-pass system and therefore provides a negative contribution to the phase of the electromechanical cycle: evaluating the sign of the partial derivatives that appear in the expression of *K*(s), it can be shown that the sign of that transfer function is always positive, and therefore the effect of the voltage regulation on the electromechanical cycle is always destabilizing.

This effect is irrelevant only in particular operating conditions:

- In the case of very slow voltage regulators, in which the effect of *K*(s) is interested in the field of low frequency oscillations.
- At open-circuit, with $P_e = 0$, or without contribution of *K*(s).

4.2 Stabilization of the system through additional feedback

The analysis of the stability of a mono-machine dynamic system, briefly discussed in the previous paragraph, highlights the need to introduce additional feedback loops that provide a correction to the voltage reference in order to ensure stability margins broader, namely running conditions safer and a field of usability of the machine more extended.

4.2.1 Characterization of additional stabilizing feedback

A signal stabilizerΔv_{ret}, which is added to the voltage reference, is obtainable as a proportional contribution to the speed of mechanical rotation (or to the derivative of the load angle) according to a transfer function $K_\Omega(s)$, to be defined, as indicated below

$$\Delta v_{ret} = K_\Omega(s)\Delta\Omega = K_\Omega(s)\frac{s}{\Omega_n}\Delta\delta \qquad (4\text{-}14)$$

This contribution may be represented, in the block diagram, through an equivalent block $\overline{K}_\Omega(s)$, which represents the effect on the generated active power rather than on the voltage reference: this is illustrated in *Figure 4-6*.

It can be shown that, the above introduced additional feedback allows both to increase the reduced phase margin, intrinsic in the electromechanical cycle and, above all, to compensate the destabilizing effect introduced by the voltage loop. This is possible through an appropriate choice of the transfer function $K_\Omega(s)$: in particular, in order to compensate the integral action exerted by the voltage loop in the pulse characteristics of the electromechanical phenomena, it is appropriate to provide through $K_\Omega(s)$ an opposite derivative action, i.e.

$$K_\Omega(s) = K_\Omega + sK'_\Omega \qquad (4\text{-}15)$$

Since the introduction of derivative regulating contributions is related to the implementation issues that can increase the risk of disturbances of measurement, the derivative term of $K_\Omega(s)$ can be more conveniently reconstructed through the measurement of the generated active power, by observing that

$$\Delta P_e = -sT_m\Delta\Omega \qquad (4\text{-}16)$$

we then obtain

$$\Delta v_{ret} = (K_\Omega + sK'_\Omega)\Delta\Omega = K_\Omega\Delta\Omega - K_p\Delta P_e \quad \text{with} \quad K_P = \frac{K'_\Omega}{T_m} \qquad (4\text{-}17)$$

In addition, it is useful to add a high-pass filter with unity gain on the introduced stabilizing signal, in order to cancel the steady state effect, namely in order not to influence the static performance of the voltage regulation loop.
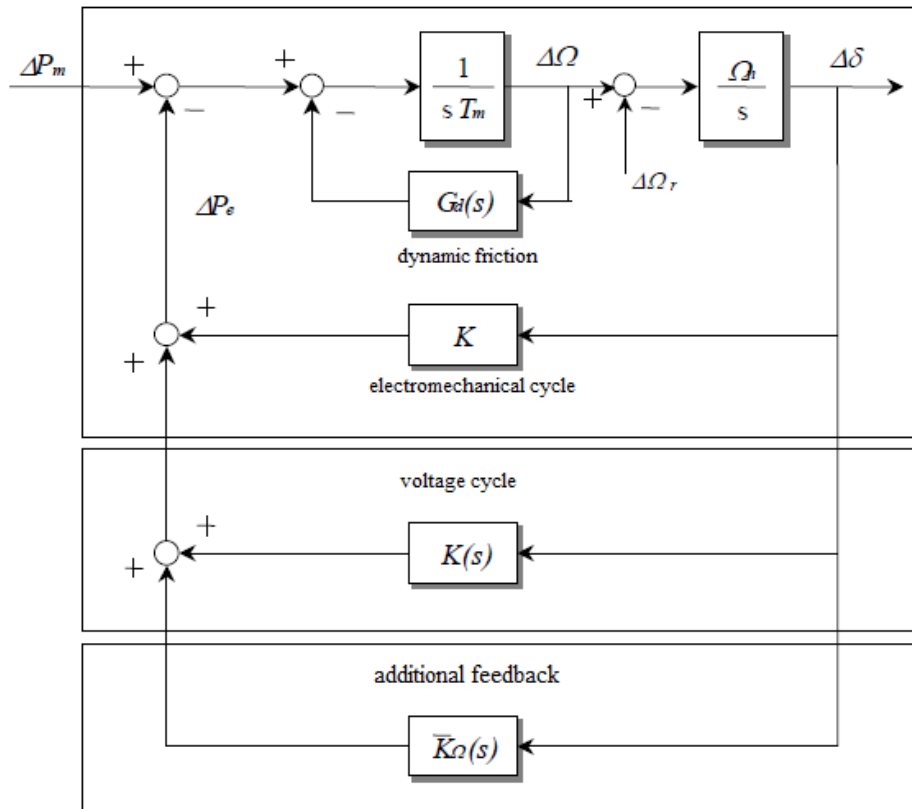
Figure 4-6 block diagram of a linearized mon-machine alternator-network with additional stabilizing feedback

And the final block diagram that can be useful for our case and carries more related data in as below
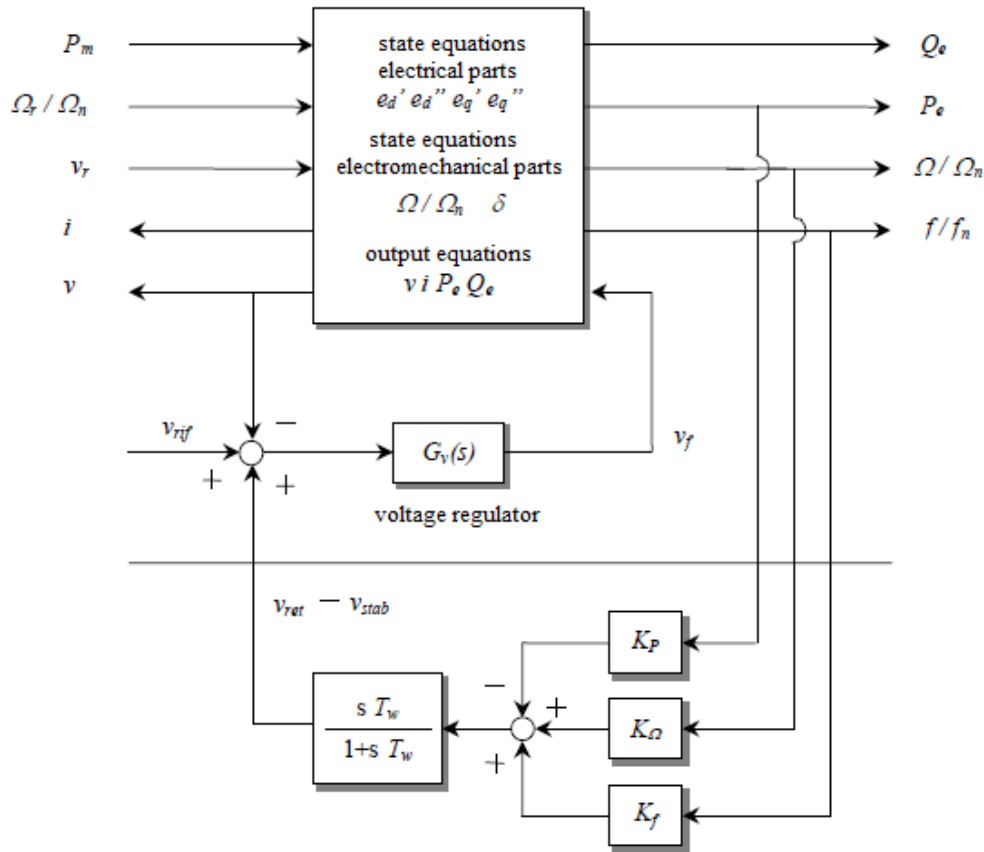
Figure 4-7 another representation of the mono-machine block diagram with voltage regulator and additional feedback

4.3 Practical examples of PSS tuning: single power plant

As it was mentioned in the beginning of this chapter, to analyze the optimization of a single power plant it was divided it into three different parts, which are *synchronous generator, automatic voltage regulator* and *power system stabilizer.* In the previous sections the focus was on the definition of these different parts and to describe each of them using block diagrams, that are useful from the control point of view and in particular for PSS (that is the main block that we want to work on).

In the following section some practical applications are discussed. The procedure is as explained below:

- First, a typical power plant[1] with the default values of the parameters is chosen. (This power plant is one of the plants of the large network that will be discussed in the next chapter). For the selection of the examined power plant some considerations are important. It is better that the selected power plant has the most general type of the AVR and PSS, because any special case can be useless to be used as the example. Thus, the aim is to choose a plant with the most common types of AVR and PSS. (While in the process of doing the thesis, different kinds of power plants with different level of difficulty were considered, but just one of them is mentioned individually in this chapter).

- Then, different optimization methods, described in chapter 3, are applied to the selected power plant, in order to see the result of the optimization on the eigenvalues (or similarly poles) of the system. These poles and consequently damping ratios and their frequency can give us very useful information about the quality of the damping of electromechanical oscillations.

- The final step is to compare the oscillating modes of the power plant, both before and after optimization, and to check if the optimization could be effective or not.

It is already mentioned that the main tool for PSS tuning, used in this thesis, is the software named ALICE. The available AVR and PSS types in ALICE are given in the following:

PSS types: standard, PSS1A, PSS2B, PSS3B, PSS4B, Ansaldo, ABBeGE2, ELIN and Toshiba.

AVR types: standard, DC1A, DC3A, DC4B, AC1A, AC2A, AC3A, AC4A, AC5A, AC6A, AC7B, AC8B, ST1A, ST2A, ST3A, ST4B, ST5B. ST6B, ST7B, Alstom, Ansaldo, ELIN, SEMIPOL.

---

[1] By "power plant", it is simply meant the composite model consists of SCR, AVR and PSS. Of course in a real power plant there are other devices such as prime mover, governor and so on, but for the purpose of this thesis they are not directly considered.

According to the type of the PSS, it is possible to use one or more methods of PSS tuning, described in the previous chapter. Therefore, the most general type should be chosen in this chapter, since we will be able to imply different methods of optimization.

The first power plant that is discussed here is named "car01". This plant is one of the plants of the large network (i.e. Chilean network) that will be shown in the next chapter. Different parameters of this plant including the parameters of SCR, AVR and PSS are given. (Please note that the values of the parameters of the PSS are the pre-optimization values). The values of the parameters are as shown in *Table 4-2*.

It can be helpful to demonstrate the block diagram of this kind of PSS, because the position of each parameter and its influence on the final output signal of the PSS can be seen. *Figure 4-8* depicts the IEEE standard model of PSS1A, while *Figure 4-9* is the linearized block diagram around the operating point. In the case of this thesis, the small signal stability is discussed; therefore, the linearized model is used.
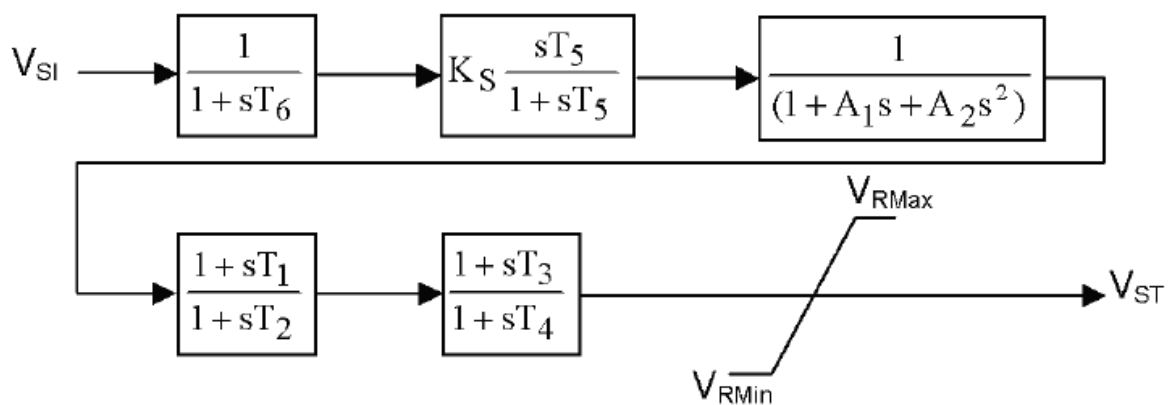
Figure 4-8 block diagram of PSS PSS1A

Table 4-2 value of the parameters of SCR, AVR and PSS for the plant "car01"

SCR 6th order machine	AVR Type: ST1A	PSS Type: PSS1A
Tdop=T'_{do}=6.5[1]	Tc=10.00	kp=0.000
Tdos=T''_{do}=0.023	Tb=0.2200	kw=0.000
Tdp=T'_{d}=0.7731	Ta=2.000	kf=0.000
Tds=T''_{d}=0.0177	ka=100.000	ks5=2.000
Tdop=T'_{do}=0.70	Tc1=1.000	T6=0.0002
Tqos=T''_{qo}=0.030	Tb1=1.000	T5=3.500
Tqp=T'_{q}=.1508	ksf=0.0787	A2=0.0017
Tqs=T''_{q} =.**0136**	Tsf=3.5300	A1=0.0610
xd=2.186	CVretf=1	T1=1.000
xq=2.043	---	T2=1.000
Tm=9.00	---	T3=1.000
xt=.1250	---	T4=1.000
xe=.2500	---	---
Td=3.00	---	---
dw=0.00	---	---

---

[1] Time constants are given in seconds, and reactances are per unit values.
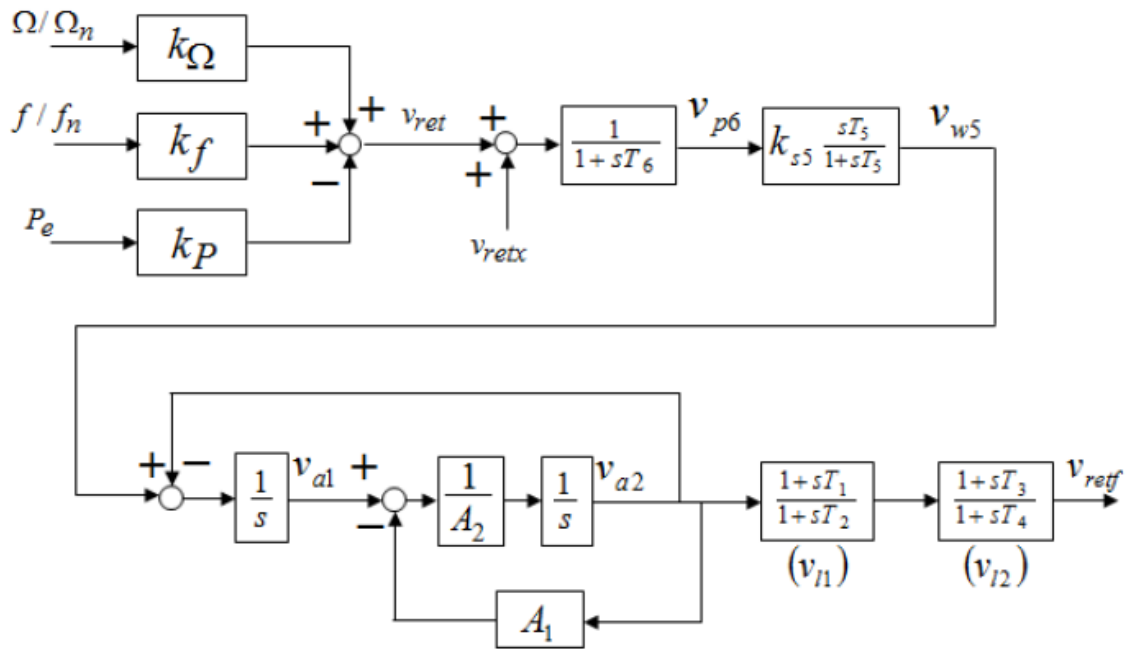
Figure 4-9 linearized block diagram of PSS PSS1A, as explained and used in ALICE

There are different kinds of analyses that can be done on this power plant in ALICE, such as:

1) Calculating the poles and damping ratios of the power plant for different frequencies, especially for the frequency range of interest, i.e. 1-2 Hz.

2) Depicting the open loop bode diagram of the system. (to analyze the phase of the transfer function between speed and active power)

3) Doing a time domain simulation to track the transition, following a step change in the reference voltage.

All of these analyses are done, both before and after optimization of the PSS parameters. The result of the calculation of the poles before optimization for the plant "car01", is shown in *Table 4-3*. (Notice that the damping ratios less than 1 are just shown).

Table 4-3 damping ratios of plant "car01", before optimization

damping ratio or zita or ζ	Frequency
0.0300	1.1318
0.7397	2.5974

As it was mentioned before, the minimum acceptable damping is 20%, thus, it is clear that in this plant, there is an oscillatory mode with the damping of 3%, which should be increased after optimization. To emphasize the effect of these oscillations, the phase of the open loop transfer function and also time domain simulations (for the load angle and the generated active power) are depicted in *Figure 4-10* to *Figure 4-12*, respectively. As it is demonstrated in *Figure 4-10*, the phase diagram is not in the satisfying area in the frequency range of interest, i.e. 0.1 to 1 Hz.
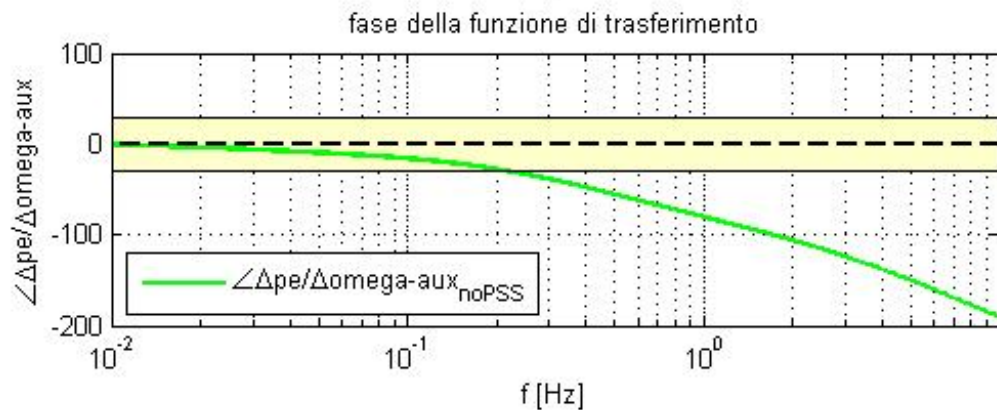
Figure 4-10 Phase of the open loop transfer function between speed and active power for plant "car01",
without PSS

Figure 4-11 transient response of the load angle to a step change in the reference voltage, before
optimization
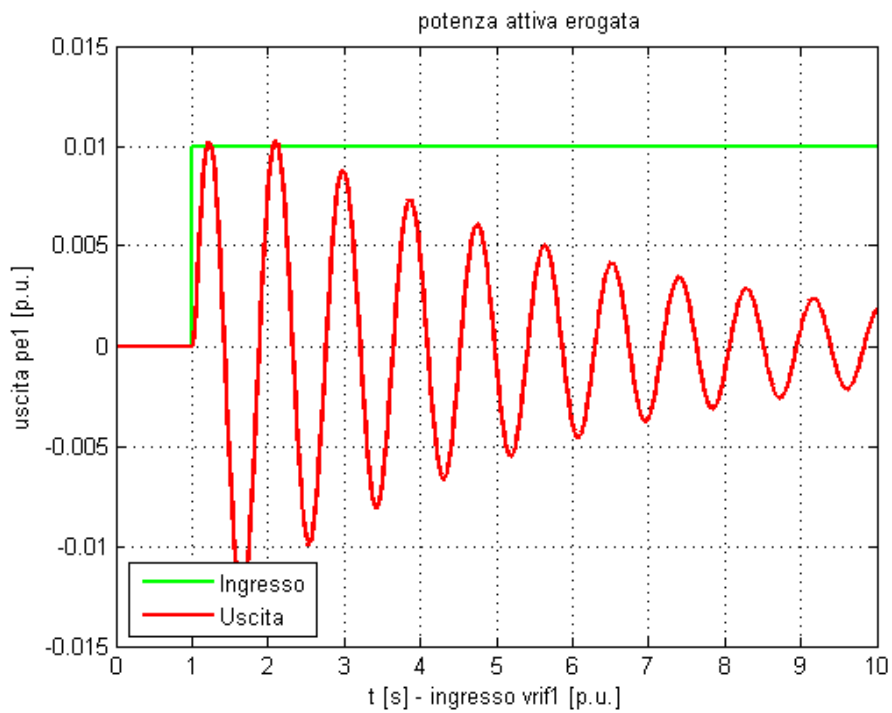
Figure 4-12 transient response of the active power to a step change in the reference voltage, before
optimization

Thus, according to exact and simplified criteria of stability analysis, this plant has to be optimized.

Figure 4-11 illustrate the electromechanical oscillations caused by the above-mentioned pole –with frequency of 1.1318 Hz. As it is seen, the amplitude of the first oscillation is pretty high, that can cause enormous stability problems, and even in some cases, to trigger protective breakers in the network. Furthermore, following the first oscillation, the other oscillations are not effectively damped.

According to the results of the preceding stability analyses that are performed for the plant "car01", the necessity of a tuning of the PSS parameters is clear. In the following, ALICE will be used to optimize the plant "car01".

In the *Figure 4-13*, the interface of ALICE is illustrated. As it is shown, the calculation mode of the PSS gain can be i) approximate or ii) iterative. To be more accurate, it is better to choose the iterative choice.

It is also possible to choose the desirable damping ratio that will be reached after optimization, (that is 20% for our purpose).

The optimization can be performed in two general ways, i) only by using one gain, like kp, kf or kw. ii) it can be done in the "multi-obiettivo" mode which means "multi-objective". In this mode, there is the possibility to choose the first or second method of PSS tuning, described in chapter 3. Therefore, the user has the chance to have two different channels at the same time, such as kp-kf or kp-kw, or by considering the second method; it is possible to have one gain together with one or two lead-lags. This is the case for plants in which by only exploiting the gains, we cannot reach the desirable damping ratio, and consequently, it is better to fix the value of one of the gains calculated by the residual method and then to apply lead-lags calibration on the other channel.

In the following diagram, the possible optimization methods –as described before-are shown.

Single-objective: with 'kp' or 'kf' or 'kw'

Optimization Methods

Residuals: 'kp-kf' or 'kp-kw'

Multi-objective

One gain with lead-lag(s):

'kp-lead-lag(s)' or 'kf-lead-lag(s)' or 'kw-lead-lag(s)'
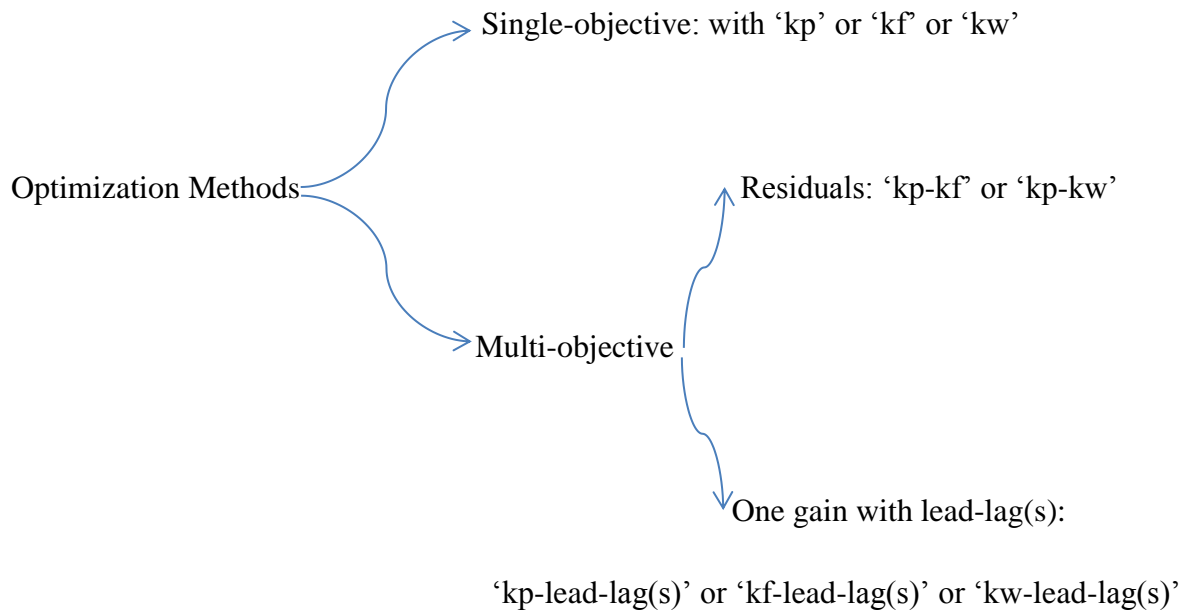
Note: in the case of power plant "car01", the PSS is PSS1A, and it is the most general case, so all of the mentioned methods are available. But in some PSS types such as PSS2B, the residuals method is not accessible.
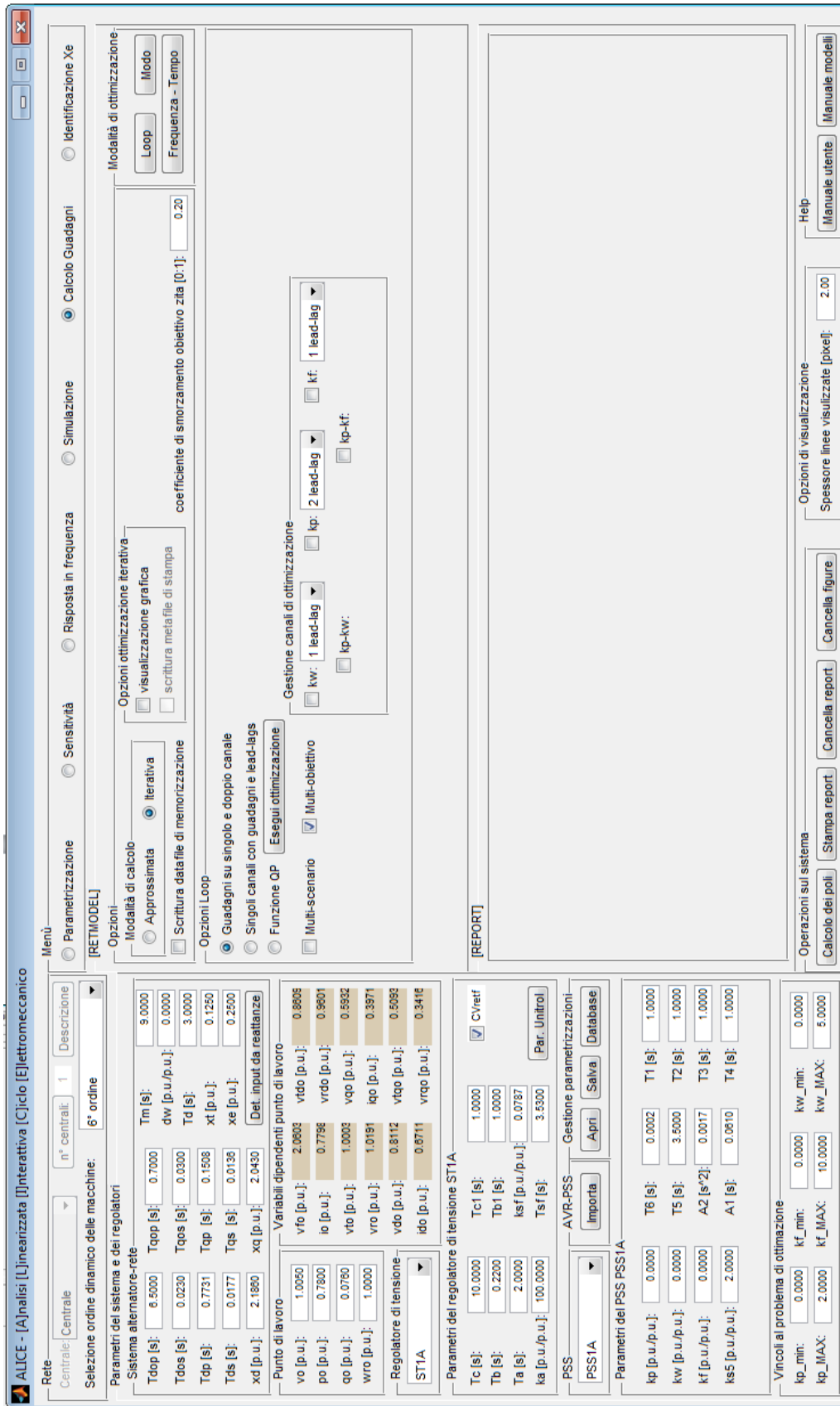
Figure 4-13 ALICE interface, for the plant "car01"

4.3.1 **Application of optimization methods for a typical plant**

In this section, the results of application of two different PSS tuning methods are given.

For the stated power plant (car01) in the previous section, the results are as following:

Table 4-4 results of different optimization methods on "car01"

case	Optimization type	Zita (ζ)	kp	kf	kw	T1	T2	T3	T4
1	kp-kf	0.200	0.1261	2.15	0	1	1	1	1
2	kp-kw	0.200	0.1332	0	1.51	1	1	1	1
3	kp-1lead-lag	0.130	2.000	0	0	0.2403	4.1204	1	1
4	kp-2lead-lags	0.200	1.6937	0	0	0.5582	1.7741	0.5582	1.7741

Regarding the results of the *Table 4-4*, it can be seen that in three cases, the damping ratio, ζ, has reached to the desirable value, i.e. 20%, and in one case it has been improved (case 3). Thus, it is meaningful to say that the optimization of this plant is not only possible, but also useful. The analyses of each case are taken into account in the following sections.

Case 1:

In this case, the aim is to optimize the stabilizers' gains using the residuals method. kp and kf are the selected channels for the first case. In *Figure 4-14* to *Figure 4-16*, the same analyses as before optimization are done, and as it can be seen the response of the angle is not oscillating anymore. Furthermore, the active power oscillations are significantly damped. In *Figure 4-14*, the phase of the open loop transfer function is shown. It is possible to compare the phase diagram before and after optimization. Comparing the green and red lines in this *Figure 4-14*, the optimization outcome is clearly shown.

Figure 4-14 Phase of the open loop transfer function between speed and active power for plant "car01",
without PSS(green line), with PSS but without lead-lag(with just gain)(red line), case 1
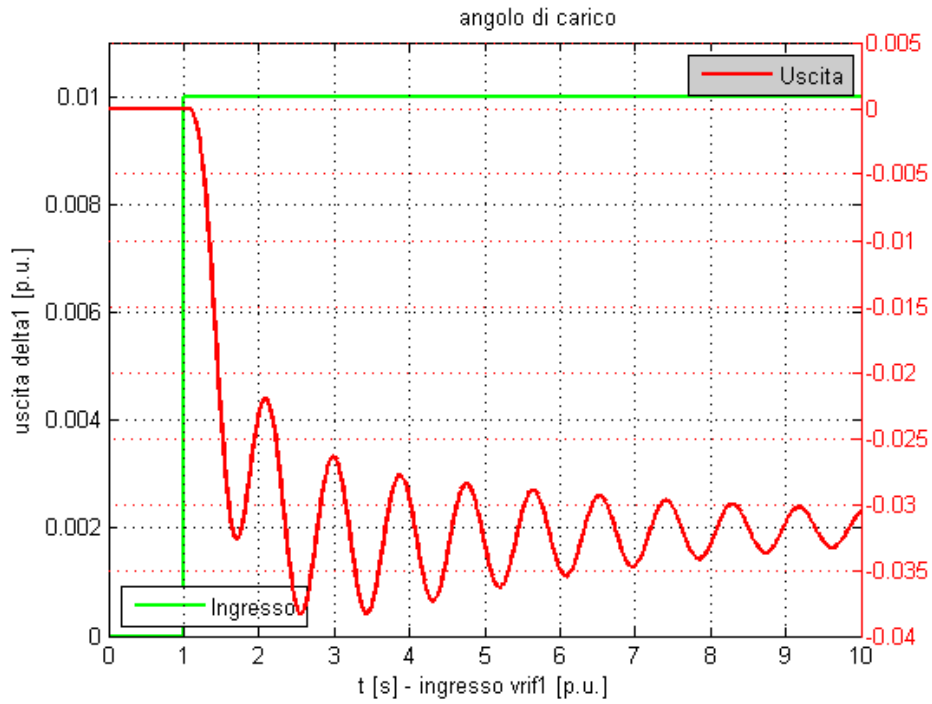

Figure 4-15 transient response of the load angle to a step change in the reference voltage, after optimization,
case 1

Figure 4-16 transient response of the active power to a step change in the reference voltage, after optimization, case 1

Case 2:

Similar to the case 1, the residuals method is utilized, but instead of kf (that is the frequency gain), kw has been used. kw is the gain that is applied on the speed feedback coming from the synchronous generator. With regard to this case, the results of the analyses are shown in *Figure 4-17* to *Figure 4-19*.

As we expected, the results are quit the same as the case 1, because in both cases, residuals method is used. Therefore, it is possible to apply each of them for the same purpose, but we have to notice that the difference between them is the feedback channel coming from the synchronous machine. Thus, it is necessary to check if it is easier to measure the frequency or the speed of the generator. In some plants, the measurement of the frequency of the rotor is not permissible; in this case the speed is a good substitution.
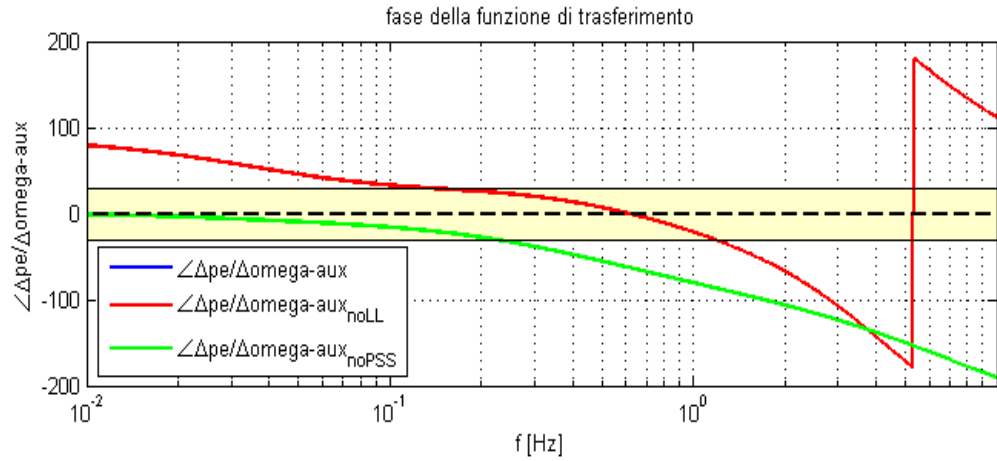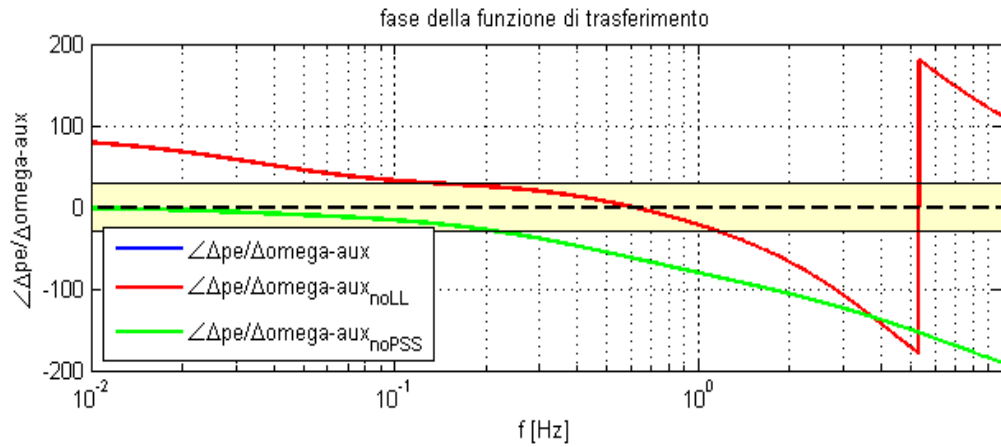
Figure 4-17 Phase of the open loop transfer function between speed and active power for plant "car01", without PSS(green line), with PSS but without lead-lag(with just gain)(red line), case 2
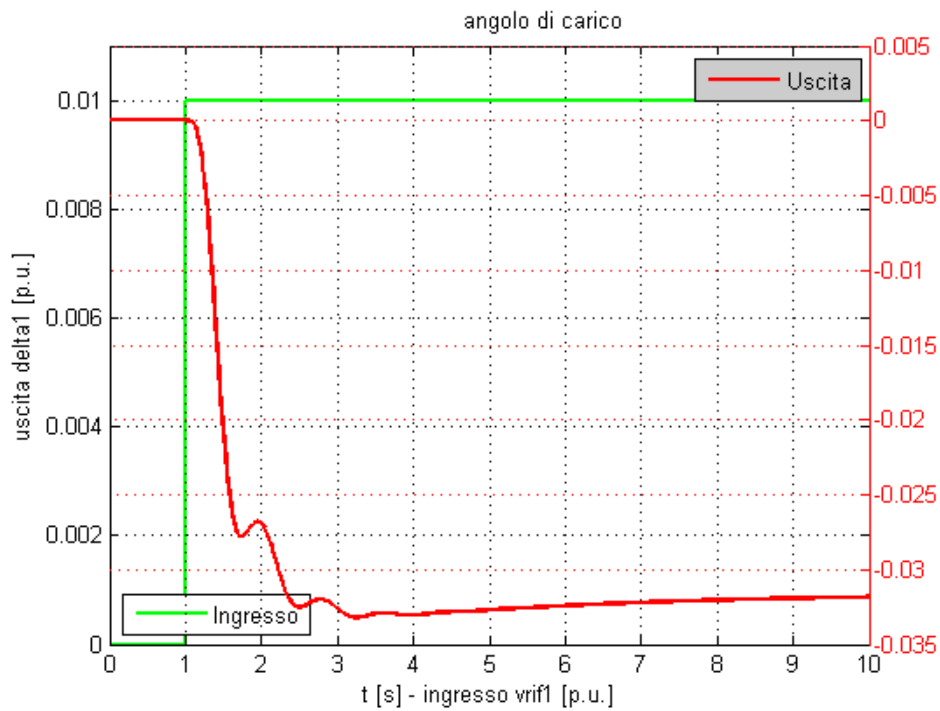
Figure 4-18 transient response of the load angle to a step change in the reference voltage, after optimization, case 2
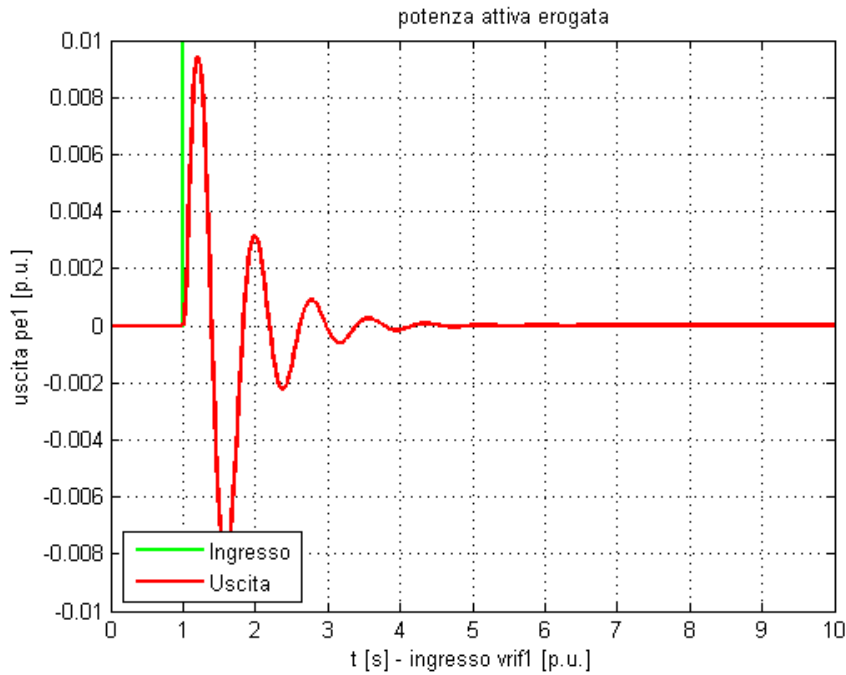
Figure 4-19 transient response of the active power to a step change in the reference voltage, after

optimization, case 2

Case 3 and 4:

In these cases, the optimization is performed by using one gain and lead-lags time constants for one feedback channel. This method is very useful when only one input of PSS is available or one of the input measurements is not enough accurate.

The difference between case 3 and 4 is the number of lead-lags used in each case. In case 3, just one lead-lag is used, while in case 4, there are two lead-lags. As it is obvious, employment of two lead-lags in case 4 can considerably improve the damping ratio. In fact, the selection of case 3 in this section was just to show the influence of the second lead-lag to optimize the PSS parameters. The same analyses are done for the cases 3 and 4, and the results are illustrated in *Figure 4-20* to *Figure 4-25*.

By comparing the case 3 with the case 4, the effect of reaching a damping ratio lower than 20% is completely clear, since in the case 3, ζ is 13%. Thus, in this case, the damping of the oscillations in both the active power and load angle responses is lower than the case 4, as we expected. On the other hand, the comparison between case 4 and case 2 tells us

91

that in both cases the desirable damping and phase diagram is reached. From the practical point of view, this is important, because it means that: if both cases reach a damping ratio of at least 20%, these two methods are alternatives. Thus, in some power plants that just one input of the PSS is available, it is possible to use lead-lags to satisfy the limitation of ζ and phase diagram.
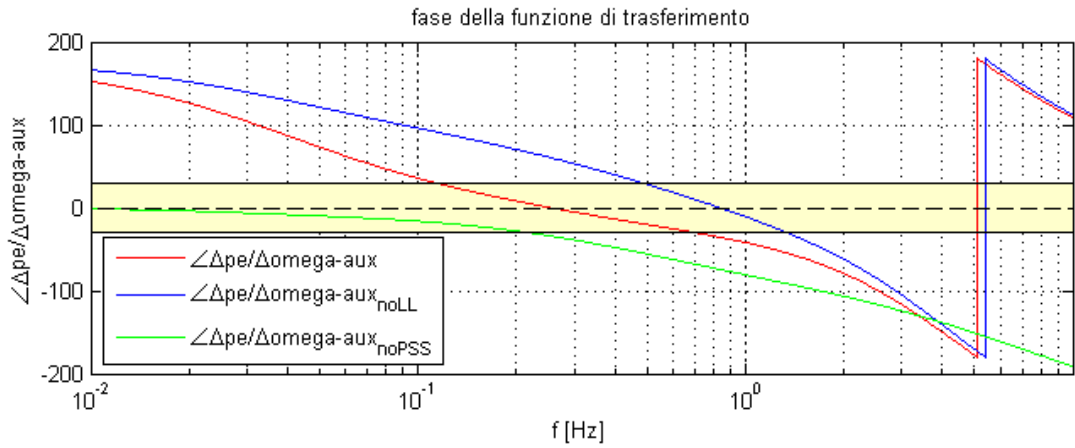
Figure 4-20 Phase of the open loop transfer function between speed and active power for plant "car01", without PSS(green line), with PSS but without lead-lag(with just gain)(red line), with PSS and lead-lag(blue line) , case 3
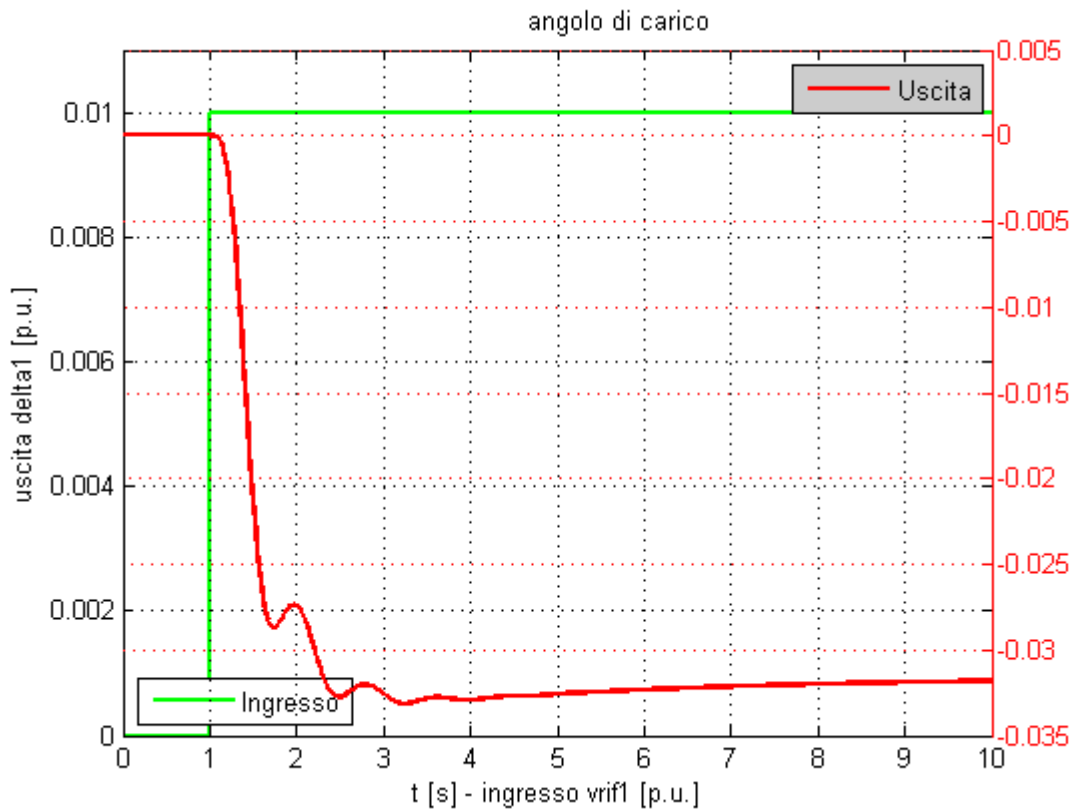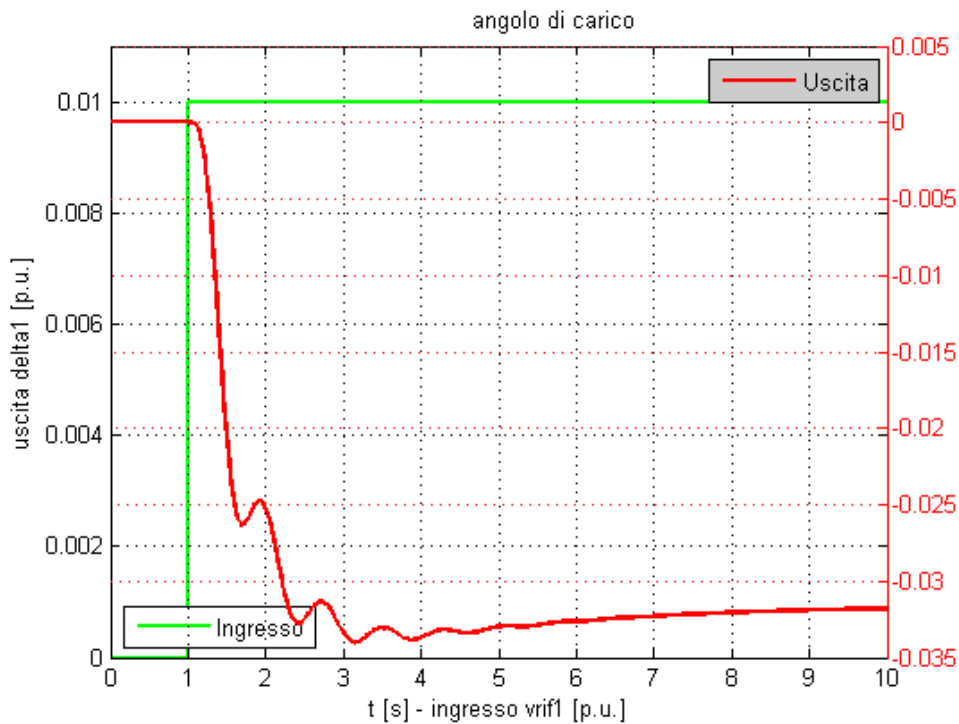
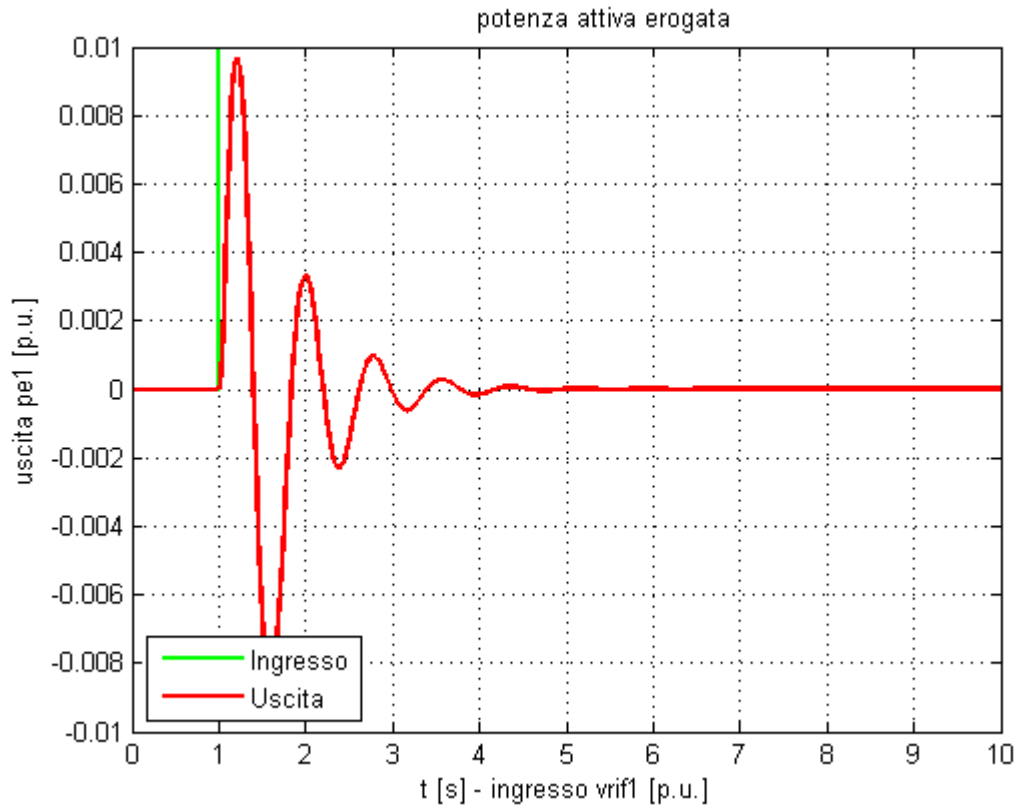*Figure 4-21 transient response of the load angle to a step change in the reference voltage, after optimization, case 3*
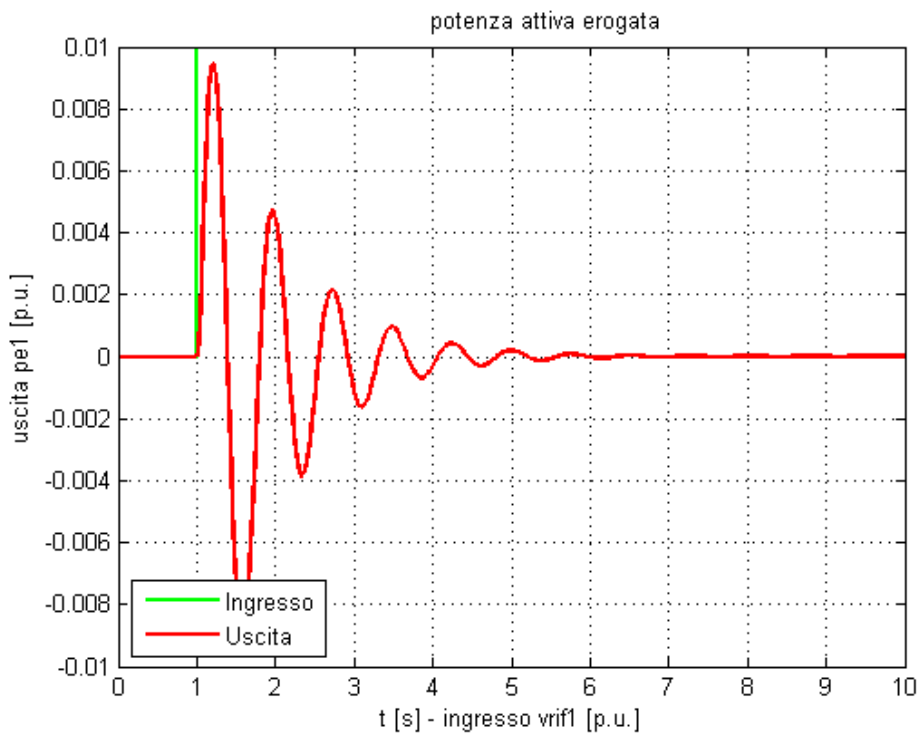
Figure 4-22 transient response of the active power to a step change in the reference voltage, after optimization, case 3

93
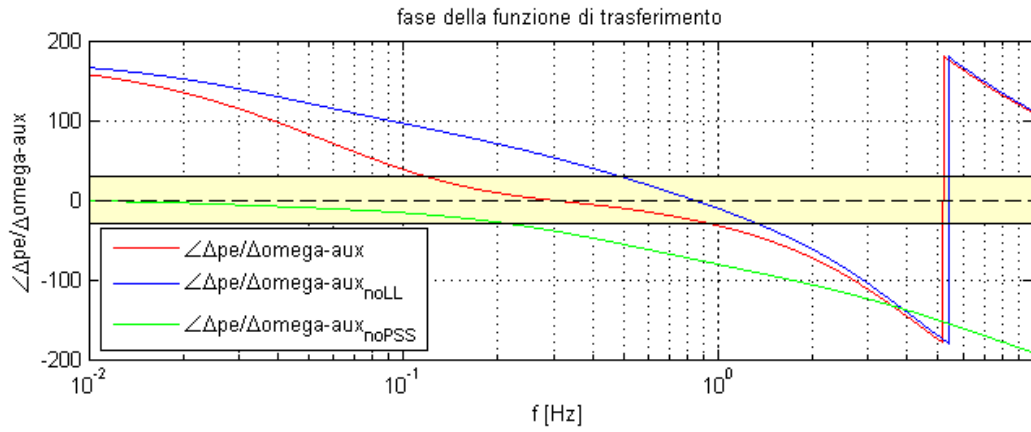
Figure 4-23 Phase of the open loop transfer function between speed and active power for plant "car01",
without PSS(green line), with PSS but without lead-lag(with just gain)(red line), with PSS and lead-lag(blue
line) , case 4
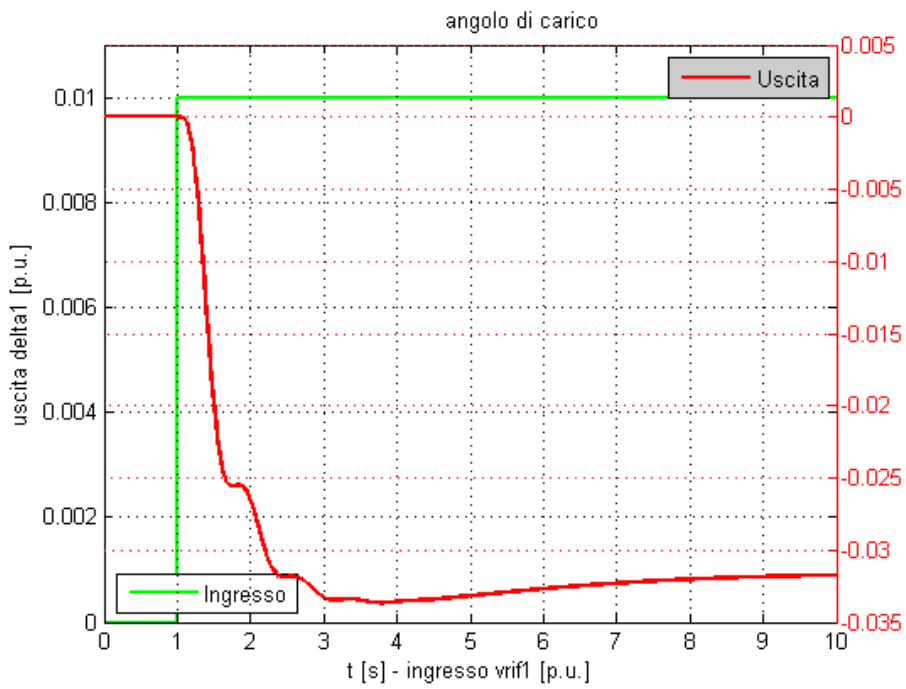
Figure 4-24 transient response of the load angle to a step change in the reference voltage, after optimization,
case 3
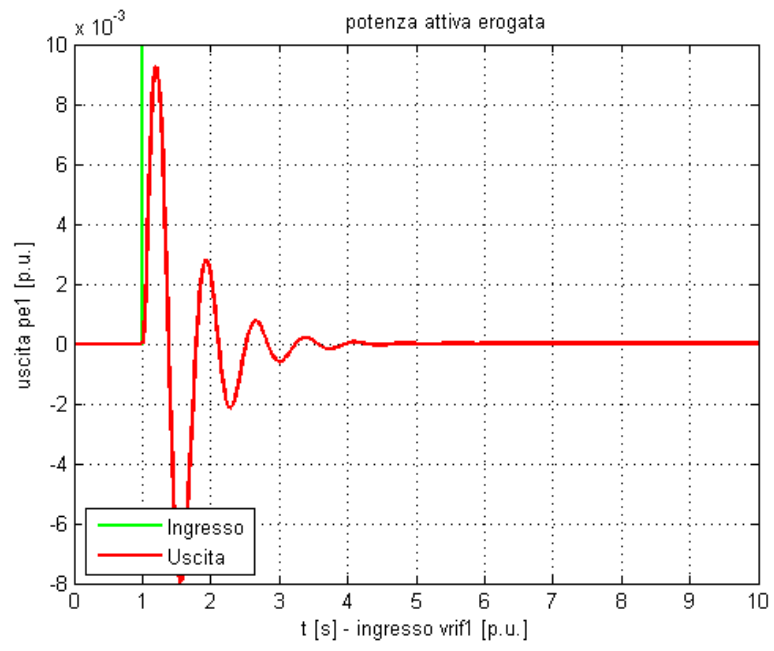
Figure 4-25 transient response of the active power to a step change in the reference voltage, after optimization, case 4

5 Application of Local Optimization Techniques on a Real Network

The optimization of an individual power plant was carried out in the previous chapter. Referring to the results achieved in chapter 4, it is possible to optimize a single power plant by using ALICE as the optimization tool. In this chapter, the aim is to develop a software product for the optimization of the parameters of the PSS of the electrical power plants of *large networks*, with the objective of maximizing the damping of electromechanical oscillations.

The practical difficulty that this goal is confronted with is the fact that almost all of the large real networks, like the network of a country, are represented in software like DigSilent or PSSE. Thus, all of the data of the network are stored in this software. While, the available application used for the optimization of PSS parameters is ALICE that is developed in MATLAB. It means that all of the data coming from the network, and consequently DigSilent, must be readable for MATLAB.

Therefore, even if the main goal of this chapter is to optimize PSS parameters of a large network, during this process we will have to deal with other issues, such as exporting the data of the power plants from DigSilent, converting them into readable data for MATLAB, importing them in MATLAB and so on. As a result, the best way to go on with this chapter is to, first explain a work flow of the process, and then go into the details with each part, and finally the results of the optimization can be reached. The optimization results consist of the tuned parameters of PSSs and also the outcome of simulations as are shown in different figures.

5.1 Outline of the Optimization Process

The optimization process can be cast in different steps as follows:

- Load the network in DigSilent
- The "Modal Analysis" followed by "Initial Conditions"
- Calculate "eigenvalues" and "eigenvectors" of the system
- Analyze the controllability and participation factor of each power plant in each eigenvalue, in order to identify the plants that have to be optimized
- Export the data of power plants as .CSV files
- Conversion of .CSV files into .MAT files to be readable for MATLAB and consequently for ALICE
- Local optimization and pre-global optimization using ALICE
- Export the optimized parameters from ALICE to have them in .MAT files
- Conversion of .MAT files into .CSV files to be readable for DigSilent
- Import the optimized parameters into DigSilent and change the previous parameters
- Execute "Modal Analysis" again to check the results of the eigenvalues after optimization

Before we go into details with each step and see the whole process, it can be beneficial if we visualize this process in a flow chart, as it is depicted in *Figure 5-1*.
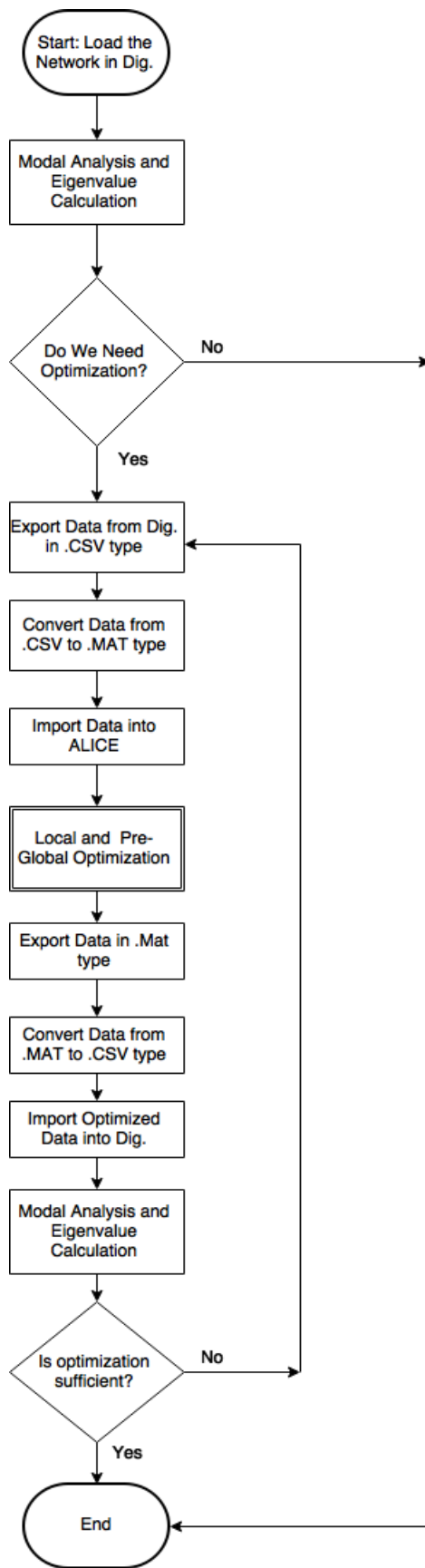
Figure 5-1 optimization process flow chart

5.2 Real Network Optimization

As it was mentioned before, the activity involves the development of a software product for the optimization of the PSS parameters of the electrical power plants of large networks. The large network used in this thesis is the Chilean network.[1] All of the data of the network, such as the network diagram (transmission and distribution lines and etc.), parameters of SCR, AVR and PSS, future developments and etc. are given in DigSilent.

According to the section 3.1, "eigenvalue analysis" is a very powerful tool to investigate the stability of a power system. Eigenvalues and eigenvectors of a dynamic multi-machine system can be calculated by the "Modal Analysis" command in DigSilent.[2]

5.2.1 Network details

In the Chilean network, used in this thesis, there are 70 power plants. Between these plants, 12 of them are facilitated with PSSs that are in service, and in 15 power plants AVR is available and in service.

Regarding to the network, the very first concern that comes up is that some of the AVRs and PSSs that are utilized are not the IEEE standard types whereas as it was already mentioned, there are 23 types of AVRs and 9 types of PSSs in ALICE that are all standard types. Thus, for our purpose it was better to modify the ones in the network in accordance with the IEEE standards. The best way is to match the real controllers in the network with the most similar IEEE standard one. As a result, after matching all of the existing AVRs and PSSs in the network, there are 12 PSSs including four different standard types. The same modifications was applied to the AVRs resulting in 15 AVRs with two different standard types.

In *Table 5-1*, different types of PSSs and AVRs that are utilized in the Chilean network are presented.

---

[1] Note that the first network used for the optimization was another large network, but due to copy right issues we report only the results of the Chilean network that is publicly shared in internet.
[2] A brief explanation about modal analysis and eigenvalue calculation in DigSilent is given in Appendix A.

Table 5-1 AVR and PSS types in Chilean network

PSS types	AVR types
standard	standard
PSS2B	AC4A
Ansaldo	---
ABBeGE2	---

5.2.2 Modal analysis and eigenvalues calculation: pre-optimized network

To analyze the stability of the network, the modal analysis is executed and following that the calculation of eigenvalues of the system is carried out. According to the first step of the process, it is required to analyze the eigenvalues of the system. The eigenvalue presentation of the network, before optimization, is shown in *Figure 5-2*. In this *Figure 5-2*, there are two pink lines that are representing the damping ratio limitations of 5 and 20%. As it is explained in 3.3, for inter-area oscillation modes, the minimum acceptable value of ζ is 5%, but for local modes this value is 20%. Thus, the oscillating modes with the frequency range of 0.1 to 1Hz must be in the left side of the line corresponding to 5% damping ratio, and the modes with the frequency range of 1 to 2Hz must be in the left side of the line which is representing 20% damping ratio.
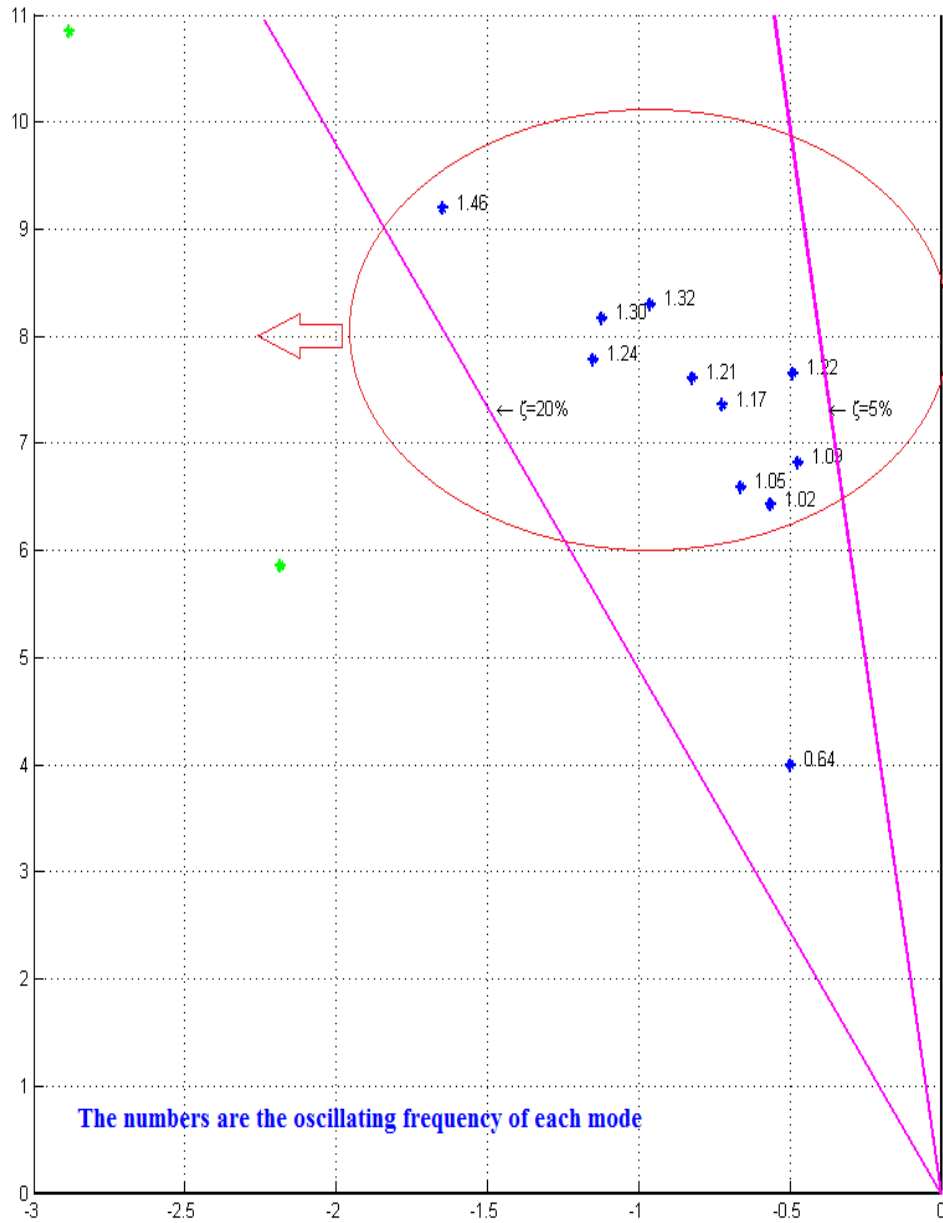
Figure 5-2 Eigenvalues of the Chilean network, before optimization

Figure 5-2 shows that between the local modes, just two of them are in the left side of the 20% line; therefore, all of the other eigenvalues must be shifted to the left side, after optimization. This is the reason which states that the optimization is compulsory for this

network. The next step is to check which power plants are mostly participating in those eigenvalues. This participation together with the controllability of that eigenvalue can give us very useful and effective information about the power plants that their PSS parameters must be tuned.

Consequently, after understanding the fact that the network has to be optimized, the eigenvalue analysis will inform us about the PSSs which must be optimized. According to *Figure 5-2*, there are 10 eigenvalues that are in the right side of the 20% line. In *Figure 5-3* to *Figure 5-6*, the participation factors of some[1] of these local modes are given.
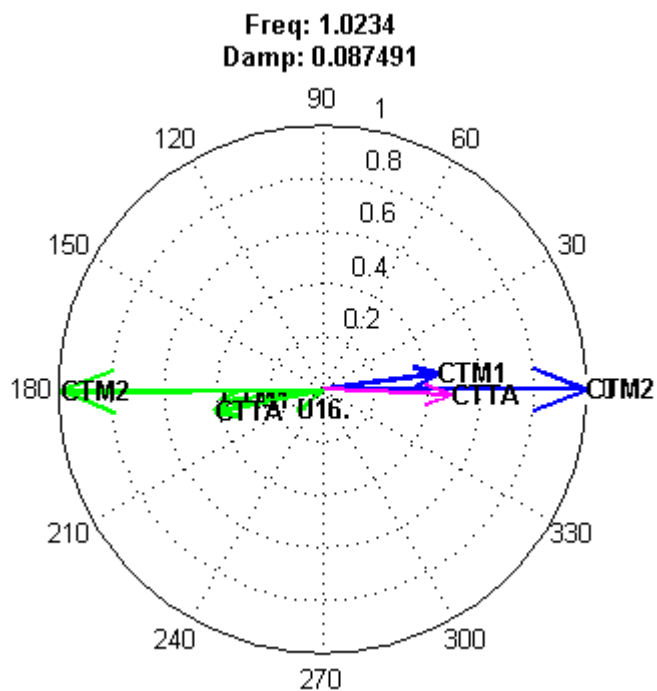
Figure 5-3 participation factor of different plants for the frequency mode of 1.023Hz, before optimization

In *Figure 5-3* to *Figure 5-6* the participation factors are shown in a polar plane. The names written on the figures are the names of the plants which are contributing in that frequency mode. As it can be seen, there are some circles with different radii depicted by dots and one circle with a bold line which has unity radius. The radius shows the amplitude of participation of each plant that is normalized to the biggest participation amplitude.

---

[1] In reality and in the course of the thesis, the participation factors for all local modes are calculated with the related profiles achieved. But since the number of figures for all modes exceeds 20, here, for the sake of brevity, a group of them are reported.

The phase of participation factor represents the direction of each contribution. For example, in *Figure 5-5*, plants U12 and U13 have 180° phase difference. It means that they have exactly opposite signs, so they affect in opposite directions.
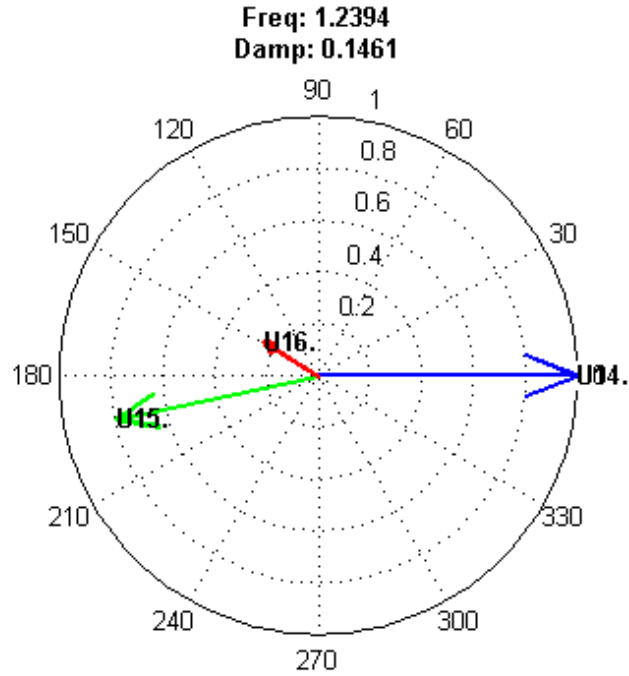
Figure 5-4 participation factor of different plants for the frequency mode of 1.239Hz, before optimization
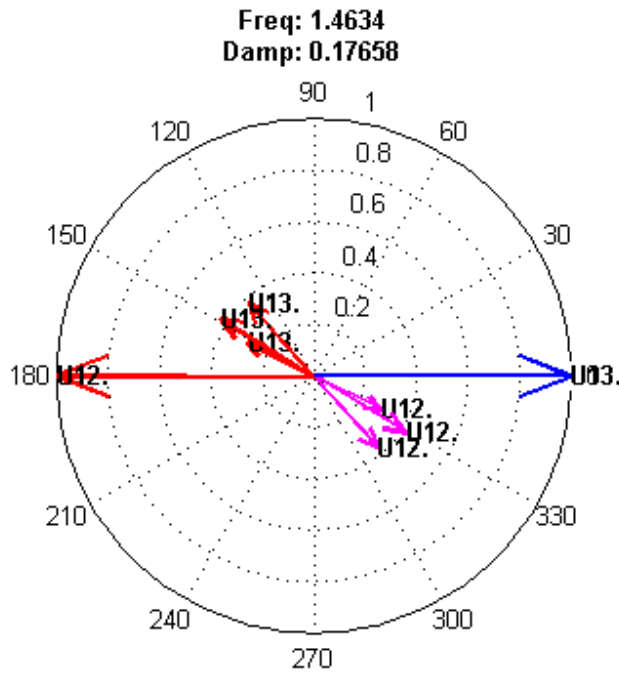
Figure 5-5 participation factor of different plants for the frequency mode of 1.463Hz, before optimization
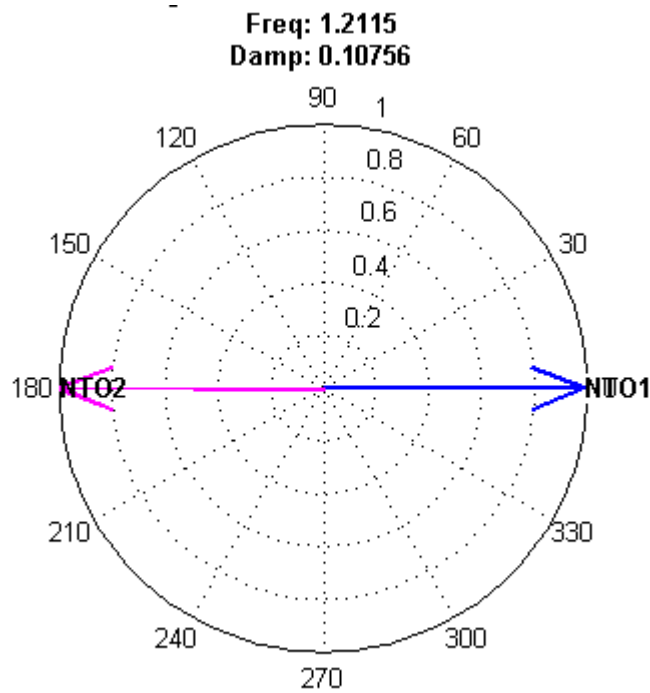
Figure 5-6 participation factor of different plants for the frequency mode of 1.211Hz, before optimization

According to participation factors, all eigenvalues that are highlighted in *Figure 5-2* are actually due to only 11 power plants in the network. It means that from 70 power plants in the network, just 11 of them are affecting these local modes. Thus, in some power plants, PSS is not necessary (at least at the moment, with existing generators and loads). Between the power plants that have a participation in the local mode oscillations of poor damping, some of them have PSS (5 plants), and the rest are realized without any PSS in the reality.

Consequently, our process of optimization can be divided into two phases. First, the network will be optimized using the existing PSSs of the real network, and the results will be illustrated. Then, it will be shown that following the first phase, there are still some modes of local oscillations that are not shifted to the left side, since their correspondent plants do not have any PSS to be optimized. As a result, the second phase of the optimization that will be discussed in the next section is to add some hypothetical PSSs to the power plants in which there is no PSS, but we know -by eigenvalue analysis- that they have a high participation in the local oscillation modes of poor damping. In *Table 5-2*, the names of the power plants which are participating in local oscillations are reported together with availability of PSS in that power plant.

Before starting the optimization of existing PSSs, it is worthwhile to remark that some of the essential functions for converting the data from .CSV to .MAT and vice versa, together with the main function of local optimization are represented in Appendix B.

Table 5-2 power plants participating in local oscillations and their PSS availability

Power Plant	PSS availability
U-12	No
U-13	No
U-14	No
U-15	No
U-16	Yes
NTO1	Yes
NTO2	Yes
CTTAR	No
CHAP	No
CTM1	Yes
CTM2	Yes

5.2.3 Modal analysis and eigenvalues calculation: optimized network

Starting from the first phase of optimization, the existing PSSs of the network will be optimized to have the tuned parameters. After accomplishment of optimization, eigenvalues of the system are calculated as a result of modal analysis performance. Eigenvalues of the optimized network are depicted in *Figure 5-7*.
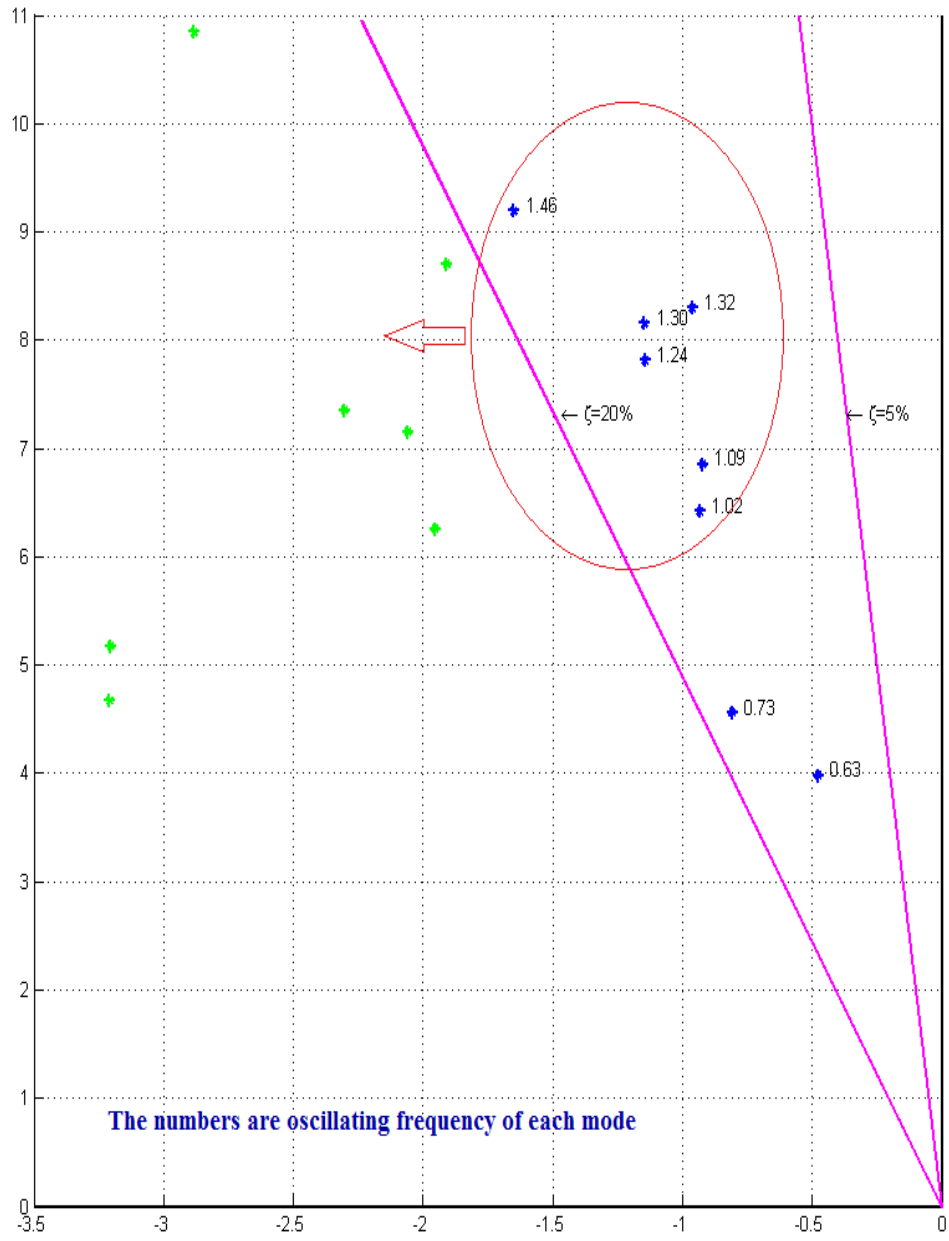
Figure 5-7 eigenvalue of the Chilean network, after optimization of existing PSSs

A better eye-casting on *Figure 5-7* reveals the ensued major points:

- After the first phase of optimization, five eigenvalues are shifted to the green area, which means that now they have a damping ratio of more than 20%.

- There are still six eigenvalues that are oscillating with local frequency, and damping ratio of less than 20%.

The occurrence of these latter points can be well justified by the participation factors corresponding to each eigenvalue. Similar to the previous case, it is possible to calculate participation of power plants into each eigenvalue. Considering these participations, the eigenvalues that are shifted to the left side of the line are those in which the corresponding power plants have PSS inside, and in contrary, those eigenvalues that did not shift to the green area are due to power plants in which PSS is not available. It can be proved by looking at the figures of participation factors of local modes after optimization. Again for the sake of brevity some of the figures are represented in this thesis. *Figure 5-8* and *Figure 5-9* illustrate both participation factors and controllability of two oscillating modes.
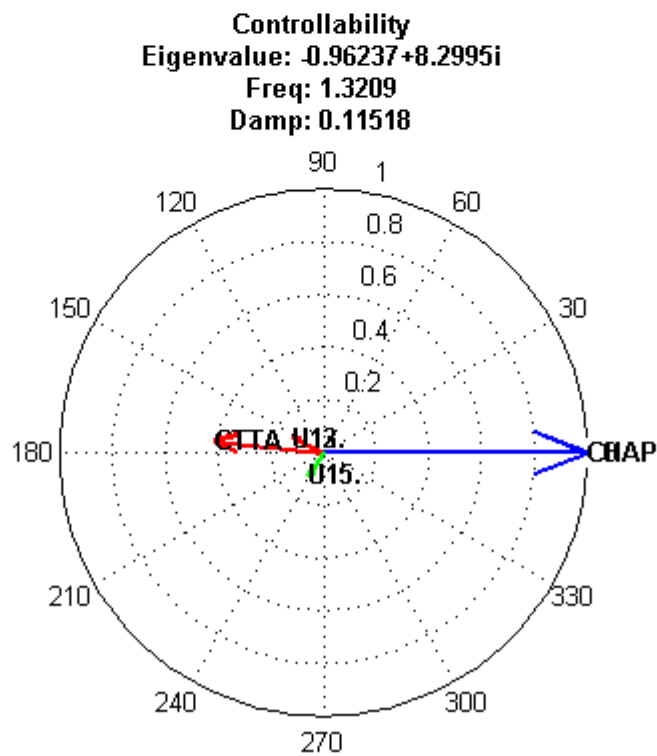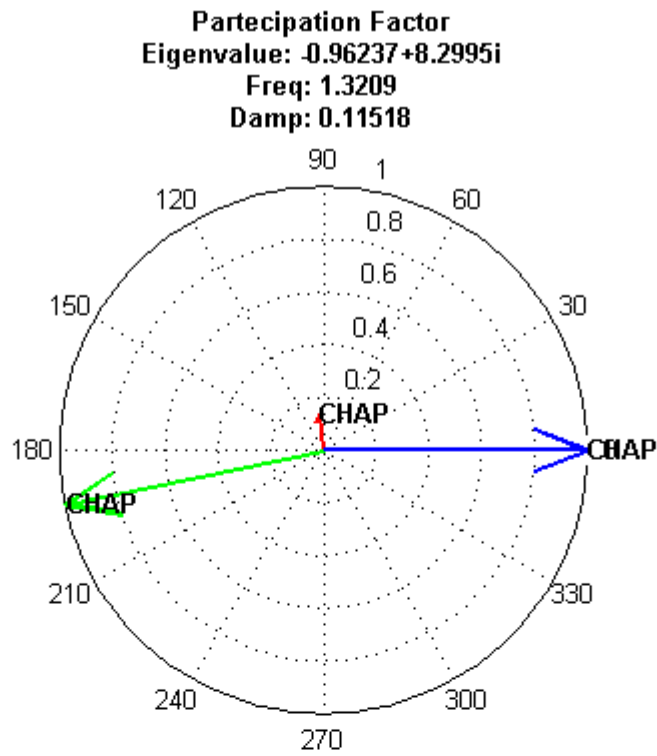
Figure 5-8 participation factor and controllability of different plants for the frequency mode of 1.3209Hz, after optimization of existing PSSs
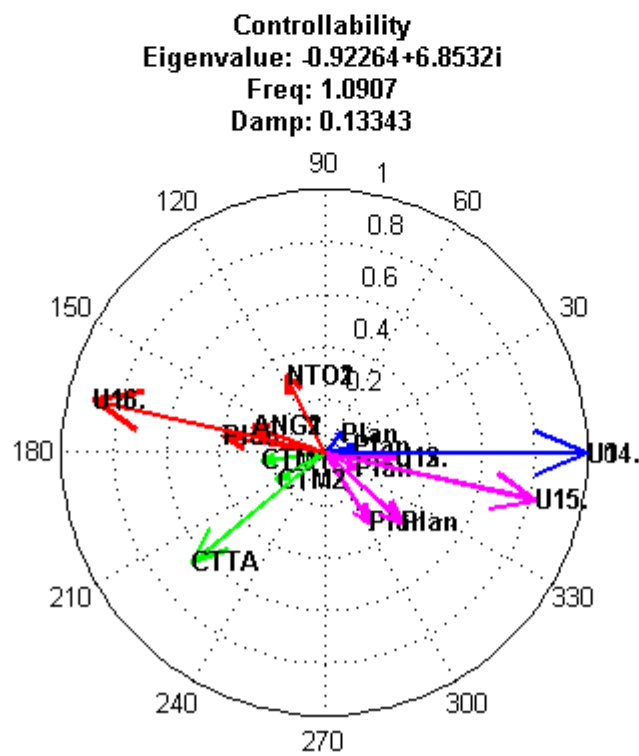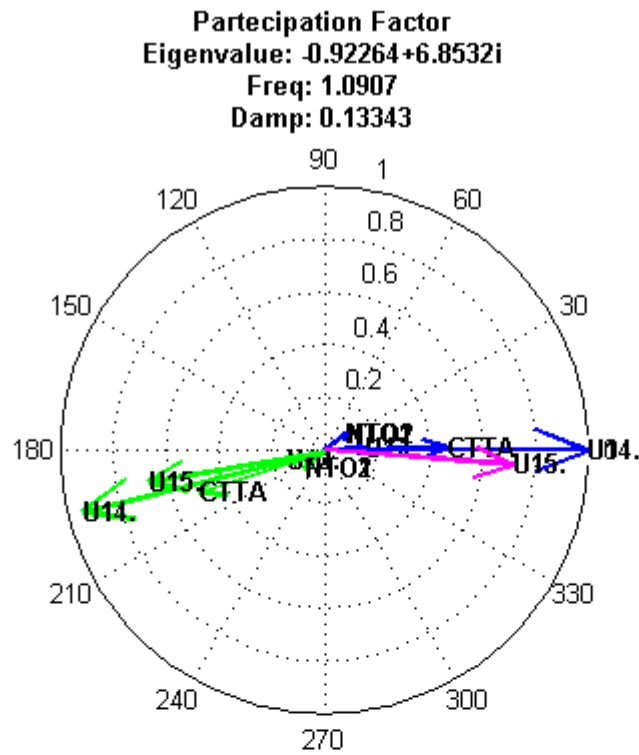
Figure 5-9 participation factor and controllability of different plants for the frequency mode of 1.0907Hz, after optimization of existing PSSs

5.2.4   **Finalization of the results**

The optimization of existing PSSs in the Chilean network leads us to the following results:

- Improvement of those damping ratios which their eigenvalue is due to the power plants equipped with PSS.
- Recognition of the power plants in which PSS is necessary in order to maximize the damping ratios of the system.
- Necessity of adding some new PSSs to the power plants that are participating in the local oscillating modes. Thus, this investigation is able to address future intervention on the network to enhance stability.

5.3 Stability Enhancement: hypothetical new PSSs

As it has been declared in the previous section, the optimization of the network using the existing PSSs cannot be sufficient, since there are still some eigenvalues that are not influenced by current PSSs. As a result, an advantageous modification that can be done in this network is to add new PSSs to the power plants that are recognized in the former section.

According to the participation factors after optimization, the power plants in which a PSS is beneficial, but it is not available, are as follows:

Power plants without PSS installation: U-12, U-13, U-14, U15, CTTAR, CHAP.

To be sure that this procedure leads us to the stability enhancement, first of all just two PSSs are added to the plants U-12 and U-13. In *Figure 5-10*, it is exposed that the eigenvalue with frequency of 1.46Hz is just controllable by the plants U-12 and U-13, and at the same time its damping ratio is 17% which must be increased. Consequently, by adding two PSSs to these two plants, we expect that this eigenvalue will be shifted to the left side of the 20% line.
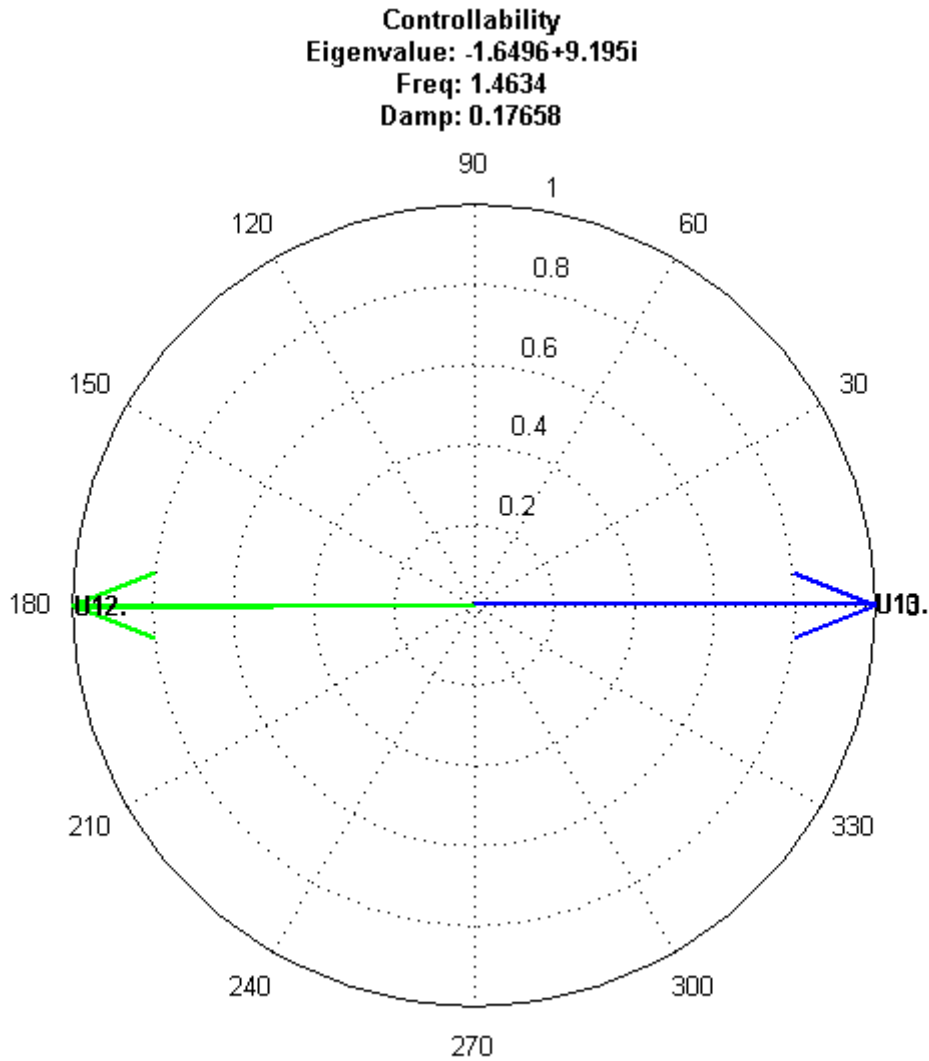
Figure 5-10 controllability of the plants U-12 and U-13 on the eigenvalue with frequency of 1.463Hz

In *Figure 5-11*, the result of eigenvalue calculations after adding two PSSs to the plants U-12 and U-13 is shown. Of course, also these PSSs are tuned in the same way as the other ones. *Figure 5-11* is perfectly proving the fact that just by adding PSSs to the plants that are participating in an eigenvalue, maximization of the damping ratio – correspondent to that eigenvalue- can be achieved.
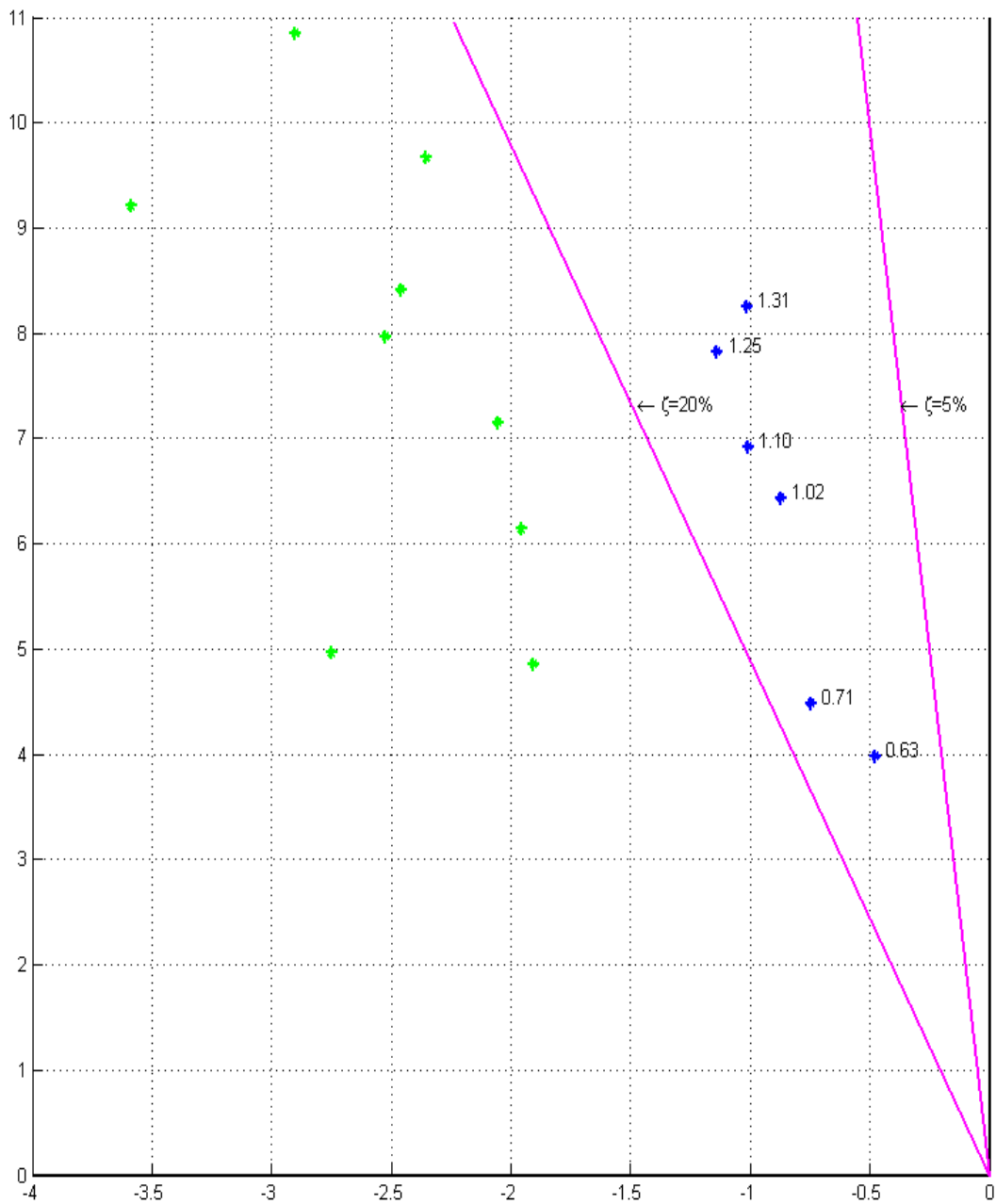
Figure 5-11 eigenvalues representation after optimization of existing PSSs and implementation of PSSs to plants 'U-12' and 'U-13'

This claim is truly verified thanks to *Figure 5-11*. As it can be seen in this figure, not only the mentioned eigenvalue with frequency of 1.46Hz is shifted to the left side of the 20% line, but also other eigenvalues which were totally or partially controlled by these plants, are improved completely or moderately, respectively.

So far the efficiency of adding new PSSs to those plants that are participating in the poorly damped modes is clarified. Thus, the procedure can be continued until all of the eigenvalues with damping ratio of less than 20% will be shifted to the left side.

This method has been applied to the rest of the plants in which PSS is not realized, but according to the modal analysis, it is needed. The new modal analysis with the presence of added PSSs will result in a completely optimized network as the point of view of the local oscillations. The eigenvalue representation after the final optimization is given in *Figure 5-12*. This figure is illustrating that all of the local modes are shifted to the left side of the 20% limitation line; therefore we can assert that the Chilean network is entirely locally optimized.
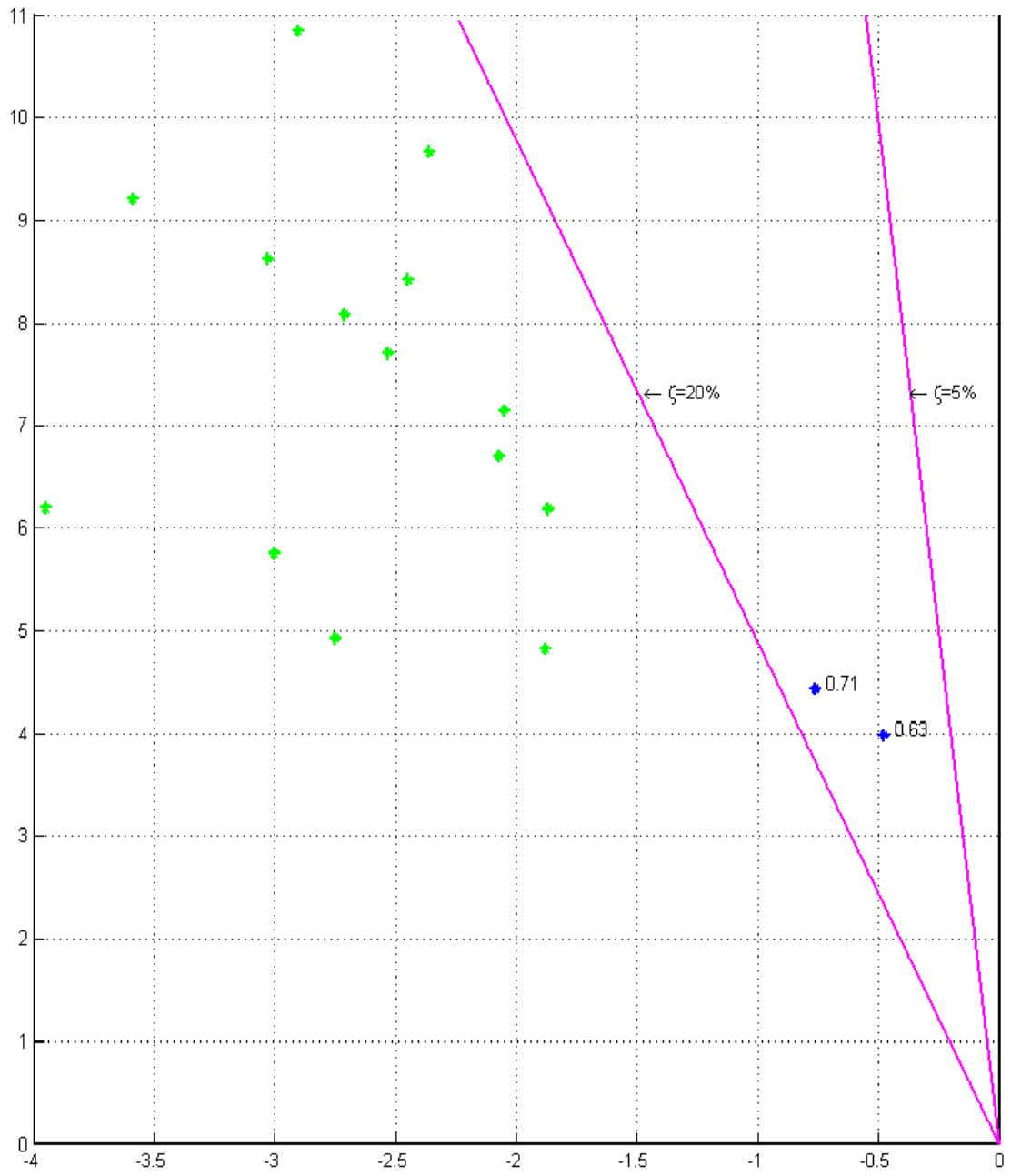
Figure 5-12 eigenvalues representation after optimization of existing PSSs and implementation of six new PSSs

6 Conclusion

This thesis addressed some methods of tuning of power system stabilizers for the damping of the electromechanical oscillations in power systems. The thesis work focused on three key issues, namely: the electromechanical oscillations problem which is worsened by using fast automatic voltage controllers, adding PSS to increase the damping of these oscillations and fine-tuning of the present PSSs to maximize the damping.

In the two first chapters the problem together with its cause and the solution to decrease it was discussed. Although this thesis dealt with all of the above-mentioned issues, the main goal was to maximize the damping of oscillations by finding the best tuning of the PSS parameters. This goal was sought in chapter 3 and 4. Finally in chapter 5, a practical network was optimized. The importance of the maximization of the damping was represented by observing the response of the rotor angle and active power of the synchronous generator to a step increment of the reference voltage. Eigenvalue analysis of pre-optimized and optimized network together with the participation factors of different power plants in each oscillating mode indicates that the optimization of PSS parameters could lead us to have well-damped electromechanical oscillations which were due to power plants with available PSS. On the other hand for those oscillation modes which are due to power plants without any PSS to decrease their influence in that mode, it was necessary to first, add a PSS in that plant, and then to optimize its parameters.

Considering the mentioned conclusion and the results of the optimization of the PSSs in the results provided for the Chilean network, it is possible to notice that in a real case sometimes the installation of a non-adequate power system stabilizer for a power plant with a certain type of controllers does not provide the expected results in terms of damping, since they are not affecting any oscillating mode. Thus, in Chilean network, in some power plants PSS are installed even if from our analysis it results that it is unnecessary (at least with the current power generation and demand and configuration of the network). Instead, it is needed in some other power plants, while it is unavailable.

According to the previous conclusion about Chilean network, in this thesis, we tried to add also some hypothetical PSSs to those power plants which are participating to the oscillating modes. The eigenvalue analysis perfectly demonstrates that with the new PSSs all of the eigenvalues are shifted to the left side of the 20% limitation line.

Therefore, a feasible conclusion has to consider both the electrical and economical aspects as seen for the Chilean network. Since this thesis clarifies that, to have a completely optimized network, PSS is not required in all power plants but they can be installed only in specific ones identified by the modal analysis. Thus, knowing which plants are participating in each oscillating mode, it is possible to find the minimum number of PSSs in order to have an "optimized" network.

This thesis focused its attention in particular on the optimization of local oscillation modes, but the next step for further improvements and developments in the proposed method for the optimization of electromechanical oscillations is to develop the methodology for the global optimizations, in order to increase also the damping on the inter-area modes. It is worthwhile to mention that the aim of this thesis was to increase the damping of the local modes but without neglecting completely the inter-area modes.

To analyse the inter-area oscillation it has been used the criterion of the analysis of transfer function phase between the generating unit speed and the electrical active power. This method is very useful for evaluating the effectiveness of the PSS parameterization. The objective of the optimization of the PSS, in fact, can also be expressed by saying that this must be calibrated so that its phase contribution is sufficient to compensate, all or at least in part, the phase difference between speed and electric active power. In particular, this compensation should be effective in the electromechanical oscillations frequency range (0.1-2 Hz) to smooth them. Therefore, while performing the local mode optimization it was also set the phase of the transfer function between +/-30° around 0° in the band of interest, in order to consider also the inter-area modes and prepare the network for the global optimization.

Appendix A

Modal Analysis / Eigenvalue Calculation

Introduction

The Modal Analysis command calculates the eigenvalues and eigenvectors of a dynamic multi-machine system including all controllers and power plant models. This calculation can be completed at the beginning of a transient simulation and at every time step when the simulation is stopped. Note that sometimes, in the literature, Modal Analysis is referred to as Eigenvalue Calculation or Small Signal Stability. Throughout, this appendix the calculation will generally be referred to as Modal Analysis. This appendix provides a brief background on the theory of Modal Analysis.

Theory of Modal Analysis

The calculation of eigenvalues and eigenvectors is the most powerful tool for oscillatory stability studies. When doing such a study, it is highly recommended to first compute the "natural" system oscillation modes. These are the oscillation modes of the system when all controller and power plant models are deactivated so every synchronous machine will have constant turbine power and constant excitation voltage. After determining these 'natural' modes, the effects of controllers (structure, gain, time constants etc.) and other models can be investigated.

After the initial conditions have been calculated successfully, which means that all time-derivatives of the state variables should be zero (the system is in steady state), or the simulation has been stopped at a point in time, the modal analysis calculates the complete system A-matrix using numerical, iterative algorithms. The representation of the electro-dynamic network model is equivalent to the representation used for the balanced RMS simulation, except for the general load model, for which the frequency dependencies are neglected.

The computation time for the Modal Analysis is approximately proportional to the number of state space variables to the power of three. Considering, that most power system objects and models will contain several (perhaps up to a dozen or more for some complex controllers), the calculation time can rapidly increase as the size of the system being considered increases. For this reason, alternative methods for calculating the system eigenvalues and eigenvectors must be used when the system grows very large.

A multi-machine system exhibits oscillatory stability if all conjugate complex eigenvalues making up the rotor oscillations have negative real parts. This means that they lie in the left complex half-plane. Electromechanical oscillations for each generator are then stable.

More formally, assuming that one of the conjugate complex pair of eigenvalues is given by:

$$\lambda_i = \sigma_i \pm jw_i$$

then the oscillatory mode will be stable, if the real part of the eigenvalue is negative

$$\sigma_i < 0$$

The period and damping of this mode are given by:

$$T_i = \frac{2\pi}{w_i}$$

$$d_i = -\sigma_i = \frac{1}{T_p} \ln(\frac{A_n}{A_{n+1}})$$

where A_n and A_{n+1} are amplitudes of two consecutive swing maxima or minima respectively.

The oscillatory frequencies of local generator oscillations are typically in the range of 0.5 to 5 Hz. Higher frequency natural oscillations (those that are not normally regulated), are often damped to a greater extent than slower oscillations. The oscillatory frequency of the between areas (inter-area) oscillations is normally a factor of 5 to 20 times lower than that of the local generator oscillations.

The absolute contribution of an individual generator to the oscillation mode which has been excited as a result of a disturbance can be calculated by:

$$\overrightarrow{w(t)} = \sum_{i=1}^{n} c_i \, \overrightarrow{\phi_i} \, e^{\lambda_i \cdot t}$$

where:

$\overrightarrow{w(t)}$ generator speed vector

λ_i i'th eigenvalue

$\overrightarrow{\phi_i}$ i'th right eigenvector

c_i magnitude of excitation of the i'th mode of the system (at t=0)
(depending on the disturbance)

n number of conjugate complex eigenvalues (i.e. number of generators-1)

In the following c is set to the unit vector, i.e. c = [1,...,1], which corresponds to a theoretical disturbance which would equally excite all generators with all natural resonance frequencies simultaneously.

The elements of the eigenvectors $\overrightarrow{\phi_i}$ then represents the mode shapes of the eigenvalue i and shows the relative activity of a state variable, when a particular mode is excited. For example, the speed amplitudes of the generators when an Eigen-frequency is excited whereby those generators with opposite signs in $\overrightarrow{\phi_i}$ oscillate in opposite phase.

The right eigenvectors $\overrightarrow{\phi_i}$ can thus be termed the "observability vectors". The left eigenvectors $\overrightarrow{\phi_i}$ measures the activity of a state variable x in the i'th mode, thus the left eigenvectors can be termed the "relative contribution vectors".

Normalization is done by assigning the generator with the greatest amplitude contribution the relative contribution factor 1 or -1 respectively.

For a n-machine power system, n-1 generator oscillation modes will exist and n-1 conjugate complex pairs of eigenvalues λ_i will be found. The mechanical speed ω of the n generators will then be described by:

$$\begin{bmatrix} w_1 \\ w_2 \\ \dots \\ w_n \end{bmatrix} = c_1 \cdot \begin{bmatrix} \phi_{11} \\ \phi_{12} \\ \dots \\ \phi_{1n} \end{bmatrix} \cdot e^{\lambda_1 \cdot t} + c_2 \cdot \begin{bmatrix} \phi_{21} \\ \phi_{22} \\ \dots \\ \phi_{2n} \end{bmatrix} \cdot e^{\lambda_2 \cdot t} + \dots + c_2 \cdot \begin{bmatrix} \phi_{n1} \\ \phi_{n2} \\ \dots \\ \phi_{nn} \end{bmatrix} \cdot e^{\lambda_n \cdot t}$$

The problem of using the right or left eigenvectors for analyzing the participation of a generator in a particular mode i is the dependency on the scales and units of the vector elements. Hence the eigenvectors ϕ_i and ψ_i are combined to a matrix **P** of participation factor by:

$$\underline{P_i} = \begin{bmatrix} P_{1i} \\ P_{2i} \\ \dots \\ P_{ni} \end{bmatrix} = \begin{bmatrix} \phi_{1i} \cdot \psi_{i1} \\ \phi_{2i} \cdot \psi_{i2} \\ \dots \\ \phi_{ni} \cdot \psi_{in} \end{bmatrix}$$

The elements of the matrix pij are called the participation factors. They give a good indication of the general system dynamic oscillation pattern. They can be used to determine the location of eventually needed stabilizing devices to influence the system damping efficiently. Furthermore, the participation factor is normalized so that the sum for any mode is equal to 1.

When are modal analysis results valid?

A modal analysis can be started when a balanced steady-state condition is reached in a dynamic calculation. Normally, such a state is reached by a balanced load-flow calculation, followed by a calculation of initial conditions. However, it is also possible to

do a balanced RMS simulation and start a modal analysis after the end of a simulation or during a simulation when you have manually stopped it.

Although, the modal analysis can be executed at any time in a transient simulation it is not recommended that you do so when the system is not in a quasi-steady state. This is because each modal analysis is only valid for a unique system operating point. Furthermore, the theory behind modal analysis shows that the results are only valid for 'small' perturbations of the system. So although you can complete a modal analysis during a large system transient, the results obtained would change significantly if the analysis was repeated a short time step later when the operating point of the system would be significantly different.

Appendix B

Essential Functions for Local Optimization

According to chapter 5.1, the process of optimization includes export of the data from DigSilent, a conversion process from .CSV to .MAT and so on. In this chapter the main functions that are written in MATLAB are represented. Those functions written in DigSilent are skipped for the sake of brevity.

Conversion from .CSV to .MAT[1]:

```matlab
function csv_or_xls2parmodel_iter(use_csv,default_folders,input_folder,output_folder)

if ~default_folders
    input_folder = uigetdir;
elseif default_folders && nargin < 4
    input_folder = 'csv_input';
    output_folder = 'mat_input';
end

if use_csv
    path(input_folder,path);
    path(output_folder,path);

    D = dir([input_folder, '\*.csv']);

    for i = 1:size(D,1)
        filename_p = eval(['D(i,1).','name']);
        filename = filename_p(end-6:end);
        if strcmp(filename,'SCR.csv')
            main_filename = filename_p(1:end-8);
            for j = 1:size(D,1)
                filename_p1 = eval(['D(j,1).','name']);
                name_len = length(main_filename)+4;
                if length(filename_p1) >= name_len
                    filename1 = filename_p1(1:name_len);
                    if strcmp([main_filename '_avr'],filename1)
                        AVR_data = importdata(filename_p1);
                        %% getting AVRType
                        SCR_name_length = length(main_filename)+6;
                        AVRType_char = filename_p1(SCR_name_length:end-4);
                        AVR_Type = {{AVRType_char}};

                    elseif strcmp([main_filename '_pss'],filename1)
```

---

[1] This function is also able to convert .XLSX files to .MAT files.

```matlab
                    PSS_data = importdata(filename_p1,';');
                    %% getting PSSType
                    SCR_name_length = length(main_filename)+6;
                    PSSType_char = filename_p1(SCR_name_length:end-4);
                    PSS_Type = {{PSSType_char}};
                elseif strcmp([main_filename '_SCR'],filename1)
                    SCR_data = importdata(filename_p1);
                end
            end
        end

        %% SCR structure
        nums_SCR_doub = SCR_data.data;
        fieldnames_SCR = SCR_data.rowheaders;
        nums_SCR_cell = num2cell(nums_SCR_doub);
        SCR = cell2struct(nums_SCR_cell,fieldnames_SCR);

        %% AVR structure
        nums_AVR_doub = AVR_data.data;
        fieldnames_AVR = AVR_data.rowheaders;
        nums_AVR_cell = num2cell(nums_AVR_doub);
        AVR1 = cell2struct(nums_AVR_cell, fieldnames_AVR);
        AVR = struct(AVRType_char,AVR1);

        %% PSS structure
        nums_PSS_doub = PSS_data.data;
        fieldnames_PSS = PSS_data.rowheaders;
        if strcmp(PSSType_char,'PSS2B')
            fieldnames_PSS(18) = {'MM'};
            fieldnames_PSS(19) = {'NN'};
            fieldnames_PSS(20) = {'w_in'};
            fieldnames_PSS(21) = {'kw'};
            fieldnames_PSS(22) = {'kf'};
            fieldnames_PSS(23) = {'kp'};
            nums_PSS_doub(20) = 1;
            nums_PSS_doub(21) = 0;
            nums_PSS_doub(22) = 0;
            nums_PSS_doub(23) = 0;
        end
        if strcmp(PSSType_char,'PSS4B')
            fieldnames_PSS(52) = {'kt'};
            fieldnames_PSS(53) = {'w_in'};
            fieldnames_PSS(54) = {'RR'};
            fieldnames_PSS(55) = {'FL'};
            fieldnames_PSS(56) = {'FI'};
            fieldnames_PSS(57) = {'FH'};
            fieldnames_PSS(58) = {'kw'};
            fieldnames_PSS(59) = {'kf'};
            fieldnames_PSS(60) = {'kp'};
            nums_PSS_doub(52) = 1;
            nums_PSS_doub(53) = 1;
            nums_PSS_doub(54) = 1.2;
            nums_PSS_doub(55)        =       1/(2*pi*nums_PSS_doub(2)*nums_PSS_doub(54));
%%nums_PSS_doub(2) is the value of Tl2
            nums_PSS_doub(56)       =       1/(2*pi*nums_PSS_doub(19)*nums_PSS_doub(54));
%%nums_PSS_doub(19) is the value of Ti2
            nums_PSS_doub(57)       =       1/(2*pi*nums_PSS_doub(36)*nums_PSS_doub(54));
%%nums_PSS_doub(36) is the value of Th2
            nums_PSS_doub(58) = 1;
            nums_PSS_doub(59) = 0;
            nums_PSS_doub(60) = 0;
        end
        nums_PSS_cell = num2cell(nums_PSS_doub);
        PSS1 = cell2struct(nums_PSS_cell, fieldnames_PSS);
        PSS = struct(PSSType_char,PSS1);

        %% building sat_quad
        sat_quad                                                            =
struct('kwmin',0,'kwmax',5,'kfmin',0,'kfmax',10,'kpmin',0,'kpmax',5);

        %% building par
        par1 = struct('SCR',SCR,'sat_quad',sat_quad,'AVR',AVR,'PSS',PSS);
        par = {par1}; %%we need a structure inside a cell
```

124

```matlab
            %% getting AVR type
            AVRType = {AVR_Type};

            %% getting PSS type
            PSSType = {PSS_Type};

            %% finding the order of the machine
            if   (par{1}.SCR.Tqp==0  &&  par{1}.SCR.Tqop==0  &&  par{1}.SCR.Tds==0  &&
par{1}.SCR.Tdos==0 && par{1}.SCR.Tqs==0 && par{1}.SCR.Tqos==0)
                macch_type = '3° ordine';
            elseif  (par{1}.SCR.Tqp==0  &&  par{1}.SCR.Tqop==0  &&  par{1}.SCR.Tds==0  &&
par{1}.SCR.Tdos==0)
                macch_type = '4° ordine';
            elseif (par{1}.SCR.Tqp==0 && par{1}.SCR.Tqop==0)
                macch_type = '5° ordine modello B';
            elseif (par{1}.SCR.Tqp==0 && par{1}.SCR.Tds==0 && par{1}.SCR.Tdos==0)
                macch_type = '5° ordine modello A';
            else
                macch_type = '6° ordine';
            end


            %% building parmodel_1
            parmodel = struct('macch_type',macch_type,'cen',[NaN],'gen',[1 1],...
                'par',par,'xe',[0.2500],'AVRType',AVRType,'PSSType',PSSType); %#ok<NBRAK>

            %% completing the par structure for synchronous machines
            sub_handles_tmp = struct('env_type','mono','parmodel',parmodel);
            xe = 0.25;
            gen1 = 1;
            par2 = calcola_var_dipendenti(sub_handles_tmp,par,xe,gen1);
            par{1} = par2;

            %% building parmodel_2
            parmodel = struct('macch_type',macch_type,'cen',[NaN],'gen',[1 1],...
                'par',par,'xe',[0.2500],'AVRType',AVRType,'PSSType',PSSType);
%#ok<NBRAK,NASGU>

            sub_handles.use_hmi=0;
            sub_handles.AVRType=parmodel.AVRType;
            sub_handles.PSSType=parmodel.PSSType;
            parmodel.par = check_AVR_par(sub_handles, parmodel.par, parmodel.gen);
            parmodel.par = check_PSS_par(sub_handles, parmodel.par, parmodel.gen);

            %% writing the .mat file
            main_filename_with_par = [main_filename '_par'];
            if default_folders
                currentFolder = pwd;
                cd(output_folder);
                save(main_filename_with_par,'parmodel');
                cd(currentFolder)
            elseif ~default_folders
                save (main_filename_with_par,'parmodel');
            end
        end
    end

else
    path(input_folder,path);
    D = dir([input_folder, '\*.xls']);
    for i = 1:size(D,1)
        SCR_name = eval(['D(i,1).','name']);
        xls_data = importdata(SCR_name);

        %% getting sheets names that are actually AVR and PSS types
        [status,sheets] = xlsfinfo(SCR_name); %#ok<ASGLU>
        AVR_Type_char = sheets{1,1};
        PSS_Type_char = sheets{1,2};
        AVR_Type_char_new = AVR_Type_char(5:end);
        PSS_Type_char_new = PSS_Type_char(5:end);
        AVR_Type = {{AVR_Type_char_new}};
        PSS_Type = {{PSS_Type_char_new}};

        %% SCR structure
```

```
            nums_SCR_doub = xls_data.data.SCR;
            fieldnames_SCR = xls_data.textdata.SCR;
            nums_SCR_cell = num2cell(nums_SCR_doub);
            fieldnames_SCR_trans = transpose(fieldnames_SCR);
            nums_SCR_cell_trans = transpose(nums_SCR_cell);
            SCR = cell2struct(nums_SCR_cell_trans,fieldnames_SCR_trans);

            %% AVR structure
            nums_AVR_doub = eval(['xls_data.data.' , AVR_Type_char]);
            fieldnames_AVR = eval(['xls_data.textdata.' AVR_Type_char]);
            nums_AVR_cell = num2cell(nums_AVR_doub);
            fieldnames_AVR_trans = transpose(fieldnames_AVR);
            nums_AVR_cell_trans = transpose(nums_AVR_cell);
            AVR1 = cell2struct(nums_AVR_cell_trans, fieldnames_AVR_trans);
            AVR = struct(AVR_Type_char_new,AVR1);

            %% PSS structure
            nums_PSS_doub = eval(['xls_data.data.' , PSS_Type_char]);
            fieldnames_PSS = eval(['xls_data.textdata.' PSS_Type_char]);
            nums_PSS_cell = num2cell(nums_PSS_doub);
            fieldnames_PSS_trans = transpose(fieldnames_PSS);
            nums_PSS_cell_trans = transpose(nums_PSS_cell);
            PSS1 = cell2struct(nums_PSS_cell_trans, fieldnames_PSS_trans);
            PSS = struct(PSS_Type_char_new,PSS1);

            %% building sat_guad
            sat_guad = struct('kwmina',0,'kwmax',20,'kfmin',0,'kfmax',10,'kpmin',0,'kpmax',1);

            %% building par
            par1 = struct('SCR',SCR,'sat_guad',sat_guad,'AVR',AVR,'PSS',PSS);
            par = {{par1}}; %%we need a structure inside a cell

            %% getting AVR type
            AVRType = {AVR_Type};

            %% getting PSS type
            PSSType = {PSS_Type};

            %% building parmodel
            parmodel         =         struct('macch_type','6°        ordine','cen',[NaN],'gen',[1
1],'par',par,'xe',[0.2500],'AVRType',AVRType,'PSSType',PSSType); %#ok<NBRAK,NASGU>
            sub_handles.use_hmi=0;
            sub_handles.AVRType=parmodel.AVRType;
            sub_handles.PSSType=parmodel.PSSType;
            parmodel.par = check_AVR_par(sub_handles, parmodel.par, parmodel.gen);
            parmodel.par = check_PSS_par(sub_handles, parmodel.par, parmodel.gen);

            %% getting the filename
            SCR_name_new = [SCR_name(1:end-4) '_par'];

            %% writing the .mat file
            if default_folders
                currentFolder = pwd;
                cd([currentFolder '\mat_intput']);
                save(main_filename_with_par,'parmodel'); %#ok<NODEF>
                cd ..
            elseif ~default_folders
                save (SCR_name_new,'parmodel');
            end
        end
    end
end
```

Conversion from .MAT to .CSV[1]:

```
function parmodel2csv_or_xls_iter(use_csv, default_folders,input_folder,output_folder)

if ~default_folders
```

---

[1] This function is also able to convert .MAT files into .XLSX files.

```matlab
        input_folder = uigetdir;
    elseif default_folders && nargin < 4
        input_folder = 'mat_output';
        output_folder = 'csv_output';
    end


path(input_folder,path);

%% counting the number of files inside the folder
D = dir([input_folder, '\*.mat']);

%% getting the file names
for i = 1 : size(D,1)
    filename = eval(['D(i,1).','name']);
    load(filename);
    parmodel_name = filename(1:end-8);

    %% suffix
    if use_csv
        suffix = '.csv';
    elseif ~use_csv
        suffix = '.xls';
    end

    SCRsuffix  = '_SCR';
    AVRsuffix  = '_avr_';
    PSSsuffix  = '_pss_';

    %% struct
    SCR_struct = parmodel.par{1}.SCR;
    AVR_struct = eval(['parmodel.par{1}.AVR.', cell2mat(parmodel.AVRType{1})]);
    PSS_struct = eval(['parmodel.par{1}.PSS.', cell2mat(parmodel.PSSType{1})]);

    %% filename for .csv
    SCR_filename = [parmodel_name SCRsuffix suffix];
    AVR_filename = [parmodel_name AVRsuffix cell2mat(parmodel.AVRType{1}) suffix];
    PSS_filename = [parmodel_name PSSsuffix cell2mat(parmodel.PSSType{1}) suffix];

    %% filename for .xls
    xls_filename = [parmodel_name suffix];

    %% cells
    SCR_cell = struct2cell(SCR_struct);
    AVR_cell = struct2cell(AVR_struct);
    PSS_cell = struct2cell(PSS_struct);

    names_SCR_struct = fieldnames(SCR_struct);
    names_AVR_struct = fieldnames(AVR_struct);
    names_PSS_struct = fieldnames(PSS_struct);

    %% some special modifications
    if strcmp(parmodel.PSSType{1},'PSS2B')
       names_PSS_struct(18) = {'M'};
       names_PSS_struct(19) = {'N'};
    end

    outSCR1 = [names_SCR_struct'; SCR_cell'];
    outAVR1 = [names_AVR_struct'; AVR_cell'];
    outPSS1= [names_PSS_struct'; PSS_cell'];

    outSCR = transpose(outSCR1);
    outAVR = transpose(outAVR1);
    outPSS = transpose(outPSS1);

    %% AVR and PSS type
    AVRType = cell2mat(parmodel.AVRType{1});
    PSSType = cell2mat(parmodel.PSSType{1});

    %% choosing between .xls or .csv
    if use_csv
        %% Csv writing
        if default_folders
            currentFolder = pwd;
            addpath(currentFolder);
```

```
            cd(output_folder);
            cell2csv(AVR_filename,outAVR,';');
            cell2csv(PSS_filename,outPSS,';');
            cell2csv(SCR_filename,outSCR,';');
            cd(currentFolder)
        elseif ~default_folders
            cell2csv(AVR_filename,outAVR,';');
            cell2csv(PSS_filename,outPSS,';');
            cell2csv(SCR_filename,outSCR,';');
        end
    else
        %% xls writing
        xlswrite(xls_filename,outAVR,['AVR_' AVRType]);
        xlswrite(xls_filename,outPSS,['PSS_' PSSType]);
        xlswrite(xls_filename,outSCR,'SCR');
        xls_delete_sheets(xls_filename);
    end
end
```

The main optimization function:

```
function local_optimization(gain1,gain2,backup_gain)

%% case of not having lead-lags
if nargin < 3
    if ~strcmp(gain2,'1ll') && ~strcmp(gain2,'2ll')
        backup_gain = gain2;
    else
        backup_gain = 'kf';
    end
end

%% path
root_dir=pwd;
lib_alice = [root_dir '\lib_alice\'];
path(lib_alice,path);
src_alice = [root_dir '\src_alice\'];
path(src_alice,path);
init_PSS = [root_dir '\src_alice\init_PSS\'];
path(init_PSS,path);
src_mono = [root_dir '\src_alice\src_mono\'];
path(src_mono,path);
sist_alice = [root_dir '\sist_alice\'];
path(sist_alice,path);
sist_mono = [root_dir '\sist_alice\sist_mono\'];
path(sist_mono,path);
parmodel2csv = [root_dir '\parmodel2csv_alice\'];
path(parmodel2csv,path);
mat_input = [root_dir '\parmodel2csv_alice\mat_input'];
path(mat_input,path);
mat_output = [root_dir '\parmodel2csv_alice\mat_output'];
path(mat_output,path);
csv_input = [root_dir '\parmodel2csv_alice\csv_xls_input'];
path(csv_input,path);
csv_output = [root_dir '\parmodel2csv_alice\csv_xls_output'];
path(csv_output,path);
errors = [root_dir '\parmodel2csv\errors'];

%% csv -> parmodel (csv_input > mat_input)
csv_or_xls2parmodel_iter(1,1,csv_input,mat_input);

%% single_parmodel_PSS_opt from mat_input
D = dir([mat_input, '\*.mat']);
for i = 1:size(D,1)
    filename = eval(['D(i,1).','name']);
    try
        single_parmodel_PSS_opt(gain1,gain2,backup_gain,[mat_input        '\'
filename],mat_output);
    catch ME
        disp(['Local Optimization failed for ' filename]);
        disp(ME);
```

```matlab
            disp(ME.message);
            disp(ME.stack);
            disp(ME.cause);
            copyfile([mat_input '\' filename],[errors '\' filename]);
        end
end

%% csv -> parmodel (mat_output > csv_output)
parmodel2csv_or_xls_iter(1,1,mat_output,csv_output);
```

7 Bibliography

[1] P. Kundur, Power System Stability and Control, McGraw-Hill, 1994.

[2] Jan Machowsky, Janusz Bialek and Jim Bumby, Power System Dynamics: Stability and Control, Wiley, 2008.

[3] P.S.R. Murthy, Power System Analysis, BS Publication, 2007.

[4] D. Piccagli, M. Barbieri, M. Pozzi, G. Giannuzzi, R. Zaottini, Techniques for the Analysis and Optimization of Electromechanical Stability, September 2012. International Federation of Automatic Control (IFAC).

[5] Ashfaque A. Hashmani, I. Erlich, "Mode selective damping of power system electromechanical oscillations using supplementary remote signals," IET Generation, Transmission & Distribution, Volume 4, Issue 10, October 2010, p. 1127 – 1138.

[6] U. Bachmann, I. Erlich, "Untersuchung von Netzpendelungen mittels Modalanalyse," 4. Tagung Netzregelung, Berlin, Germany, VDIBerichte 1329, pp. 85-99, 1997.

[7] F. P. DeMello and C. Concordia, "Concepts of synchronous machine stability as affected by excitation control," IEEE Transactions on Power Apparatus and Systems, vol. PAS-88, pp. 316-329, April 1969

[8] E. V. Larsen, D. A. Swann, "Applying Power System Stabilizers,parts IIII," IEEE Trans. on Power Apparatus and Systems, vol. PAS-100, pp. 3017-3046, 1981.

[9] E. V. Larsen and D. A. Swann, "Applying power system stabilizers parti: General concepts," IEEE Trans. on Power Apparatus and Systems, vol. PAS-100, no. 6, pp. 3017-3024, June 1981.

[10]   E. V. Larsen and D. A. Swann, "Applying power system stabilizers part ii: General concepts," IEEE Trans. on Power Apparatus and Systems, vol. PAS-100, no. 6, pp. 3025-3033, June 1981.

[11]   R.Marconato, "Electric Power Systems, volume 3", CEI 2008.